

43562



National Library of Canada

Bibliothèque nationale du Canada

Canadian Theses Division / Division des thèses canadiennes

Ottawa, Canada
K1A 0N4

PERMISSION TO MICROFILM — AUTORISATION DE MICROFILMER

• Please print or type — Écrire en lettres moulées ou dactylographier

Full Name of Author — Nom complet de l'auteur

RAYMOND ALEXANDER STEWART

Date of Birth — Date de naissance

3 MARCH 1952

Country of Birth — Lieu de naissance

REPUBLIC OF IRELAND

Permanent Address — Résidence fixe

21 KINGSTON
GALWAY
IRELAND

Title of Thesis — Titre de la thèse

PORE PRESSURES IN EARTH DAMS DURING IMPOUNDING

University — Université

UNIVERSITY OF ALBERTA

Degree for which thesis was presented — Grade pour lequel cette thèse fut présentée

MASTER OF SCIENCE

Year this degree conferred — Année d'obtention de ce grade

1979

Name of Supervisor — Nom du directeur de thèse

DR. Z. EISENSTEIN

Permission is hereby granted to the NATIONAL LIBRARY OF CANADA to microfilm this thesis and to lend or sell copies of the film.

L'autorisation est, par la présente, accordée à la BIBLIOTHÈQUE NATIONALE DU CANADA de microfilmer cette thèse et de prêter ou de vendre des exemplaires du film.

The author reserves other publication rights, and neither the thesis nor extensive extracts from it may be printed or otherwise reproduced without the author's written permission.

L'auteur se réserve les autres droits de publication; ni la thèse ni de longs extraits de celle-ci ne doivent être imprimés ou autrement reproduits sans l'autorisation écrite de l'auteur.

Date

OCT. 16 1979

Signature

Raymond Stewart



National Library of Canada

Cataloguing Branch
Canadian Theses Division

Ottawa, Canada
K1A 0N4

Bibliothèque nationale du Canada

Direction du catalogage
Division des thèses canadiennes

NOTICE

The quality of this microfiche is heavily dependent upon the quality of the original thesis submitted for microfilming. Every effort has been made to ensure the highest quality of reproduction possible.

If pages are missing, contact the university which granted the degree.

Some pages may have indistinct print especially if the original pages were typed with a poor typewriter ribbon or if the university sent us a poor photocopy.

Previously copyrighted materials (journal articles, published tests, etc.) are not filmed.

Reproduction in full or in part of this film is governed by the Canadian Copyright Act, R.S.C. 1970, c. C-30. Please read the authorization forms which accompany this thesis.

**THIS DISSERTATION
HAS BEEN MICROFILMED
EXACTLY AS RECEIVED**

AVIS

La qualité de cette microfiche dépend grandement de la qualité de la thèse soumise au microfilmage. Nous avons tout fait pour assurer une qualité supérieure de reproduction.

Si il manque des pages, veuillez communiquer avec l'université qui a conféré le grade.

La qualité d'impression de certaines pages peut laisser à désirer, surtout si les pages originales ont été dactylographiées à l'aide d'un ruban usé ou si l'université nous a fait parvenir une photocopie de mauvaise qualité.

Les documents qui font déjà l'objet d'un droit d'auteur (articles de revue, examens publiés, etc.) ne sont pas microfilmés.

La reproduction, même partielle, de ce microfilm est soumise à la Loi canadienne sur le droit d'auteur, SRC 1970, c. C-30. Veuillez prendre connaissance des formules d'autorisation qui accompagnent cette thèse.

**LA THÈSE A ÉTÉ
MICROFILMÉE TELLE QUE
NOUS L'AVONS REÇUE**

THE UNIVERSITY OF ALBERTA

PORE PRESSURES IN EARTH DAMS DURING IMPOUNDING

by

©

Raymond A. Stewart

A THESIS

SUBMITTED TO THE FACULTY OF GRADUATE STUDIES AND RESEARCH
IN PARTIAL FULFILMENT OF THE REQUIREMENTS FOR THE DEGREE
OF MASTER OF SCIENCE

DEPARTMENT OF CIVIL ENGINEERING

EDMONTON, ALBERTA

FALL 1979



THE UNIVERSITY OF ALBERTA
 FACULTY OF GRADUATE STUDIES AND RESEARCH

The undersigned certify that they have read, and recommend to the Faculty of Graduate Studies and Research, for acceptance, a thesis entitled PORE PRESSURES IN EARTH DAMS DURING IMPOUNDING submitted by Raymond A. Stewart in partial fulfilment of the requirements for the degree of MASTER OF SCIENCE.

Z. Eisenstein

Z. Eisenstein

N.R. Morgenstern

Supervisor
N.R. Morgenstern

F.W. Schwartz

F.W. Schwartz

Date...17 September 1979...

To Tom and Joy

ABSTRACT

This thesis deals with the pore pressure behaviour within embankment dams resulting from reservoir impounding and the transition to steady state seepage. The theories, analyses and results are specifically related to the case history of the Mica dam in British Columbia.

The processes which affect the pore pressures within the core during reservoir loading and transient seepage have been discussed and analysed. The relative contribution of each mechanism; total stress change, transient seepage and consolidation, has been evaluated. As a product of this analysis hydraulic fracture has been investigated and some conclusions are drawn regarding its likelihood. Steady state seepage analyses have been carried out for the Mica dam, and the influence of such parameters as anisotropy, non-homogeneity and underseepage have been investigated. A short discussion on piezometer reliability is included within the text.

The effect of instrument-lead placement technique has been investigated both in a general sense and specifically related to the Mica dam.

It is concluded as a result of these studies that the method of instrument installation is critical for narrow core dams. The method employed in the Mica dam has caused local anomalies to the pore pressure distribution and so the core piezometers are not reflecting the average pore pressure distribution.

ACKNOWLEDGEMENTS

The author would like to thank Dr. Z. Eisenstein for suggesting this thesis topic and for his guidance and support during all stages of the thesis.

The author also wishes to thank Dr. N. R. Morgenstern for his invaluable comments and advice on the topic.

The financial support provided by the Transportation Development Agency, the Province of Alberta, the Alberta Research Council and the University of Alberta is greatly appreciated.

Cooperation from B. C. Hydro and Caseco. consultants was invaluable. In particular the author wishes to thank Mr. H. Nussbaum.

Thanks are extended to all my fellow graduate students and the staff in the Department of Civil Engineering who have all contributed time to assist in this thesis. In particular John Simmons, Bryan Watts, Alan Gale, Jeff Weaver, and Erman Evgin deserve special thanks for their continual patience, discussion and advice.

The author would like to thank all his family for their wholehearted support during the last two years, both moral and financial.

The author would like to acknowledge the excellent job of data entry provided by Donna and Bryan.

Also appreciation is felt for the excellent advice provided by Adrian Wightman, without which this thesis would never have materialised.

Finally the author would like to extend his heartfelt thanks to all those people who helped turn Edmonton into a home. In particular, Louise and John, Fran and Kevin, Sandra and Sean, Betty and Dave, Merle and Garth, and Genny and Paul.

Thank you everyone.

Table of Contents

Chapter	Page
CHAPTER 1	
INTRODUCTION.....	1
1.1 <u>Modern Dam Design</u>	1
1.2 <u>Aim of this Thesis</u>	3
1.3 <u>Outline of the thesis</u>	4
CHAPTER 2	
THE MICA DAM.....	6
2.1 <u>General Description</u>	6
2.2 <u>Piezometer Types and Locations</u>	10
2.2.1 Standpipe Piezometers.....	13
2.2.2 Hydraulic Piezometers.....	13
2.2.3 Pneumatic Piezometers.....	13
2.2.4 Electric Piezometer.....	14
2.3 <u>Method of Piezometer Installation</u>	15
2.3.1 Deviation From Specifications.....	18
CHAPTER III	
OBSERVED PIEZOMETRIC RESPONSE.....	21
3.1 <u>Introduction</u>	21
3.2 <u>Piezometers - Failures and Reliability</u>	22
3.3 <u>Instrumentation Response in Major Sections</u>	26
3.3.1 Data Source.....	26

3.3.2	General trend of response.....	28
3.4	Instrumentation Details and Behaviour Within Major Sections.....	31
3.4.1	Section 22+50.....	31
3.4.2	Section 24+50.....	33
3.4.3	Section 16+50.....	33
3.4.4	Section 30+50.....	35
3.5	Conclusions.....	36

CHAPTER IV

	STEADY STATE SEEPAGE ANALYSIS.....	38
4.1	Introduction.....	38
4.2	Finite Element Computer Program - EPMS.....	39
4.3	Boundary Conditions and Material Properties of the Mica Dam.....	40
4.3.1	Location of the downstream water level.....	44
4.3.2	Location of the upstream water level.....	46
4.3.3	Seepage through the bedrock foundation.....	46
4.4	Details and Results of Analysis.....	48
4.4.1	Section 22+50.....	49
4.4.2	Section 24+50.....	61
4.4.3	Section 16+50.....	61
4.4.4	Section 30+50.....	61
4.4.5	Conclusions.....	65

CHAPTER V

	COMPARISON OF OBSERVED AND PREDICTED PORE WATER PRESSURES.....	67
5.1	Introduction.....	67

5.2	<u>Comparison of Individual Sections</u>	67
5.2.1	PE24...PH1.....	67
5.2.2	PH6...PH7.....	72
5.2.3	PE35...PH10 and PH11.....	74
5.3	<u>Conclusions</u>	75

CHAPTER VI

	<u>INVESTIGATION OF PORE PRESSURE ANOMALIES</u>	77
6.1	<u>Introduction</u>	77
6.2	<u>Pore Pressures Resulting from Total Stress Changes</u>	79
6.2.1	Model for Reservoir Filling.....	79
6.2.2	Pore Pressure Parameters.....	84
6.2.3	Degree of saturation of core.....	90
6.2.4	Calculation of pore pressure increments.....	92
6.2.5	Suitability of adopted procedure.....	94
6.3	<u>Hydraulic Fracture Potential</u>	96
6.4	<u>Transient Seepage</u>	99
6.4.1	Governing Equation.....	100
6.4.2	Rigid soil skeleton - Transient seepage.....	105
6.4.3	Discussion of results from transient seepage analysis.....	109
6.4.4	Consolidation -- Transient Seepage.....	116
6.5	<u>Conclusions</u>	117

CHAPTER 7

	<u>EFFECT OF PIEZOMETER INSTALLATION METHOD ON PORE PRESSURE DISTRIBUTION</u>	122
--	---	-----

7.1	<u>Introduction</u>	122
7.2	<u>Design of Instrumentation Lead Trenches for Mica Dam</u>	123
7.3	<u>General Model for Piezometer Lead Trenches</u>	124
7.4	<u>Model Specifically Applied to Mica Dam Core</u>	133
7.5	<u>Conclusions</u>	142
Chapter 8		
	<u>Conclusions</u>	145
8.1	<u>Significance of the Processes Involved during Reservoir Impoundment and Transient Seepage</u>	146
8.1.1	Total stress changes.....	146
8.1.2	Transient seepage.....	146
8.1.3	Hydraulic fracturing.....	147
8.1.4	Justification for simplified analysis.....	147
8.2	<u>Comparison with Observed Behaviour</u>	148
8.3	<u>Selection of Piezometer Type</u>	150
8.4	<u>Recommendations for Further Research</u>	151
	<u>references</u>	153

List of Figures

Figure		Page
2.1	Location of Mica dam.....	7
2.2	Mica dam - General fill arrangement.....	8
2.3	Piezometer locations.....	12
2.4	Instrument lead trench and riser detail.....	17
2.5	Location of instrument lead trenches and risers....	19
3.1	Composite section showing functioning piezometers (1978).....	25
3.2	General piezometer levels versus time.....	27
3.3	Contours of end-of-construction pore pressures.....	30
4.1	Core permeability vs. compaction moisture content (after Law 1975).....	42
4.2	Model for steady state seepage analysis.....	45
4.3	Bedrock model and piezometer locations.....	47
4.4	Sensitivity of analysis to mesh size and tolerance.....	51
4.5	Steady state analysis. Section 22+50. Res. elev. 754m.....	52
4.6	Steady state analysis. Section 22+50. Res. elev. 734m.....	53
4.7	Steady state analysis. Section 22+50. Res. elev. 660m.....	54
4.8	Calculated steady state piezometer readings.....	55
4.9	Effect of material anisotropy. Section 22+50.....	56
4.10	Effect of material non-homogeneity. Section 22+50.....	58
4.11	Results from bedrock seepage model.....	59
4.12	Comparison of bedrock model and piezometric readings. 60	
4.13	Steady state analysis. Section 24+50.....	62
4.14	Steady state analysis. Section 16+50.....	63

4.15	Effect of material anisotropy. Section 16+50.....	64
4.16	Steady state analysis. Section 30+50.....	66
5.1	Piezometric level (PE24) versus time.....	68
5.2	Piezometric level (PH1, PE35) versus time.....	69
5.3	Piezometric level (PH2, PH6, PH7) versus time.....	70
5.4	Piezometric level (PH10, PH11) versus time.....	71
5.5	Pore pressure distribution (22+50) across elev. 590.7m with time.....	73
6.1	Schematic diagram of processes occurring in core...	78
6.2	Reservoir loading model and results.....	81
6.3	Mohr circles for elements B, C, and D.....	82
6.4	Stress paths.....	83
6.5	"A" values for Mica till.....	89
6.6	Results of total stress analysis.....	93
6.7	Reservoir filling curve and approximations.....	108
6.8	Wetting fronts for various reservoir paths.....	110
6.9	Wetting front compared with movement gauge readings.....	112
6.10	Advance of wetting front and calculated piezometer readings.....	114
6.11	Predicted piezometric levels during transient seepage.....	115
6.12	Pressure head versus time.....	118
7.1	Instrument lead trench model.....	125
7.2	Design chart for trench connected to upstream shell.. 127	
7.3	Design chart for centrally located trench.....	128
7.4	Design chart for trench connected to downstream shell.....	129
7.5	Typical finite element mesh for trench model.....	130

7.6 Typical results of trench (upstream) analysis.....131

7.7 Typical results of trench (downstream) analysis...132

7.8 Results of trench analysis on PE38...PP36 and
PE44...PP44.....134

7.9 Equipotential distribution around trench PE38...PP36.
137

7.10 Equipotential distributions around trenches
PE36...PH11, PE34...PH9, PE24...PH1.....138

7.11 Equipotential distribution around trench PE25...PH7..
139

7.12 Theoretical pore pressure distribution compared
to actual, PE24...PH2.....140

7.13 Theoretical pore pressure distribution compared
to actual, PE25...PH7, PE35...PH10, PE37...PH12...141

CHAPTER 1

INTRODUCTION

1.1 Modern Dam Design

During the last two decades there have been significant advances in embankment design techniques. An improved understanding of the physical processes occurring during embankment construction has been achieved largely through the development of analytical methods for stress and strain analysis coupled with an increase in the use of instrumentation to monitor embankment performance.

Although present day analytical tools are powerful and sophisticated, the designers predictive capabilities are reduced by an incomplete knowledge of the constitutive relationships for, and interaction between, the composite soil types. These laws and interactive behaviour mechanisms are being refined through careful back-analysis of well instrumented case histories.

In current practice the finite element method (F.E.M.) is often used to provide insight into possible problem areas in the design. It may also provide a rough qualitative assesment of the expected instrument readings. The F.E.M. is

used for the analysis of stress, deformation, consolidation, and seepage conditions within the embankment.

The factor of safety against slope failure is determined by the use of conventional limit equilibrium methods. These methods employ the principle of effective stress which requires the prediction of the pore pressure distribution within the embankment. Conventionally factors of safety are calculated for the end of construction, first filling, steady state and rapid drawdown conditions in order to establish the critical case when the factor of safety is a minimum. The pore pressure distribution for both the end of construction and steady state cases are well defined by routine analysis, however the first filling and rapid drawdown conditions require simplifying assumptions for the pore pressure distributions in order to continue with the analysis.

It is apparent that little attention has been given to estimating the pore pressure distribution during the period between the end of construction and the establishment of steady state seepage, which is defined here as the 'transient' seepage stage. The reason for this is the complex interaction of the processes involved during reservoir loading. Clearly it is desirable to gain further insight into the behaviour of the pore pressure distribution within the embankment during and subsequent to reservoir filling. This is particularly important because the first filling of a reservoir is considered as a critical stage in

the working history of a dam.

A recent addition to modern dam design is the evaluation of hydraulic fracture potential. This is a poorly understood phenomenon which certainly requires further research and clarification.

Even though the embankment dam designers' technical expertise and understanding is improving rapidly there remain periods in the life of an embankment which are not well understood. The most critical of these is the 'transient' seepage stage. There may be significant changes in the pore pressure distribution during this phase which the designer is at present unable to analyze accurately. The early part of this period, the reservoir filling stage, is probably the most critical period for the evaluation of hydraulic fracture potential, which may be of major concern with some embankment configurations.

1.2 Aim of this Thesis

This thesis was undertaken with the following objectives:

1. To take a carefully instrumented and well documented case history, namely the Mica Dam, and investigate the pore pressure distribution within the embankment during the 'transient' seepage stage (between end-of-construction and steady seepage).
2. To define the processes taking place during this

period which cause alterations in the pore pressure distribution, and to evaluate the relative contribution of each process.

- 3. To attempt to evaluate the hydraulic fracture potential in the core of this dam during resevoir filling.
- 4. To briefly discuss the performance of the pore pressure measuring devices installed in the dam.

In summary this thesis is an attempt to provide some insight into the behaviour of the pore pressure distribution during and subsequent to resevoir filling, with specific reference to the Mica Dam.

1.3 Outline of the thesis

The thesis is organised in the following sequence:

Chapter 2 provides a general description of the Mica Dam including a discussion on the piezometer types and methods of installation.

Chapter 3 discusses the reliability and performance of the piezometers in general.

Chapter 4 details the steady state seepage analysis.

Chapter 5 compares the observed and calculated pore pressure distribution within the core.

Chapter 6 analyses the seperate physical processes involved during resevoir filling. It studies the transient flow and evaluates the hydraulic fracture potential within the core. Finally these results are compared to the observed

pore pressure distribution.

Chapter 7 evaluates the effect of imperfect instrument installation procedure both generally, and specifically for the Mica Dam core. These results are compared to the observed distribution calculated from the piezometer readings.

Chapter 8 presents the conclusions of the thesis and discusses some recommendations for further research.

CHAPTER 2

THE MICA DAM

2.1 General Description

Mica dam is situated on the Columbia River in British Columbia immediately west of the Rocky Mountains, and 135 kilometers north of Revelstoke. The site is in a narrow gorge where the Columbia River leaves the Rocky Mountain Trench. The location is shown in Fig. 2.1.

The dam was constructed as part of the Columbia River Treaty (1964), which provides regulation for maximum production of power and flood control of the river. The project includes a 2500 MW powerplant which develops the head created by the dam. The storage provided by the dam is approximately $25 \times 10^9 \text{ m}^3$ and the length of the reservoir created is about 208 kilometers, from Golden to Valemont in the Trench.

The dam is a zoned earthfill embankment, with a near-vertical central impervious core of heavily compacted glacial till. The shells are compacted sand and gravel of which the outer edges are compacted and dumped rock. The general fill arrangement is shown in Figure 2.2. The

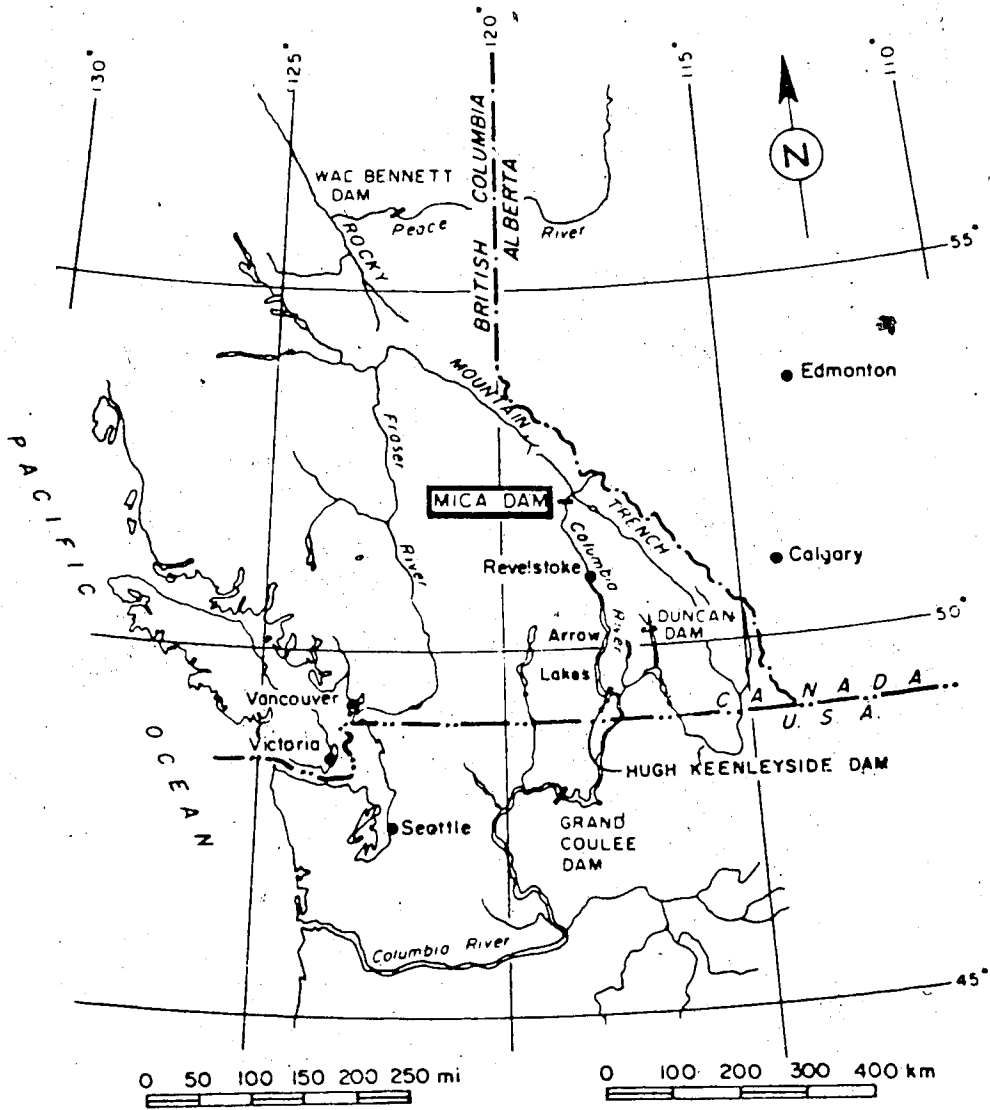
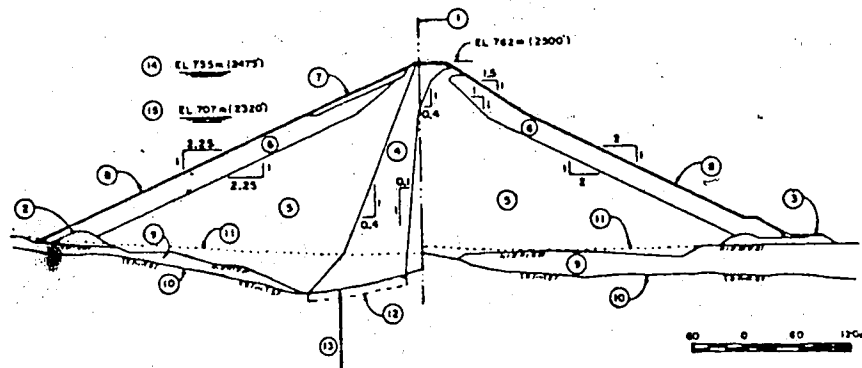


FIGURE 2.1. Location of Mica Dam
(after Law 1975)



- (1) Axis of dam
- (2) Upstream cofferdam.
- (3) Downstream cofferdam.
- (4) Core-glacial till.
- (5) Shells-sand and gravel.
- (6) Outer shells-sand and gravel or rock.
- (7) Drawdown zone-gravel, cobbles, boulders or rock.
- (8) Slope protection.
- (9) River overburden.
- (10) Bedrock.
- (11) Original riverbed.
- (12) Limit of blanket grouting.
- (13) Deep exploratory holes.
- (14) Normal maximum reservoir level
- (15) Minimum drawdown level.

FIGURE 22 Mica Dam - General Fill Arrangement
(after Nussbaum 1976)

embankment was constructed over 4 seasons between April 1969 and November 1972. The reservoir filling commenced in April 1973 and operating level was reached in August 1974. Further details of the Mica dam are available in published papers by Meidal and Webster (1973), Mylrea (1969), Webster (1970), and Webster and Lowe (1971), and in unpublished reports by Caseco Consultants Limited.

At the time of completion the Mica dam was the highest earthfill dam in the world. Due to its great height, 244 metres, careful consideration was given during design to control possible settlements and cracking (Webster, 1970). Extensive testing and analyses were carried out (Insley and Hillis 1965, Skermer 1975) in order to predict the embankment behaviour in advance of construction.

Some special features of the design to minimize cracking potential were; slight upstream arching of the core, removal of river overburden material beneath the central portion of the embankment, very heavy compaction of the core till and the sand and gravel shells. In the event of a crack forming through the core the excellent self-healing properties of the shell material increase the Factor of Safety against piping development.

In order that the dam performance could be monitored closely and analyzed an extensive instrumentation program was initiated. The instruments were installed in 4 main sections to measure horizontal and vertical movements, strains, earth pressures and pore water pressures. The

measuring devices included; 82 surface monuments, 15 vertical and near-vertical movement gauges, 6 horizontal movement gauges, 207 horizontal strain gauges, 53 earth pressure cells, 86 piezometers and 9 accelographs.

The instrumentation has been carefully monitored both during and subsequent to construction. A number of back-analyses have been carried out since construction in an attempt to model the observed behaviour by finite element methods (Simmons 1974, Law 1975, Skermer 1975). In general the calculated movements match the observed movements reasonably well when the correct boundary conditions and material properties are entered in the analyses. No analysis has been carried out to predict the behaviour of the dam during and subsequent to reservoir filling.

2.2 Piezometer Types and Locations

A large number of piezometers were installed in the body of the dam and in the foundation. The foundation piezometers were placed both to indicate the degree of success of the grouting program and to provide information on the seepage through the bedrock due to the differential head induced by the dam. The piezometers in the main body were installed to monitor the buildup of pore pressures during construction and to indicate the behaviour of the dam during reservoir filling and during the subsequent years.

Due to the pervious nature of the shell material only a few piezometers (13) were placed in strategic locations in

these zones, to ensure that no build-up of pore pressure was occurring in the sand and gravel shells. The majority of the piezometers (32) were placed within the till core. One main section and three minor sections were instrumented. The sections are shown in Fig.2.3.

A variety of piezometer types were installed in order that their reliability and behaviour could be compared. Having a mixture of models could be valuable, in the event of one particular model developing a problem, then at least some readings could be obtained from the remaining piezometers in the section.

The types of piezometers installed were:

1. Standpipe - Casagrande type
2. Hydraulic - USBR type
3. Pneumatic - Hall type and Geosistemas S.A. type
4. Electric - Maihak type

These piezometers are described by Hanna (1973), United States Bureau of Reclamation (1963), Scott and Kilgour (1967) and their advantages and disadvantages are discussed by Vaughan (1973), Little (1973).

The choice of a particular type of piezometer in each location depended on the following factors:

1. The dam zone or foundation material.
2. The distance from piezometer tip to readout unit.
3. The relative elevation of piezometer tip to readout location.

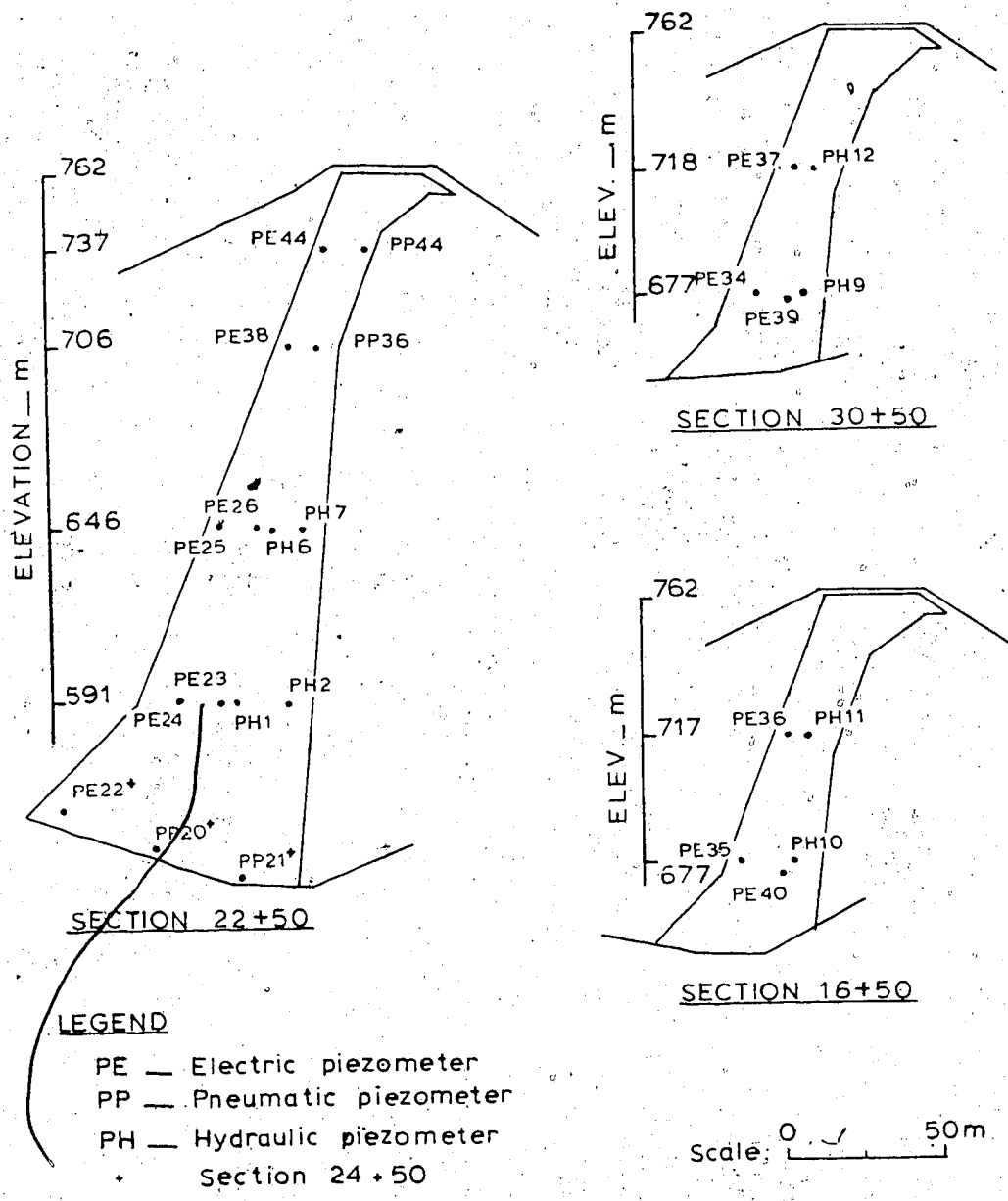


FIGURE 2.3 Piezometer Locations

Where long lead lengths were required electric piezometers were installed. Hydraulic piezometers could only be used where the instrument house was below the tip elevation. Standpipe piezometers were located in the cofferdams and were only temporary in nature. All piezometers, except the standpipes, were fitted with high air entry porous stones.

2.2.1 Standpipe Piezometers 7

These piezometers were ordinary Casagrande type piezometers. All these piezometers were abandoned during construction and are not important for this thesis. One of these standpipes was installed in the foundation, this was destroyed in late 1974.

2.2.2 Hydraulic Piezometers

These piezometers are the USBR embankment type and were manufactured by Advance Industries Ltd., Vancouver. They were originally intended for the Bennett dam, B.C.

13 of these were installed, 8 in the core and 5 in the downstream shell. There have been no failures up to early 1979.

2.2.3 Pneumatic Piezometers

Two types of pneumatic piezometers were installed. The majority were supplied by Geo-testing Inc., California and are otherwise known as Hall piezometers.

35 Hall piezometers were installed. Of these 6 have

failed and 12 have been abandoned from the cofferdams. The remainder are still functioning, 8 in the core, 4 in the shells and 8 in the downstream river overburden.

The second type of pneumatic piezometer was manufactured by Geosistemas S.A. of Mexico. These 3 piezometers were installed in the upper core and are still functioning.

The basic differences between the two models are the body materials and the reading method. The Hall piezometer has a stainless steel body, the Geosistemas a PVC body. The Hall type is read by maintaining a steady flow of nitrogen through the system, whereas the Geosistemas type is read as a pressure value upon closure of the diaphragm.

2.2.4 Electric Piezometer

The electric piezometers are the vibrating wire type supplied by H. Malhak A.G. of Germany. An excellent review of these piezometers is given by Scott and Kilgour (1967).

45 of these units were installed. 18 have failed and 11 were abandoned from within the cofferdams. Of the remaining 16 one in the core may be suspect. The functioning units are 3 in the core, 3 in the shells, 8 in the core foundations, 1 in the downstream cofferdam.

The location and type of each core piezometer is shown on Figure 2.3. The vertical and near-vertical movement gauges are being utilized as open standpipes as well as their normal function.

2.3 Method of Piezometer Installation

Two methods of piezometric installation are used in the Mica dam, one for the foundation piezometers and the other for embankment piezometers. Readout houses are located both in the upstream shell and the downstream shell. Three of these houses located in the upstream shell are now flooded by the reservoir and are abandoned. One house remains above reservoir level in the upstream shell. Three houses are located at various levels in the downstream shell and it is in these that most of the piezometer leads terminate. Two houses are located in the abutments. The instrument houses are well designed and are frost and weather-proof, containing both heating and lighting.

The piezometers were read once monthly during the reservoir impoundment period. Subsequent to this they were read a minimum of 3 times yearly. The readings were carefully tabulated and plotted on charts of level versus time. The charts are published in monthly or yearly instrumentation reports by Casco. Consultants Limited.

The foundation piezometers are of a limited interest for this thesis and will not be described in detail. The reason for this is that too few of the foundation piezometers are still functioning to provide an accurate and consistent picture of the exact conditions in the bedrock. These units are simply installed in vertical drillholes with the instrument lines rising vertically out of the drillhole and then traversing across the embankment, in association

with the other instrument leads in the area, to the readout house. The piezometers are sealed just above the tip with a bentonite plug, and the holes are carefully backfilled to ground level. The trench detail for these instrument leads is the same as for the embankment type.

The embankment piezometers are installed as the embankment construction proceeds. The tips are carefully placed just below construction level. Then the leads are laid in a trench which is offset from the tip. This trench contains a number of leads from piezometers at different locations, these leads are brought to an instrument readout house. This is normal procedure for embankment piezometer installation (USBR 1963, Blight 1970).

The specifications for the trenches are shown in Caseco Consultants Ltd., 'Contract documents' - vol.2 of 4, dated September 6, 1967. Details of the layout are shown on Figure 2.4. The backfill for the core trenches was the core material with the soil sizes greater than 9.5 mm (3/8 in.) removed (Type A). An alternate provided for was a fine concrete aggregate with up to 10% bentonite by volume added (CSA A23.1). The backfill was to be hand compacted in 75 mm (3 in) layers. Cut-offs were to be provided of Type A backfill plus 5% by volume of bentonite, not less than 0.3 m (1 ft) thick and extending 0.3 m (1 ft) outside the sides of the trench at 15 m (50 ft.) intervals or between 2 piezometer tips, whichever is lesser.

Riser leads were required for elevation changes between

Note: All dimensions in mm.

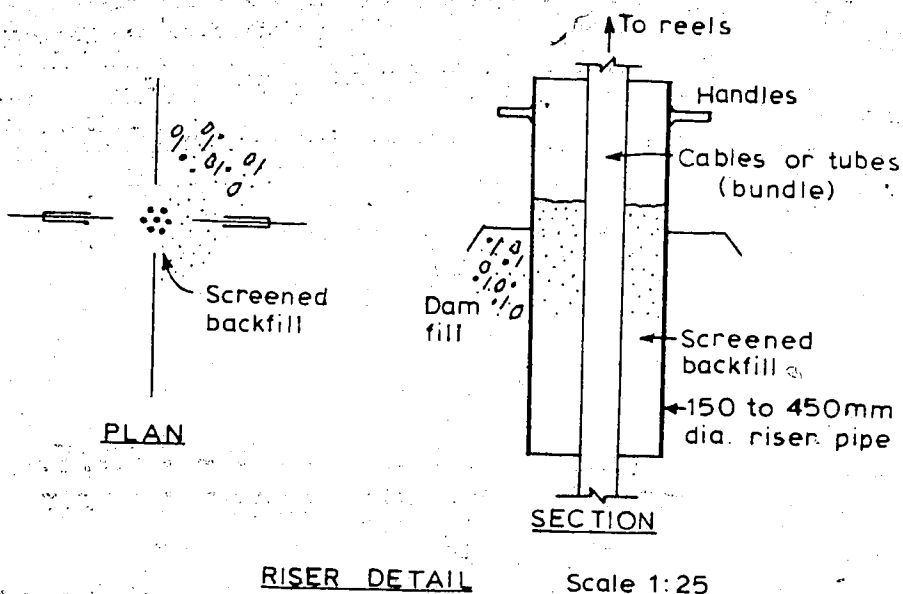
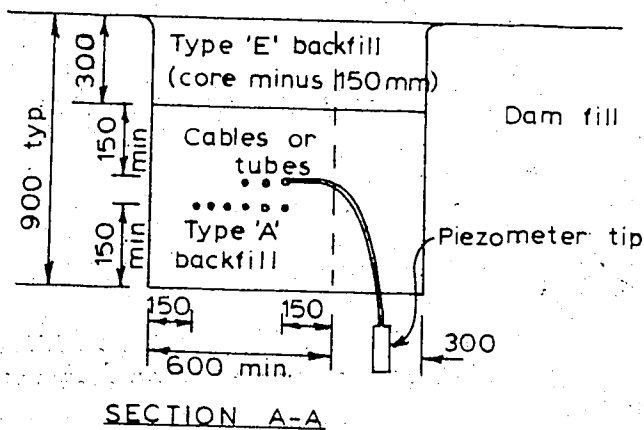
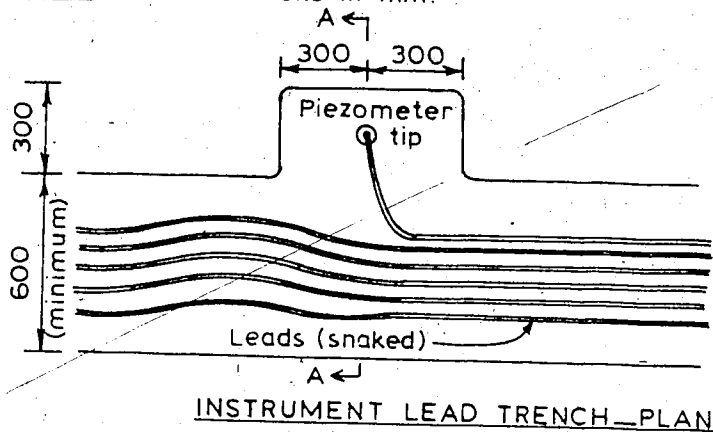


FIGURE 2.4 Instrument-Lead Trench and Riser Detail

lead trenches. Details are shown in Figure 2.7. Backfill should be Type A material, with bentonite added every 15 m (50 ft.) vertically, to act as a cutoff.

The locations of the piezometer lead trenches and riser pipes are shown in Figure 2.5. These details were taken from Caseco Consultants Ltd., 'Dam Instrumentation construction notes' 1969-1972, (unpublished). It appears from the notes that there was some deviation from the specifications during construction, which requires further discussion.

2.3.1 Deviation From Specifications

During 1969 the installation of the leads in the trenches closely followed the specifications. That is, 5% bentonite-sand with a small amount (0.15%) of cement was used 150 mm above and below the instrument leads. The remainder of the trenches were filled with minus 150mm till. Cut-offs were provided as specified. The risers were backfilled with minus 9.5 mm till.

During 1970 the only reported change was that the bulk of the trench was backfilled with minus 75 mm till. However, from the limited data available it appears that the moisture content of the backfill was very low, although the densities were reasonably high.

Throughout the 1971 construction season the complete trench was backfilled with sand-bentonite-cement mixture rather than screened till. This was at the contractors' choice. Also a statement was made in the construction notes,

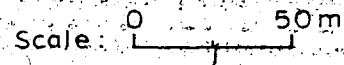
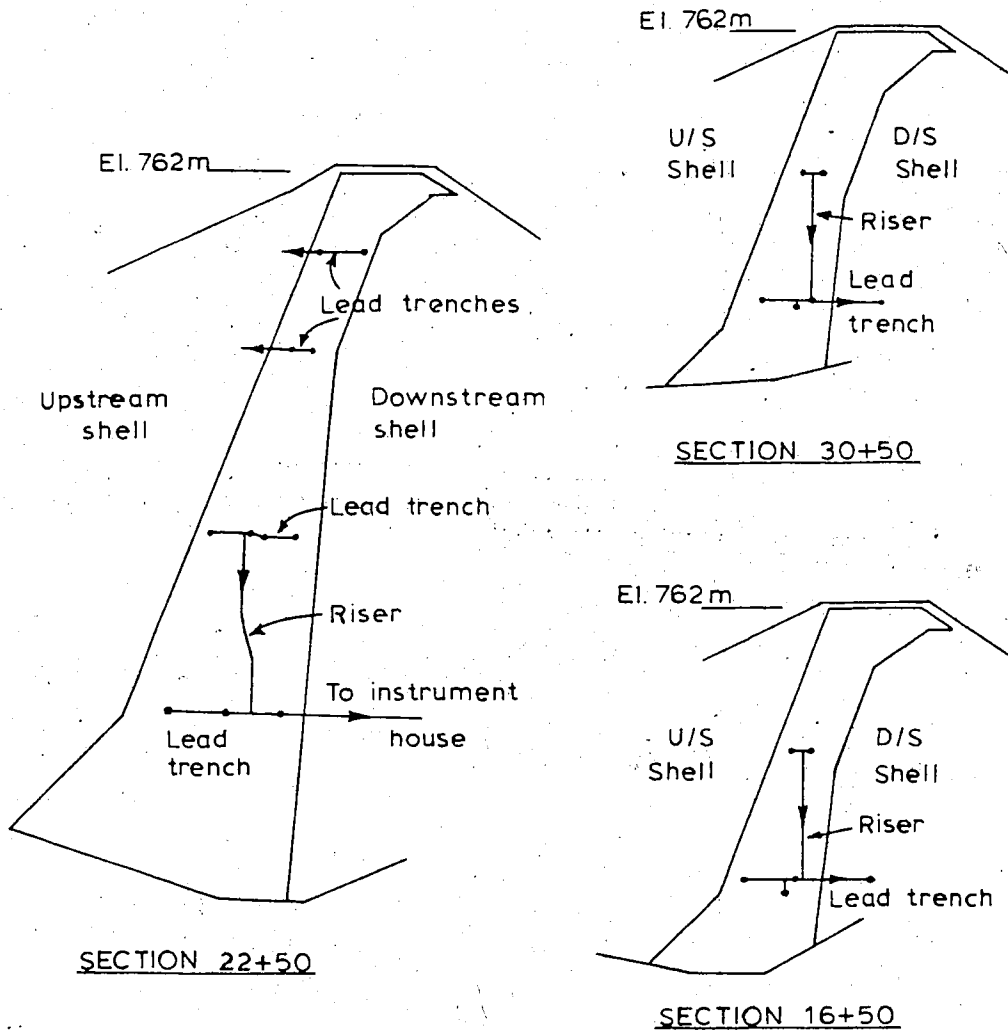


FIGURE 2.5: Location of Instrument-Lead Trenches and Risers

"It was found that the initial field moisture contents of both Wood River gravel and sand-cement-bentonite mix were considerably below optimum and moisture was added to improve compaction."

It is apparent that some difficulties were encountered with the risers,

"Oversize rocks and roots scalped from the fill were frequently piled around risers and the contractor had to be reminded continuously to keep risers clear."

The construction procedure for 1972 was similar to that of the 1971 season discussed above.

It should be noted that specific details of the trench and riser installation were difficult, and in many cases impossible to acquire, mainly because 7 years have passed since the construction was completed. However, the "construction notes" quoted from above do provide some insight into the average method of the installation and some variations encountered. The significance of these variations is discussed later in Chapter 7.

CHAPTER III

OBSERVED PIEZOMETRIC RESPONSE

3.1 Introduction

Construction of the embankment commenced in April 1969 and continued over the next four construction seasons to November 1972 when the dam was topped out at elevation 763 m, the core depth being about 244 m. Reservoir filling commenced on the 29th March, 1973. The "first-filling" took place over 2 filling seasons, this was in order that the water level would not be raised too quickly. A small drawdown (33 m) was observed between the two filling stages. Elevation 734 m was reached during this "first-filling" stage by mid-August 1974. Following this the reservoir has fluctuated seasonally between "full pool" elevation (754 m) and a winter level of about 730 m. Maximum allowable drawdown rates are limited to about 1.5 m/day over a 10 day period, with much lower rates over extended periods to a minimum of 0.15 m/day. Filling has averaged about 0.3 m/day over the last 5 years.

The purpose of this chapter is to discuss why the piezometers detailed in Chapter 2 have failed and to briefly review the response of the piezometers to the reservoir filling and to subsequent reservoir fluctuations.

3.2 Piezometers - Failures and Reliability

A considerable number of piezometers in the embankment have either failed or been abandoned. The reason for the abandonment is that early in the construction of the cofferdams some piezometers were installed to provide additional design data. On reservoir filling many of these piezometers have become inaccessible, this does not present any problem as the data to be obtained was only significant during the early construction period.

The failures, however, were not anticipated and it is of interest to evaluate the reasons for these failures. Table 3.1 shows the piezometer category, number of units, number of failures and percentage success. It is obvious that the electric piezometers have the worst record by far.

From a close inspection of the failure dates of the Maihak units a trend was immediately obvious. Six piezometers failed in July 1973. If the problem was straining of the leads, a common cause suggested by Scott and Kilgour (1967), then the piezometers would not all fail at the same time. The explanation is that two separate lightning strikes on the dam caused voltage surges which were too high for the overvoltage protection. This phenomenon has been noted in the literature by Pinkerton and McDonnell (1964) on the Tooma Dam (Australia) where 8 out of 15 Maihak piezometers failed. Also Hosking and Hilton (1963) suggest that the progressive failure of the electric piezometers in the Eucualene Dam were probably due to a

series of minor strikes because these gauges were entirely unprotected. It becomes obvious from a scan of the literature that the phenomenon of lightning strikes is a rare event, many authors have had excellent success with Malhak piezometers and although the literature does draw attention to the problem it does not emphasize lightning as a potential danger (Little 1973, Scott and Kilgour 1967, Speedie 1963).

It is interesting to note that after the first failures were diagnosed in 1970 the leads were altered in future installation from unshielded (GG) type to shielded G(C)G type. This precaution was not sufficient, however, because of the large number of failures in 1973. Perhaps because of the random nature of lightning strikes this problem has not been given enough attention, but the consequences are serious and more thought should be paid to the overvoltage protection detail in future installations.

One piezometer in the core (PE35) experienced a zero shift after the lightning strike in 1973 and so its readings were re-calibrated for this thesis after this date.

A serious consequence of these failures is that there are virtually no reliable readings to be obtained from the upstream side of the core.

The pneumatic piezometers have a moderate record and the failures tended to be progressive rather than sudden. The cause of the failures has not been established definitely but are probably due to excessive straining and

rupture of the leads or leakage into the tubing over a long period (Little 1973, Vaughan 1973, Caseco Consultants Ltd. 1970). Pneumatic piezometers are a relatively new innovation and, as such, their long term reliability is not confirmed to date. They may suffer from operator error, as reported by Little (1973). Fortunately, the pneumatic piezometers are not placed in critical locations in the core.

The U.S.B.R. type hydraulic piezometers have an excellent record in the Mica dam and are considered to be very reliable. This optimistic view of hydraulic piezometers has been shared by many authors over the years.

The locations of the functioning piezometers are shown on a composite section in Fig.3.1.

All of the piezometers are fitted with high-air-entry (H.A.E.) porous stones and therefore should record the pore water pressure in the unsaturated fill. However, as noted by many authors (Vaughan 1965, Scott and Kilgour 1967) in the case of an electric piezometer with no de-airing facility even a H.A.E. porous stone will not preclude air saturation of the stone and cavity. In areas of high pore pressure the difference between the pore air pressure and pore water pressure will be small. However, in areas of low pore pressures the reliability of the electric piezometers could be questioned. Pneumatic piezometers also suffer from the drawback of no de-airing facility. So the pneumatic piezometers in the upper core should be treated with caution as they could very well be reading pore air

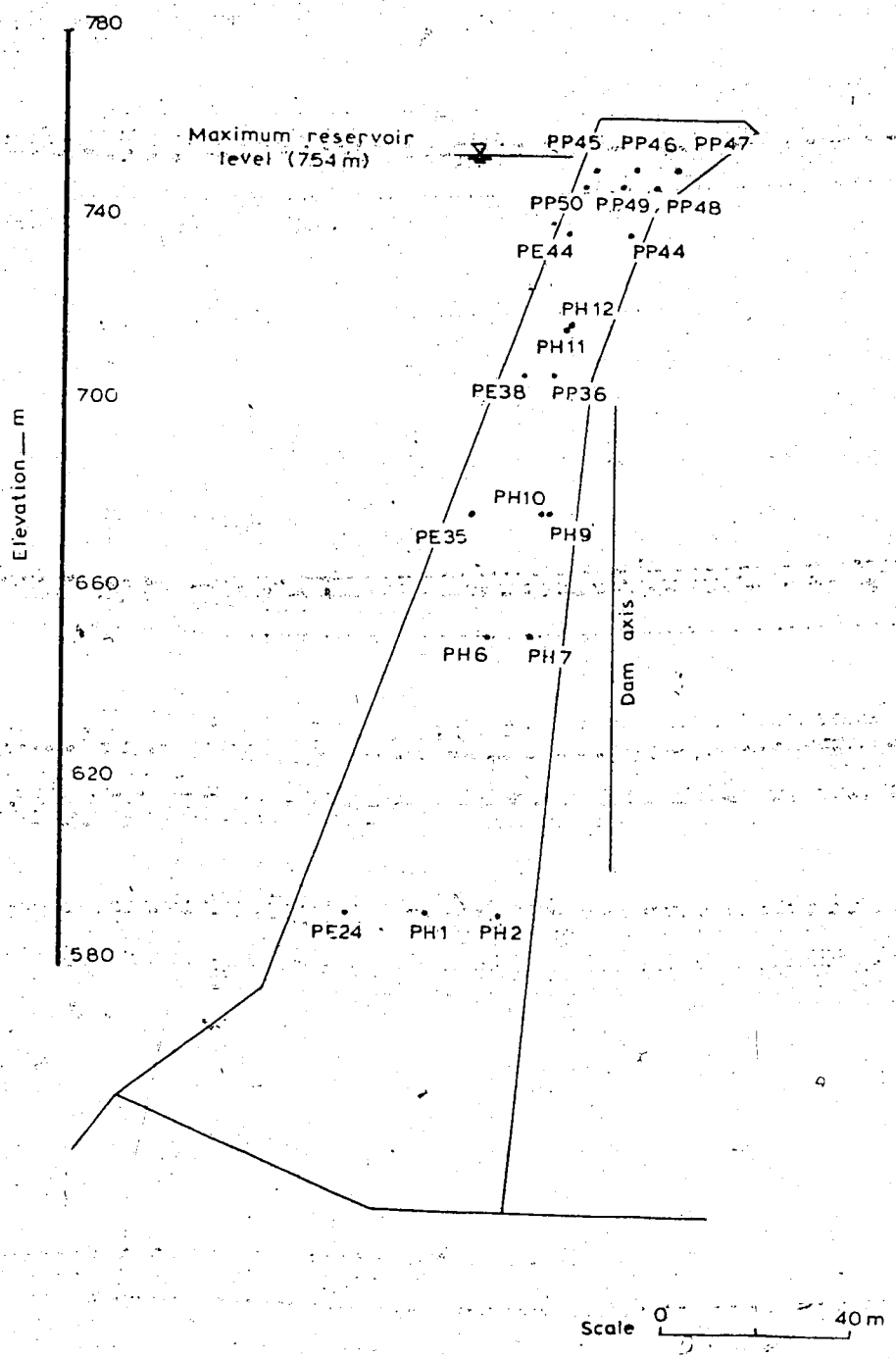


FIGURE 3.1 Composite Section Showing Functioning Piezometers (1978)

pressures. The hydraulic piezometers have been de-aired every few years when necessary and so it is felt that they are indeed reflecting the pore water pressures.

The conclusion is that the hydraulic piezometers are behaving excellently and the readings are reliable. The electric units have a very poor record and the surviving piezometers may reflect pore air pressures in areas of low pore pressure. One electric piezometer (PE35) is known to have suffered a zero shift in 1973 and so is considered unreliable. The pneumatic piezometers have a moderate record and may also be recording pore air pressures in areas of low pore pressure. These pneumatic piezometers are not located in critical areas of the core. The nett result is that the pore pressure record for the downstream section of the core is very good, whereas the upstream section is very poor.

3.3 Instrumentation Response in Major Sections

3.3.1 Data Source

The piezometer readings for the years 1969 to 1979 required for this thesis were obtained from the Caseco Consultants Ltd. "Mica Project: Reports on Dam Instrumentation" 1969 - 1979.

Readings were taken on an average of once per month with the exception of the winter when no readings were made.

The monthly readings were taken from the original reports and combined in continuous plots over the 7 year period from 1972 to 1979 (Fig.3.2.)

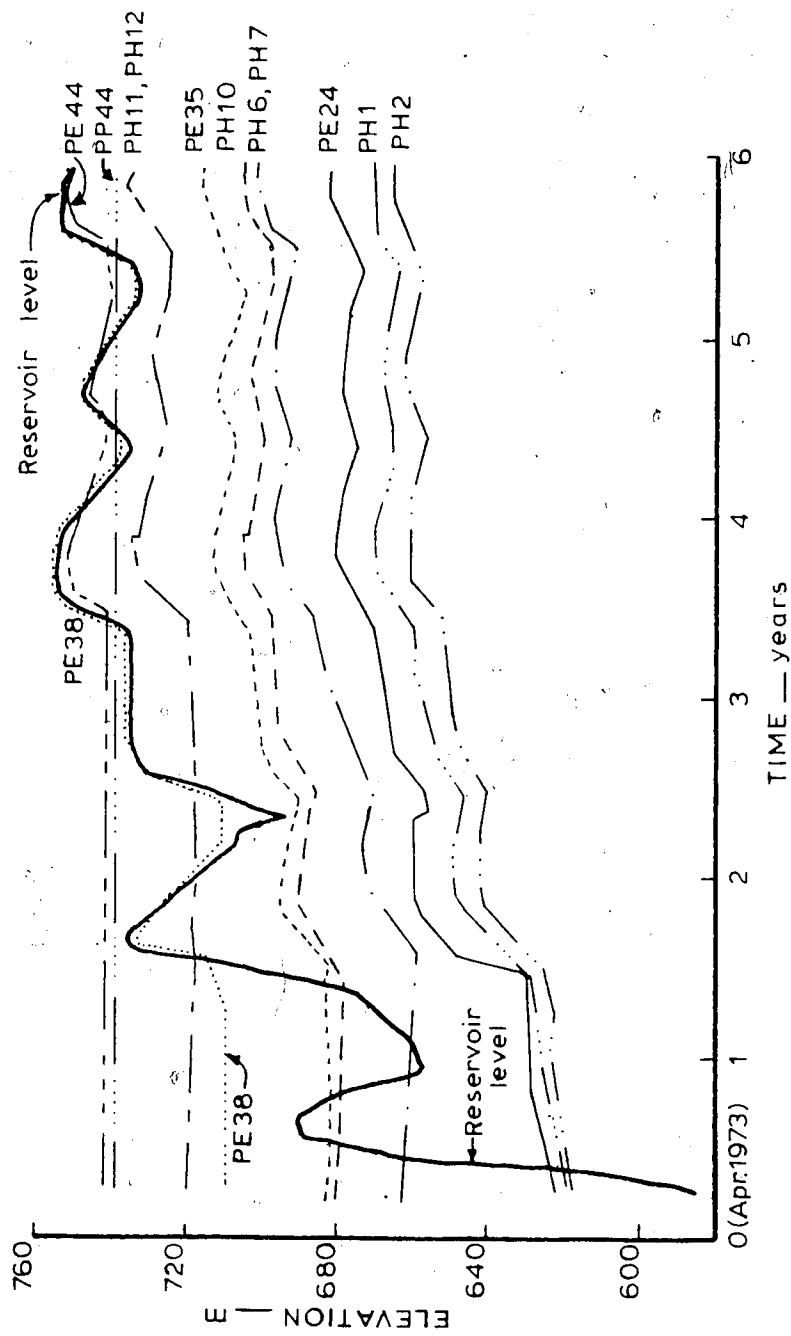


FIGURE 32 General Piezometer Levels versus Time

3.3.2 General trend of response

A cursory examination of all the data indicates a similar pattern for all core piezometers. The upstream shell piezometers reflect the reservoir head as expected and the downstream piezometers show no excess pore water pressures.

The placement pore water pressures were examined. The readings obtained within the core were all positive or very slightly negative. These were all electric piezometer readings and the reason could very easily be that the piezometers were reading the pore air pressure. At a compaction water content minus 2% of optimum it is expected that fairly large negative pore pressures would develop. It has been noted previously by Little (1973) that electric piezometers may not reflect this negative pore water pressure successfully. The reason that no hydraulic piezometric measurements were available immediately after placement was that the instrument house installations were not prepared at that time.

Next the end of construction pore pressures were inspected. As expected with the increased total stresses due to the application of the remaining fill the pore pressures had become positive. Contours of the end of construction pore pressures are shown in Fig.3.7.

Some consolidation is apparent between the end-of-construction and first filling in all the lower piezometers. The picture is confused in the upper elevations because the applied overburden stresses were not large

enough to indicate specific pore pressure gradients, coupled with probable ambiguity over pore air and pore water pressures. (Figure 3.3) One unusual feature noted during this phase is that the central core zones appear to consolidate more rapidly than the outer core zones which might be unexpected.

"First-filling" of the reservoir was reflected in the lower core piezometers by a small increase in pore pressures. However, during the second stage of the "first-filling" there is a very noticeable increase in the pore pressure response. This change in response occurred approximately 1 1/4 years after filling commenced. Following the next filling peak some of the piezometers show a decrease in pressure.

From September 1974 onwards is termed the 'steady reservoir level' even though there are seasonal fluctuations of approximately 24 m. The lower core piezometers tended to model these fluctuations with a time lag, the upper piezometers also show some response to the reservoir fluctuations.

The general conclusion was that perhaps the piezometers were reacting to the two processes involved during reservoir filling and transient flow leading to "steady state" conditions. These two processes are:

1. Total stress change.
2. Transient seepage.

The term "steady state" refers to a condition which is close

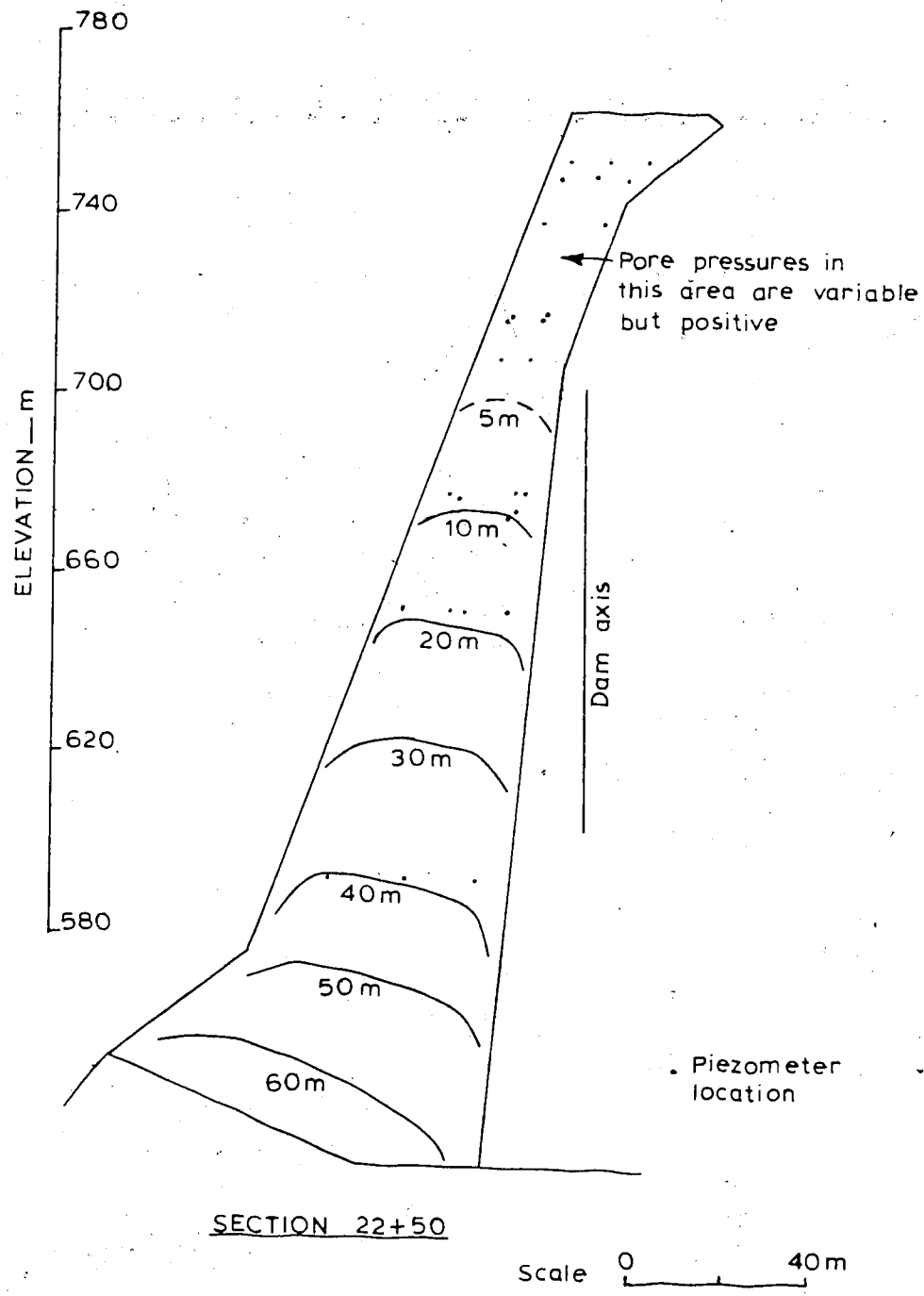


FIGURE 33 Contours of End-of-Construction Pore Pressures

to the long term steady state. This state may never be completely reached while the reservoir fluctuates.

3.4 Instrumentation Details and Behaviour Within Major Sections

3.4.1 Section 22+50

This is the major instrumentation section. The layout of the piezometers is shown in Fig.2.3. There are 4 rows of piezometers at elevations 590.7 m, 650.7 m, 706 m, and 736 m. The upper two rows contain 2 piezometers each, and the lower two rows contain 4 piezometers each. Theoretically, this would have supplied an excellent indication of the pore pressure distribution within this section. Unfortunately, a number of piezometers either failed or their readings are invalidated for other reasons discussed previously.

Piezometer PE23 failed in August 1970, PE25 and PE26 failed in July 1973, the remainder performed satisfactorily. However, the readings from PE38, PP36 and PE44 are invalidated because the leads from these piezometers were installed in trenches which ran north into the upstream shell and these piezometers are essentially reflecting the upstream water levels. From a total number of 12 piezometers only 5 are considered to be functioning and reliable. All these piezometers are located in the downstream section of the dam core with the exception of PE24. Water levels have been read continuously in the vertical movement gauges e.g. MV8, MV9. These movement gauges have been founded in the

bedrock, and they permit the entrance of seepage along their length. For this reason they should reflect the phreatic surface location with time. It is unlikely that high bedrock seepage pressures are distorting the readings because the gauges are grouted into the bedrock.

Elevation 590.7 m

Piezometer tips PE24, PH1 and PH2 are located at this elevation. These three piezometers show a similar trend, each reflecting the consolidation in the core until the pool elevation raises above 590.7 m when a continuous but slight increase in pore pressure is shown. During the first drawdown in the winter of 1973, PE 24 and PH1 continue to rise whereas PH2 decreases slightly. During the second filling the 3 piezometers respond more strongly and from this time on they all respond in a similar but damped manner to the reservoir. At all times the pore pressure at PE24 is greater than PH1 which is in turn greater than PH2. In principal the trend is correct and the magnitudes will be investigated in following sections.

Elevation 650.7 m

Piezometer tips PH6, PH7 are installed at this elevation. The first notable characteristic of these two piezometers is that their respective pore pressures are very close in magnitude and they fluctuate in a very similar manner.

They both continue to decrease at an average rate of 0.5 m/mo. until the second filling stage when they begin to react to the reservoir level. They continue to rise until the 'steady' reservoir condition is reached in 1976 when they appear to stabilize and follow the reservoir level. The difference in readings between PH6 and PH7 appears to be too small to reflect normal behaviour.

3.4.2 Section 24+50

This is the only other instrumented deep section. It contains 3 piezometers and these were all installed close to the bedrock/fill interface (see Fig.2.3). One of these, PE22, failed in August 1970. The remaining two PP20 and PP21 functioned until July and August 1974, respectively. It would appear that these piezometers were reflecting rather high pore pressures and this may have been due to the proximity of the foundation boundary. Their more rapid and more extreme response at the early stage of filling is probably due to the higher degree of saturation of the core material at this level, which is a function of the higher stresses, seepage from bedrock, and seepage from riverbed.

The most likely cause of failure was the rupture of the leads from the pneumatic piezometers, caused by excessive straining of the tubes.

3.4.3 Section 16+50

This section contains 2 rows of piezometers,

PE35...PH10 at elevation 677 m and PE36...PH11 at elevation 716.6 m. PE40 (which is located below PH10) and PE36 both failed in July 1973.

From a total of 5 piezometers, 2 have failed. This section is important though because PE35 is still functioning and it is located close to the upstream edge of the core.

Elevation 677.0 m

Piezometers PE35 and PH10 are located at this elevation. During July/August 1973 PE35 suddenly dropped about 6.5 m. This drop was not reflected by any other piezometer and the reservoir was still rising. It is apparent that this drop of 6.5 m is a direct consequence of the electric storm which caused the other electric piezometers to malfunction. Another observation to indicate the malfunction is that piezometer PH10 which is downstream of PE35 was actually reading higher than PE35 during 1975. However, the general trend of PE35 seems correct during the following years, and it is reasonable to assume that the lightning strike may have only caused a zero shift in the readings. So the readings have been corrected upward by 6.5 m. Any conclusions drawn solely from PE35 though, should be treated with due caution.

PH10 performs normally. The only unusual occurrence is a sudden drop of approximately 0.75 m on Dec.1 1976. This was caused by a gauge recalibration at that time. Otherwise

PH10 is quite similar in form to the other piezometers.

Elevation 716.6 m

PH11 is similar in most respects to PH10. Including a recalibration on December 1, 1976.

3.4.4 Section 30+50

This section contains 2 rows of piezometers. PE34, PH9 at elevation 677 m and PE12 at elevation 718 m. Included in this section is PE39 which is projected from Section 31+15. PE34, PE37 and PE39 all failed in August 1973 and once again all these piezometers were located on the upstream side of the core.

Elevation 677 m

PH9 is functioning normally. It does not begin to react until the second filling phase in 1974 and then it slowly begins to model the reservoir behaviour.

Elevation 718 m

PH12 also appears to be functioning normally. It reacts only very slightly until mid-1976 when it too models the reservoir behaviour. This is expected because of the relatively high tip elevation.

Some individual piezometers are located between sections 14+00 to 15+30 and 34+35 to 36+05. These are piezometers PP48, PP49, PPS0 and PP45, PP46, PE45, PP47,

respectively. The tip elevations of these groups are at approximately 747 m and 750.7 m.

The reservoir level does not reach elevation 747 m until mid-1976; it remains above this level for 6 months, it does not cross this elevation again until mid-1978, except for a month in 1977 when the reservoir peaks at 748 m.

As expected, these piezometers show very limited response, the upstream piezometer PP50 showing more fluctuations than the others.

These piezometers have not been subject to detailed analysis.

3.5 Conclusions

The installation of 32 piezometers in the embankment core has resulted in 12 failures, 4 completely unreliable (PE38, PE36, PE44, PP44), 1 may be unreliable, leaving a remainder of 15 piezometers functioning normally. The distribution of the reliable piezometers is unfortunate in that only 2 of these reflect the pore pressure behaviour in the upstream side of the core.

The general behaviour of the piezometers appears normal; however, this chapter did not investigate the magnitudes of the pore pressures which are dealt with in later chapters in more detail.

The very poor performance with electric piezometers could probably have been avoided by the installation of more reliable overvoltage protection devices. The installation

method itself appears to have been good because there are no failures due to excessive straining or rupture of the leads, a common fault noted by Scott and Kilgour (1967).

The performance of the pneumatic piezometers has not really been conclusive in the embankment, because the majority of these piezometers are at very high elevations where the responses are not easy to analyze.

The hydraulic piezometers have behaved excellently. The reliability of hydraulic piezometers has been noted by many authors (Little 1973, Vaughan 1973, Mackellar et al 1973, Hosking and Hilton 1963) provided the installation is carefully handled by experienced personnel.

The recommendation based on the Mica Dam performance is that in critical locations, where possible, hydraulic piezometers should be used.

CHAPTER IV

STEADY STATE SEEPAGE ANALYSIS

4.1 Introduction

One of the major concerns of this thesis is to study the process leading to steady state flow conditions in the Mica Dam. In order to ascertain this it is necessary to know what the theoretical steady state conditions are for this dam. A number of methods are available to analyse the dam for steady state conditions.

These are as follows:

1. Closed form solutions
2. Electric analogue or viscous fluid models
3. Graphical solutions (flow nets)
4. Approximate solutions by numerical methods
(finite difference or finite element)

Graphical solutions are probably the simplest, but because of the large number of flow nets which would be required and the difficulties encountered with the seepage face, this method was not adopted. The most suitable method appeared to be by finite element techniques. A computer program already existed within the department which could handle this problem. This program (FPM5) was developed by Taylor and Brown at the University of California in 1967.

4.2 Finite Element Computer Program - FPM5

The finite element seepage program used during this thesis was originally proposed by Taylor and Brown (1967). The program has been used previously at the University of Alberta by Guther (1972b) during his Master of Science thesis work. Guther (1972a) prepared the Users Manual, Soil Mechanics No. 16 entitled "Axisymmetric and Plane Flow in Porous Media", which describes the preparation of input and use of the program. Further details on the use of this program are given by Kealy and Busch (1971).

The finite element theory for use in seepage problems through porous media has been adequately described elsewhere (Zienkiewicz 1971, Taylor and Brown 1967, Guther 1972), and so will not be further discussed here.

The program FPM5 deals with the flow of liquids through a saturated porous medium where motion is governed by a generalized Darcy equation. It has the capability of dealing with a free surface and axisymmetric or plane flow problems.

The finite element method is very versatile and can easily handle effects such as anisotropy, non-homogeneity and difficult boundary geometries. The accuracy of the program is indicated by Guther (1972) in a comparison with a closed form solution.

An ambiguity does exist at the point of intersection of the free surface with the boundary, because the nodal flow at this point cannot be zero. It is important to reduce the mesh size in this area to minimize this ambiguity effect,

and so reduce the error. This problem is discussed by Neuman and Witherspoon (1970) and they show a case where the solution diverges rather than converges; however, it is felt that with careful attention to the mesh size in this area the program would then tend to converge on the correct answer.

The core in the Mica dam overhangs the downstream shell. This results in an unsaturated zone below the seepage face in the downstream shell (Casagrande, 1937). The FPM5 program cannot deal with this situation so the core has been treated as a single unit with appropriate boundary conditions.

4.3 Boundary Conditions and Material Properties of the Mica Dam

A general section of the Mica Dam is shown in Fig.2.2. The material properties of the different zones are discussed in detail by Law (1975), Simmons (1974), Meical and Webster (1973), and Webster (1970). Some till properties are listed below:

Liquid limit 18%
 Plastic limit 13%
 Plasticity index ... 5%

The most important parameters required for the seepage analysis were the relative permeabilities of the different zones, the effectiveness of the foundation grouting, and the degree of anistropy within the compacted fill. These

properties have been reported in Caseco Reports (various), Simmons (1974), Law (1975), with the exception of the degree of anisotropy of the fill.

The shell material has a permeability of about 10^{-3} cm/sec. which is approximately 3 to 4 orders of magnitude larger than the core permeability. It is reasonable then to treat the core as a separate unit because the shells are essentially 'free-draining' and will not have any influence on the pore pressure distribution within the core.

The permeability of the core fill is a function of many variables such as particle size, void ratio, composition, fabric and degree of saturation (Lambe and Whitman, 1969) or, in other terms, the permeability is a function of the soil structure which in turn is influenced by the compaction method, compaction water content and effective confining pressure. These values were obtained from direct permeability tests during extensive triaxial testing on representative samples reported by Insley and Hillis (1965). A figure (Law 1975) has been extrapolated to provide values of permeability at the low compaction water contents observed in the upper core. These results may be slightly in error but they do indicate a lower bound, see Fig. 4.1.

The minor principal effective stress is estimated to range from 500 kPa in the lower core to 350 kPa in the upper core (Simmons 1974). Using these values it is assumed that the lower core has an average permeability of 10^{-7} cm/sec.

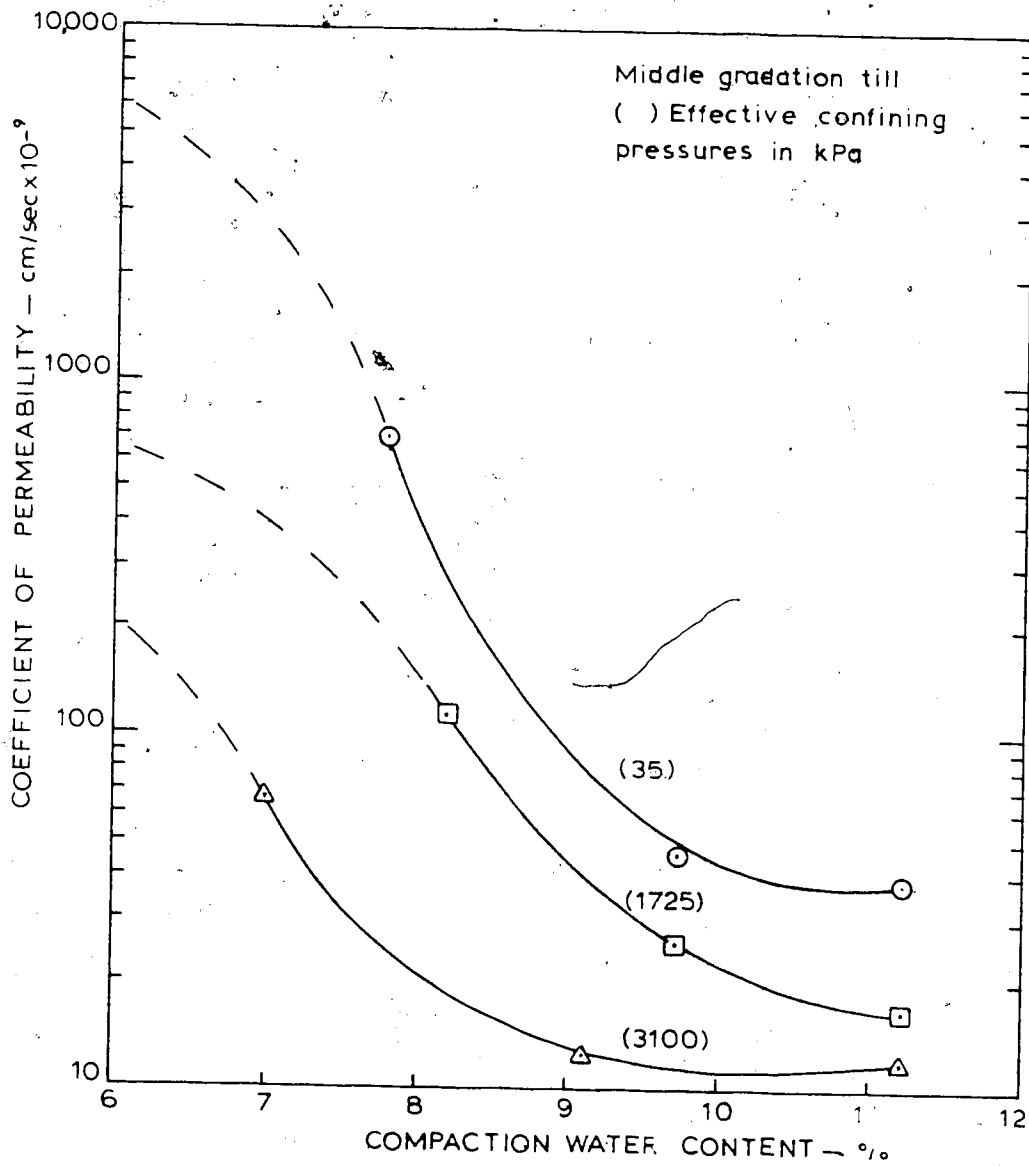


FIGURE 4.1 Core Permeability vs. Compaction Moisture Content (after Law 1975)

and the upper till at the lower water content has a permeability of 10^{-6} cm/sec. or greater. The reason for this extrapolation is justified by examination of the figures in the paper by Mitchell et al (1965) which clearly shows the influence on permeability of a wider range of moisture contents. Webster (1970) indicates the till permeability to be about 10^{-7} cm/sec. and the sand and gravel shells to be between 2×10^{-3} cm/sec. and 9×10^{-3} cm/sec. depending on the dry densities.

The degree of anisotropy of the till core has never been evaluated but it is unlikely to be greater than 4 (Sherard et al. 1963). Values as high as 10 were used in this analysis, which is certainly an upper bound.

The seepage through the bedrock foundation was more difficult to evaluate. Three piezometer sections were installed to obtain information on the effectiveness of the grouting program. Unfortunately, a number of the piezometers have failed and the information from the remaining piezometers is rather confusing. It would appear that the grouting program was not wholly successful in reducing the underseepage. Sensitivity of the pore pressure distribution to this boundary condition was investigated.

The assumption with respect to the shells was much more straightforward. The piezometers located in the upstream shell indicate that the head loss in this zone is indeed negligible. Therefore, the reservoir level is assumed to act directly on the upstream face of the core. The piezometers

in the downstream shell indicate that this material is 'free-draining', some small positive pore pressures are probably due to surface run-off and infiltration. The lower piezometers give a reasonable indication of the 'tailwater' elevation in this shell.

Figure 4.2 shows the model assumed for the steady state seepage analysis.

4.3.1 Location of the downstream water level

The flow in the downstream shell was assumed to be horizontal or sub-horizontal, so the pore pressures in the piezometers should indicate the phreatic surface in this zone. For the main Section 22+50 the readings indicate a phreatic surface which is more or less constant (fluctuations less than 6 m) the fluctuations probably being due to rainfall and run-off. There is a consistent drop in phreatic surface towards the toe and the lower piezometer PP23 has a greater pore pressure than PP26 which may indicate a slight upward flow from the bedrock. These variations are not significant.

The phreatic surface in the downstream shell is taken at 573 m (+ or 3 m) with some confidence. It may be seen later from the analysis that the pore pressure distribution is not very sensitive to this exact elevation.

Sections 16+50 and 30+50 are less precise. There are no piezometers located in the downstream shell below the phreatic surface. PH14 and PH15 are both above this level.

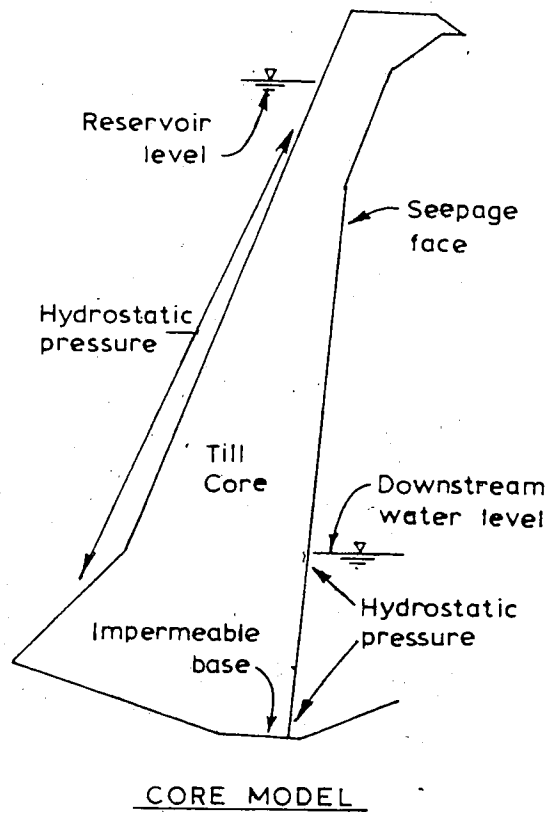
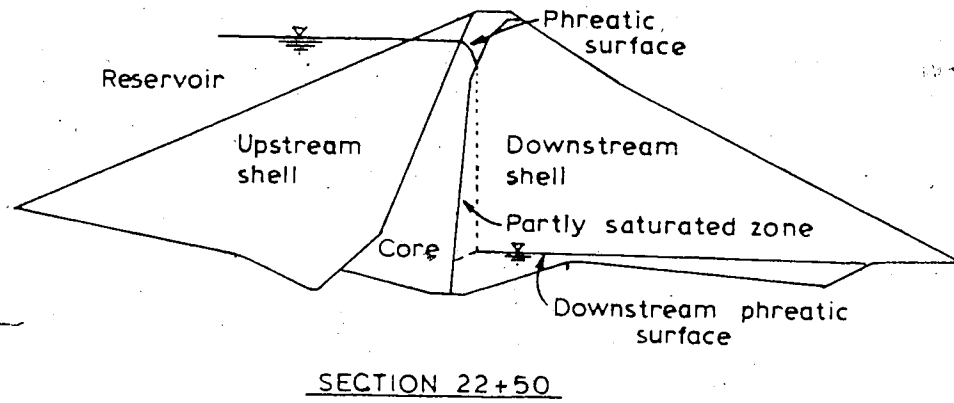


FIGURE 4.2 Model for Steady State Seepage Analysis

The phreatic surface assumed (65.6 m) is relatively low which results from a consideration of the 3 dimensional nature of the valley and the high shell permeability.

4.3.2 Location of the upstream water level

As discussed previously this level is assumed equivalent to the reservoir level. The piezometers in this zone substantiate this assumption, as do the vertical movement gauges. So there is negligible head loss across the upstream shell and there is no time lag involved.

4.3.3 Seepage through the bedrock foundation

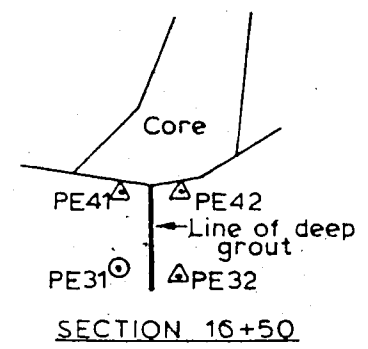
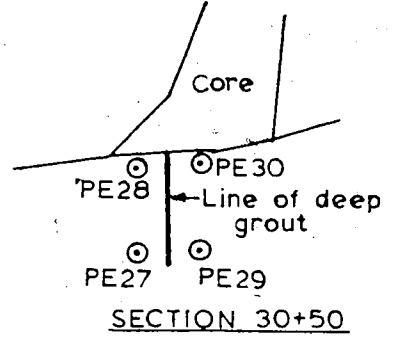
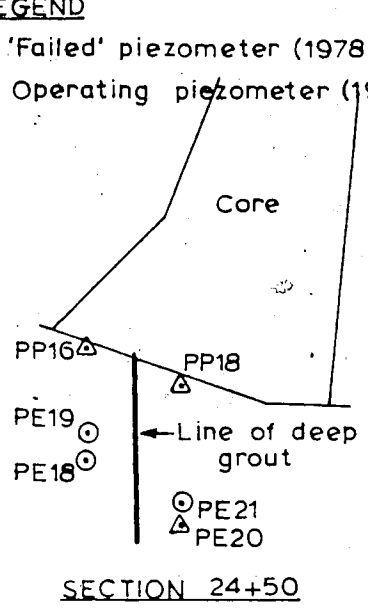
The bedrock beneath the core is described as "a metamorphic series of late Precambrian age with main rock types of mica schists and granite gneisses" (Meidal and Webster 1973). Joint spacing is often less than 0.6 m near the surface increasing with depth to more than 15 m. Water testing in the exploration drill holes indicated the rock to be "relatively tight" except near the surface.

A grouting program was considered necessary. Blanket grouting was carried out to a depth of 9 m on a 6 m square grid. In addition, a line of deep (approx. 30 m) holes 12 m apart were grouted. The effectiveness of these measures was monitored by piezometers (Fig.4.3).

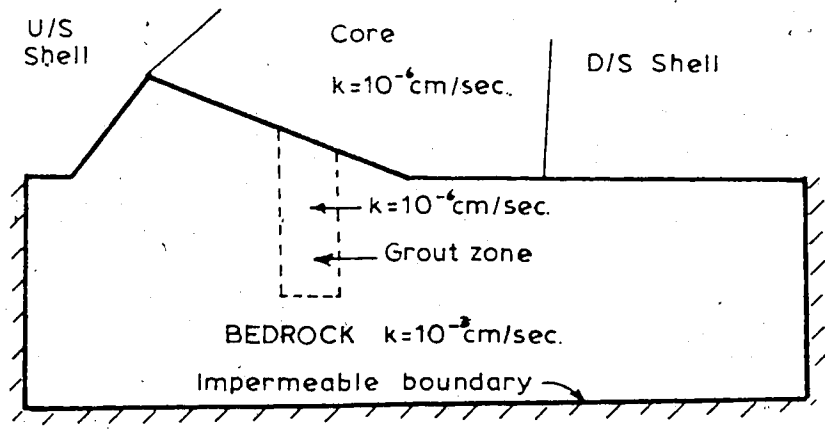
Section 22+50 indicates grouting to be about 30% effective. Section 31+15 indicates about 85% effectiveness. Section 16+50 showed the grouting to be ineffective up to

LEGEND

- △ 'Failed' piezometer (1978)
- ⊙ Operating piezometer (1978)



Scale: 0 60m



Scale 0 40m

FIGURE 4.3 Bedrock Model and Piezometer Locations

the piezometer failures in July 1973.

The instrumented sections indicate the possibility of significant underseepage. So sensitivity to this boundary condition was investigated.

A permeability value for the bedrock was assumed of the order of 10^{-3} cm/sec., there is no accurate basis for this assumption but it is considered to be an upper bound value.

4.4 Details and Results of Analysis

Finite element meshes were drawn for the four main instrument sections. The meshes were varied for different reservoir levels. Initially, the piezometer locations were not modelled by fixed nodes. However, to increase the accuracy it was later decided to provide fixed nodes at each piezometer location where practical. It should be noted that in the early stages of analysis PE24 was located incorrectly, too close to PH1. Because of an erroneous statement in a Caseco Instrumentation report dated 1970,

"...pore pressure values in PH1, which is installed very close to PE24,..."

This report is confusing PE23 with PE24. The location error was observed during later inspection of construction notes, and the location of PE24 was corrected.

The value of permeability chosen initially for the analyses was 10^{-6} cm/sec. The absolute magnitude of permeability does not have to be exact for the analysis, unless the flow values are of interest. It is the various

permeability ratios which control the pore-pressure state within the core. The permeability ratios used in the analysis are interpreted from the published laboratory testing (Law, 1976).

4.4.1 Section 22+50

Firstly, the sensitivity of the analysis to the downstream water level was checked. A range of levels from 527 m to 597 m was chosen for a constant reservoir level at 734 m. In the range of interest, 573 + or - 3 m, the variation in piezometric levels at elevation 590.7 m (PE24, PH1, PH2) was less than 0.5 m. At the higher elevations there was no significant variation. The conclusion was that moderate variations in downstream water elevation have only a local effect on the pore pressure distribution in the vicinity of the water elevation.

Next the accuracy of the solution was checked with respect to mesh size and tolerance value. A fine mesh (184 elements) and a coarse mesh (120 elements) were compared. The coarse mesh provided results within 2% of the finer mesh. This was considered accurate enough because a slight change in tip location would cause an error of this magnitude. Of course using the coarse mesh caused the boundary ambiguity effect to be more pronounced.

The tolerance level was checked on the fine mesh by altering the tolerance from 0.2 m to 0.02 m. This increased the number of iterations required from 6 to 15 with no

significant change in phreatic surface level. The results of these analyses are shown on Fig.4.4. The conclusion was that the coarse mesh is satisfactory and a tolerance level of 0.1% of the available head is adequate to give results of acceptable accuracy.

A number of computer runs were made, with the assumptions discussed above, for varying reservoir levels. The core was considered homogeneous and isotropic. A sample of the resulting grids and equipotential distributions are shown in Figs.4.5 to 4.7. The total head was plotted versus reservoir level for each piezometer. The results are shown on Fig.4.8.

Next the effect of anisotropy was investigated. A horizontal to vertical permeability ratio of 10 was chosen as an upper bound. The effect of this anisotropy was very slight indeed. The phreatic surface was close to horizontal but the piezometric readings were not effected in the lower areas. The area of major difference is the area close to the phreatic surface in the downstream section. In other words, the anisotropy causes only a local disturbance of pore pressure distribution. Sample results are shown in Fig.4.9.

The effect of non-homogeneity was investigated for the differing core properties at elevation 610 m. Above elevation 610 m the permeability chosen was 10^{-6} cm/sec. below this elevation 10^{-7} cm/sec. This effect was also studied for isotropy and anisotropy. When the reservoir is at higher elevations (734 m) the disturbance is not

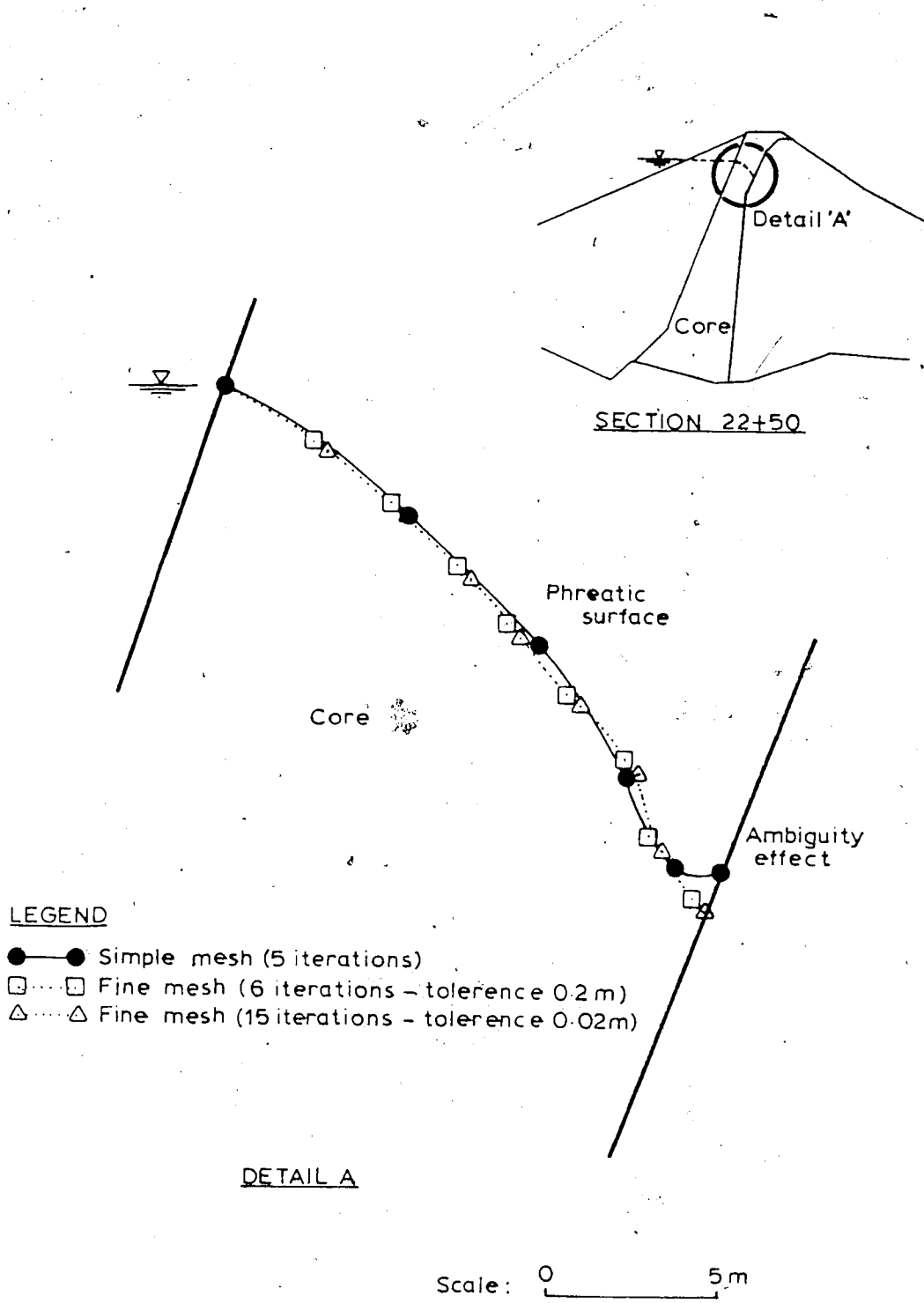


FIGURE 4.4 Sensitivity of Analysis to Mesh Size and Tolerance

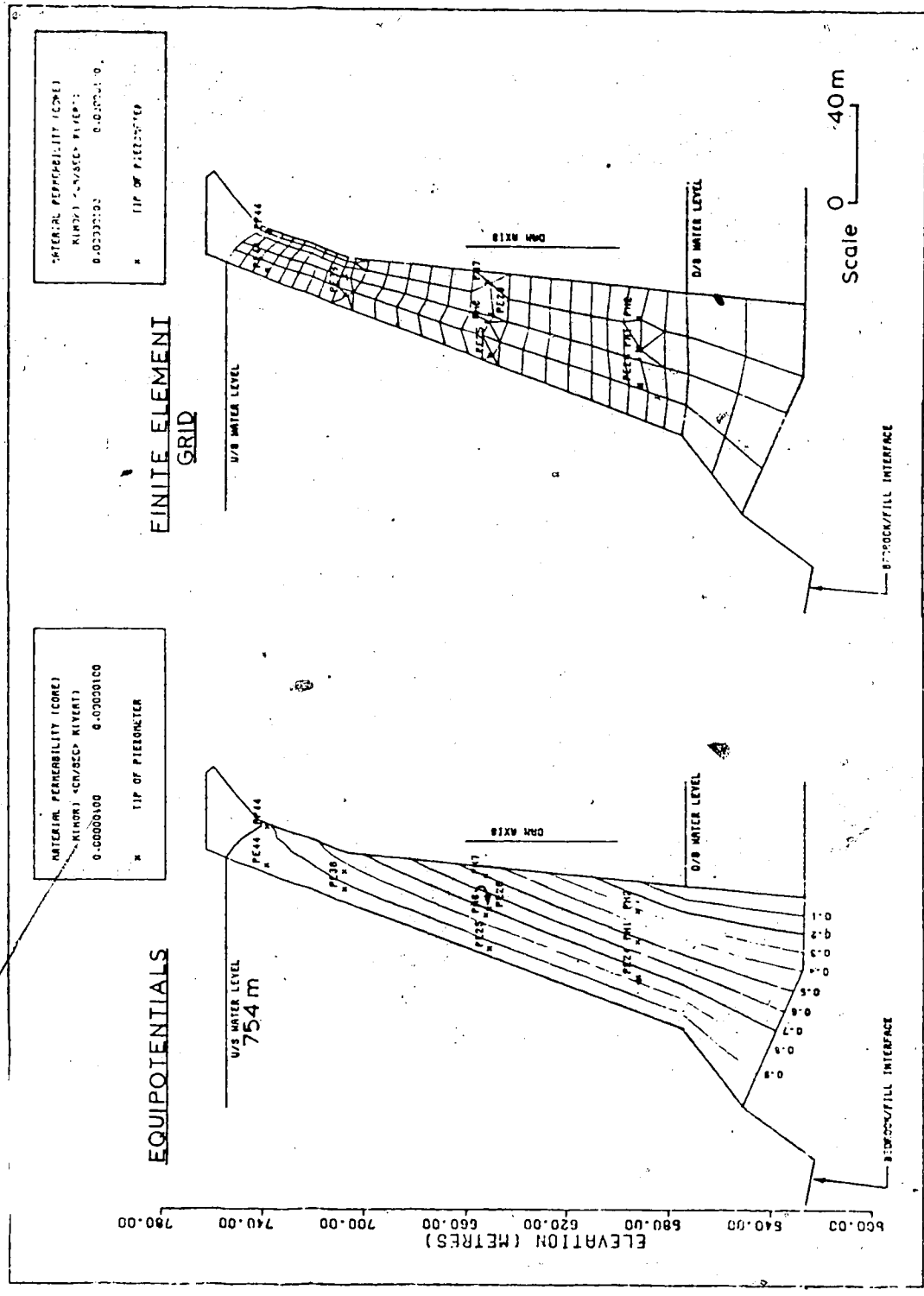


FIGURE 45 Steady State Analysis. Section 22+50. Res. Level 754m.

SECTION 22+50

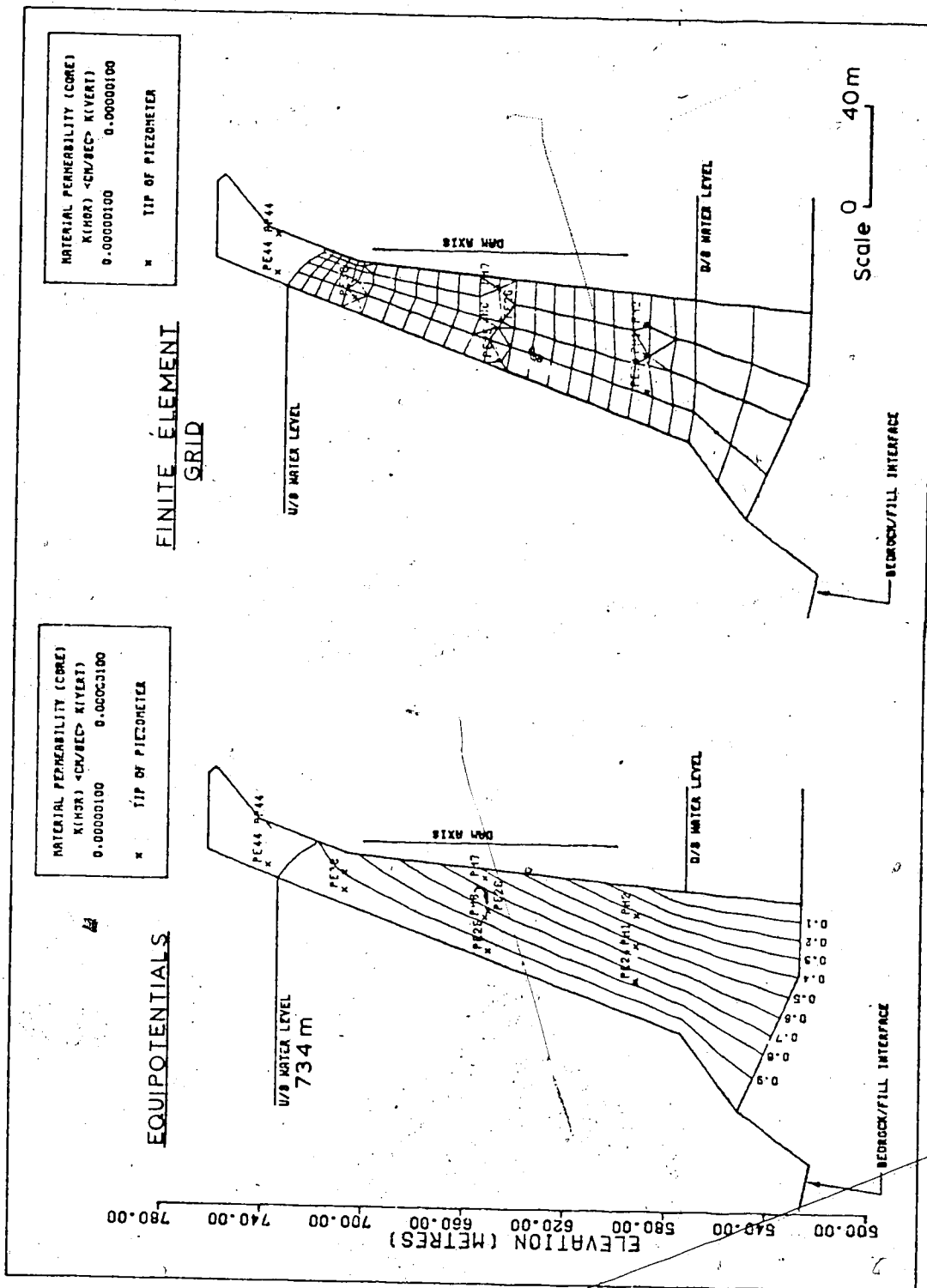


FIGURE 4.6 Steady State Analysis. Section 22+50. Res. Level 734 m.

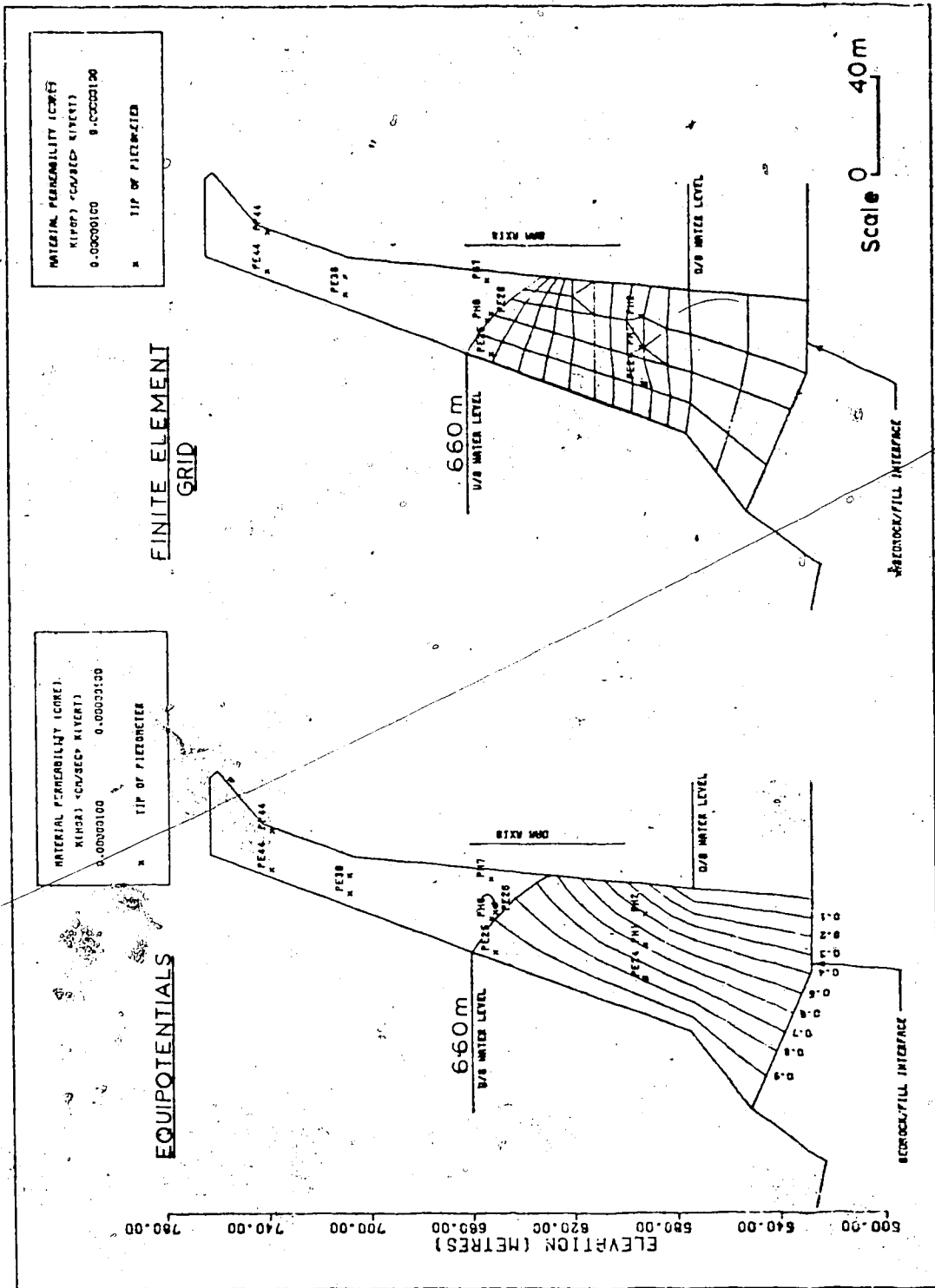


FIGURE 47 Steady State Analysis. Section 22+50. Res. Level 6.60 m.

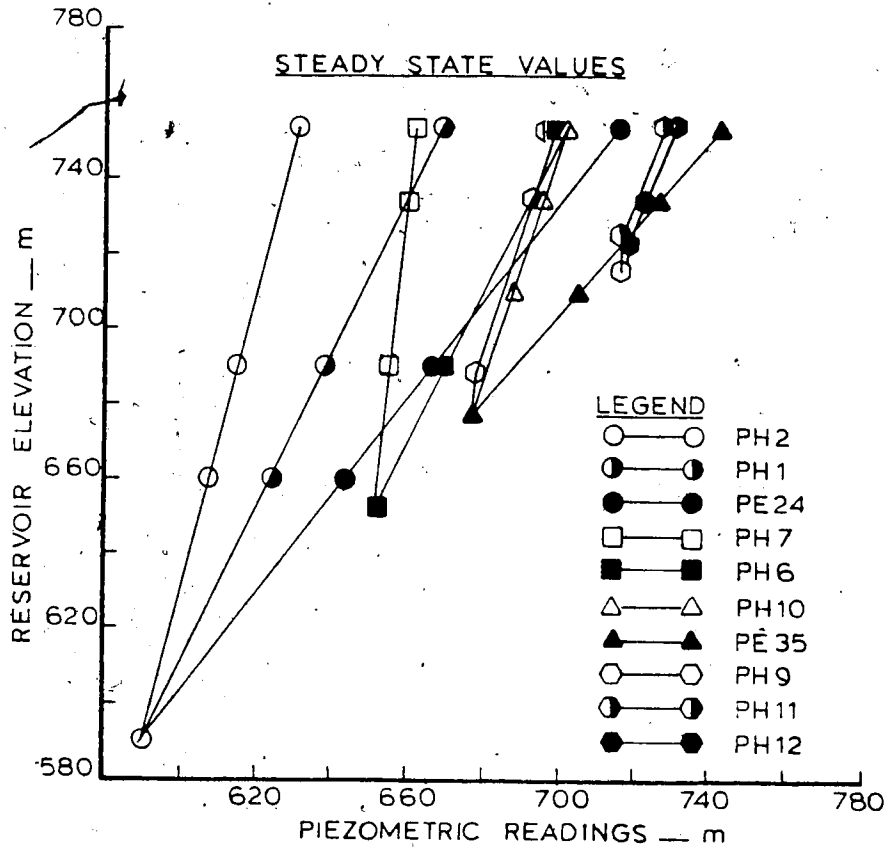


FIGURE 4.8 Calculated Steady State Piezometer Readings

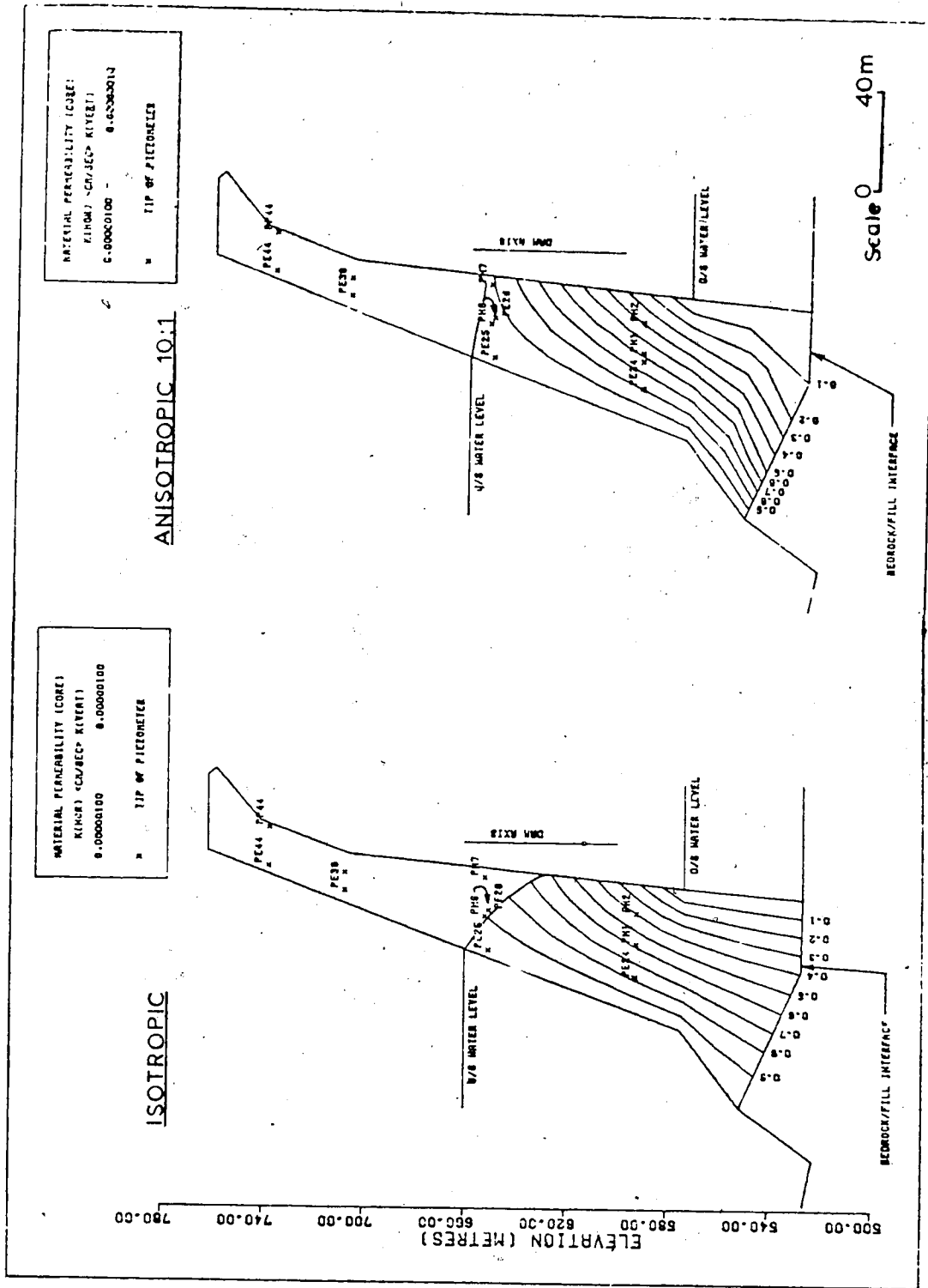


FIGURE 4.9 Effect of Material Anisotropy. Section 22+50

pronounced but remains quite local in the area of the material change. However, for lower reservoir levels (660 m) the alteration in pore pressure distribution is more severe but still only locally. The net result is that the piezometric readings above elevation 590 m do not exhibit any noticeable change in readings due to this non-homogeneity. The results are shown on Fig.4.10.

The final boundary condition investigated was concerned with the foundation bedrock seepage. A simple model was chosen with reservoir level at 660 m. Isotropy was assumed. Three material types were chosen:

1. core material: $k = 10^{-6}$ cm/sec.
2. Bedrock : $k = 10^{-3}$ cm/sec.
3. Grouted section : $k = 10^{-4}$ cm/sec.

This model assumes the grout curtain to be efficient but the bedrock below to be of high permeability.

The results, Fig.4.11 compared to Fig.4.7, indicate a local change in potential distribution around the base of the core, close to the grouted section. No effect is felt at higher elevations in the core. Although this model is very crude and the behaviour is not closely reflected by the foundation piezometers it was felt that since this underseepage has only a localized effect on the core pore pressure distribution, it was not worthwhile refining the model. The results are compared with the piezometric readings in Figs.4.12.

The conclusion from this parametric study is that none

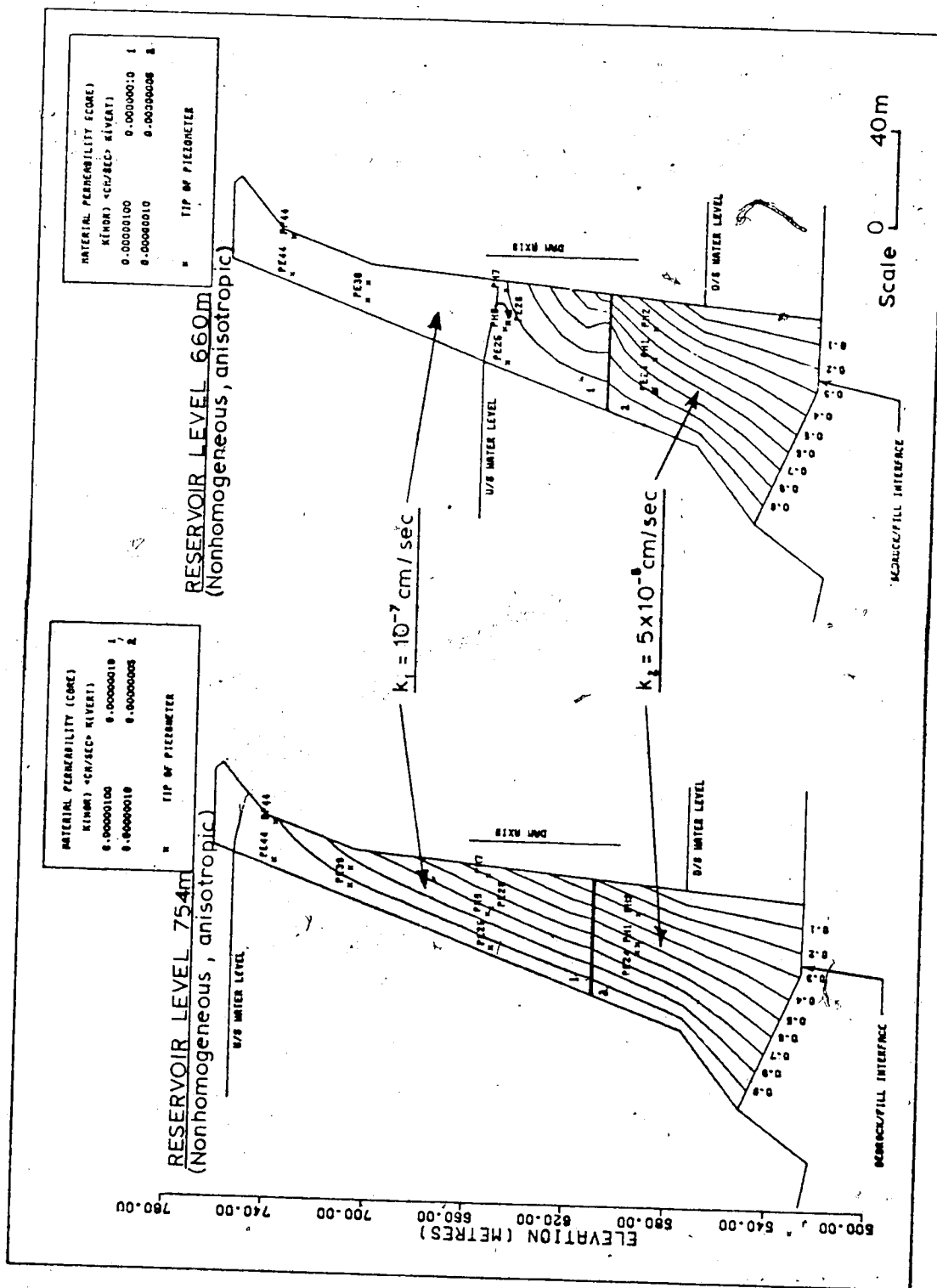


FIGURE 4.10 Effect of Material Non-Homogeneity Section 22+50

SECTION 22+50

SECTION 22+50
(UNDERSEPAGE)

MATERIAL PERMEABILITY (CODE)		TYP
K(HOR) -CM/SEC	K(VERT) -CM/SEC	
0.0000100	0.0000100	1.
0.00100000	0.00100000	4.
0.00010000	0.00010000	5.

* TIP OF PIETOMETER

MATERIAL PERMEABILITY (CODE)		TYP
K(HOR) -CM/SEC	K(VERT) -CM/SEC	
0.0000100	0.0000100	1.
0.00100000	0.00100000	2.
0.00001000	0.00001000	9.

* TIP OF PIETOMETER

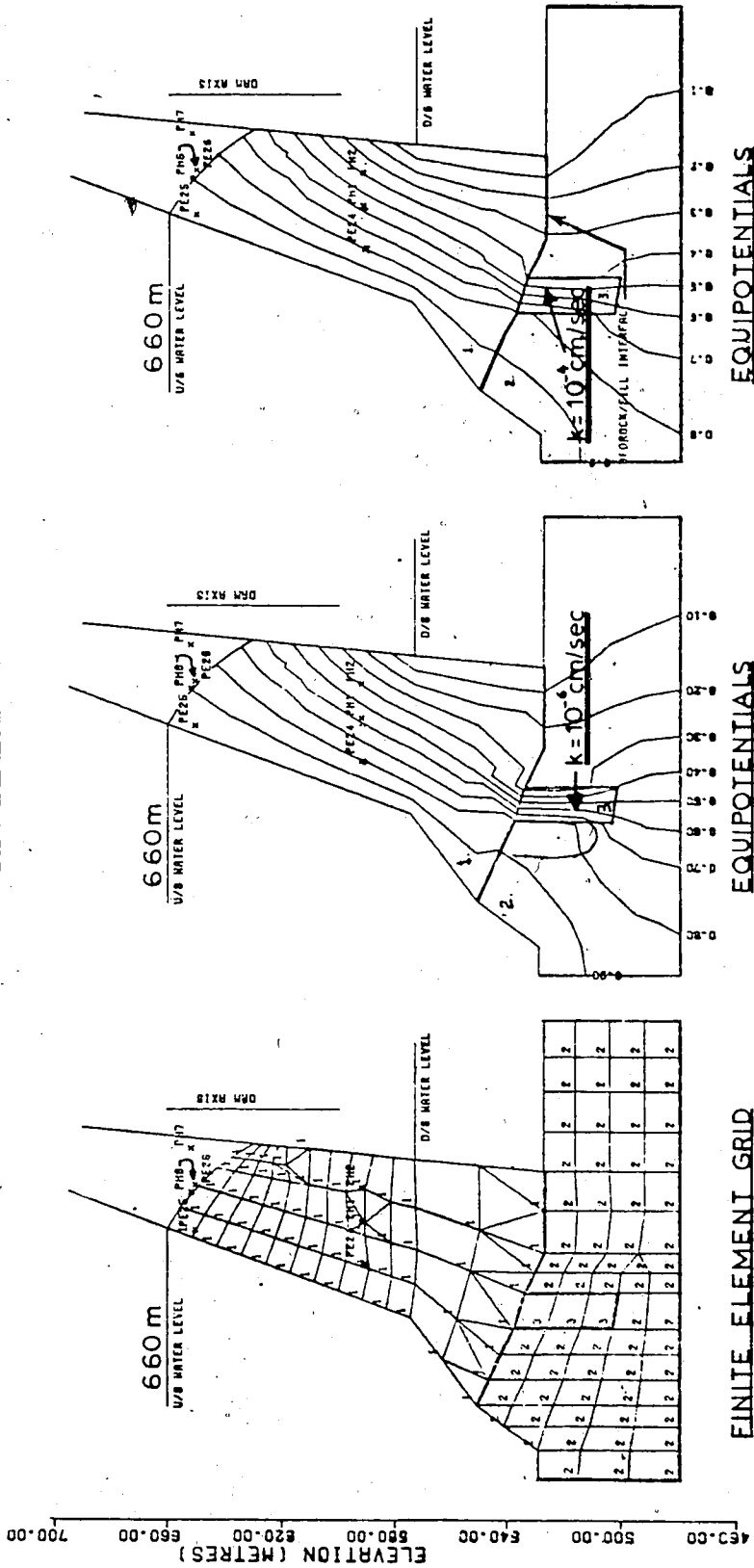
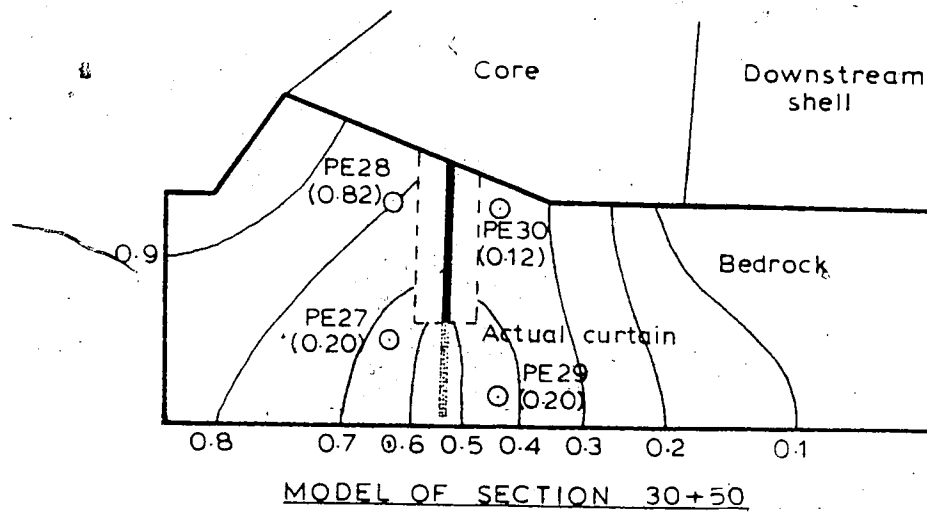
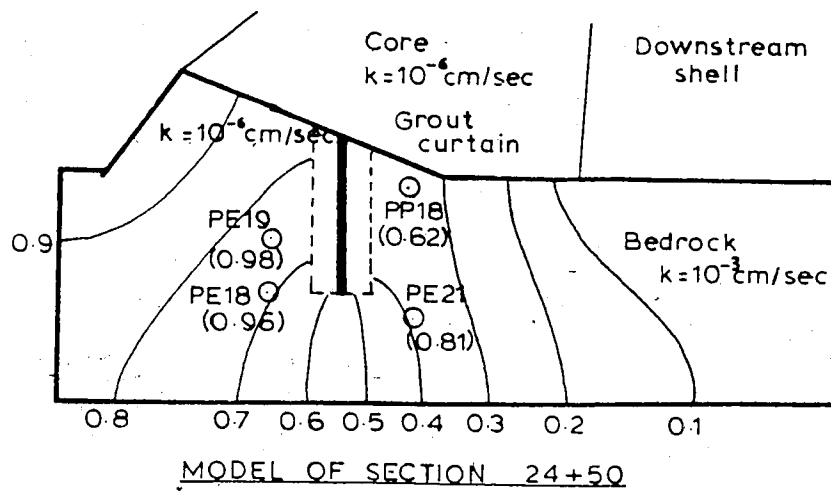


FIGURE 4.11 Results from Bedrock Seepage Model

Notes

Scale: 0 40m

1. Reservoir elevation 660m for model.
2. Downstream water level 573m for model.
3. All piezometers referred to grout curtain as origin.
4. Figures in brackets () are measured potentials.
5. Measured potentials are for a reservoir level at 732m.

FIGURE 4.12 Comparison of Bedrock Model and Piezometric Readings

of the conditions investigated change the pore pressure distribution within the core in a significant manner, with the exception of very local effects. The use of homogeneous isotropic material properties will be sufficiently accurate.

4.4.2 Section 24+50

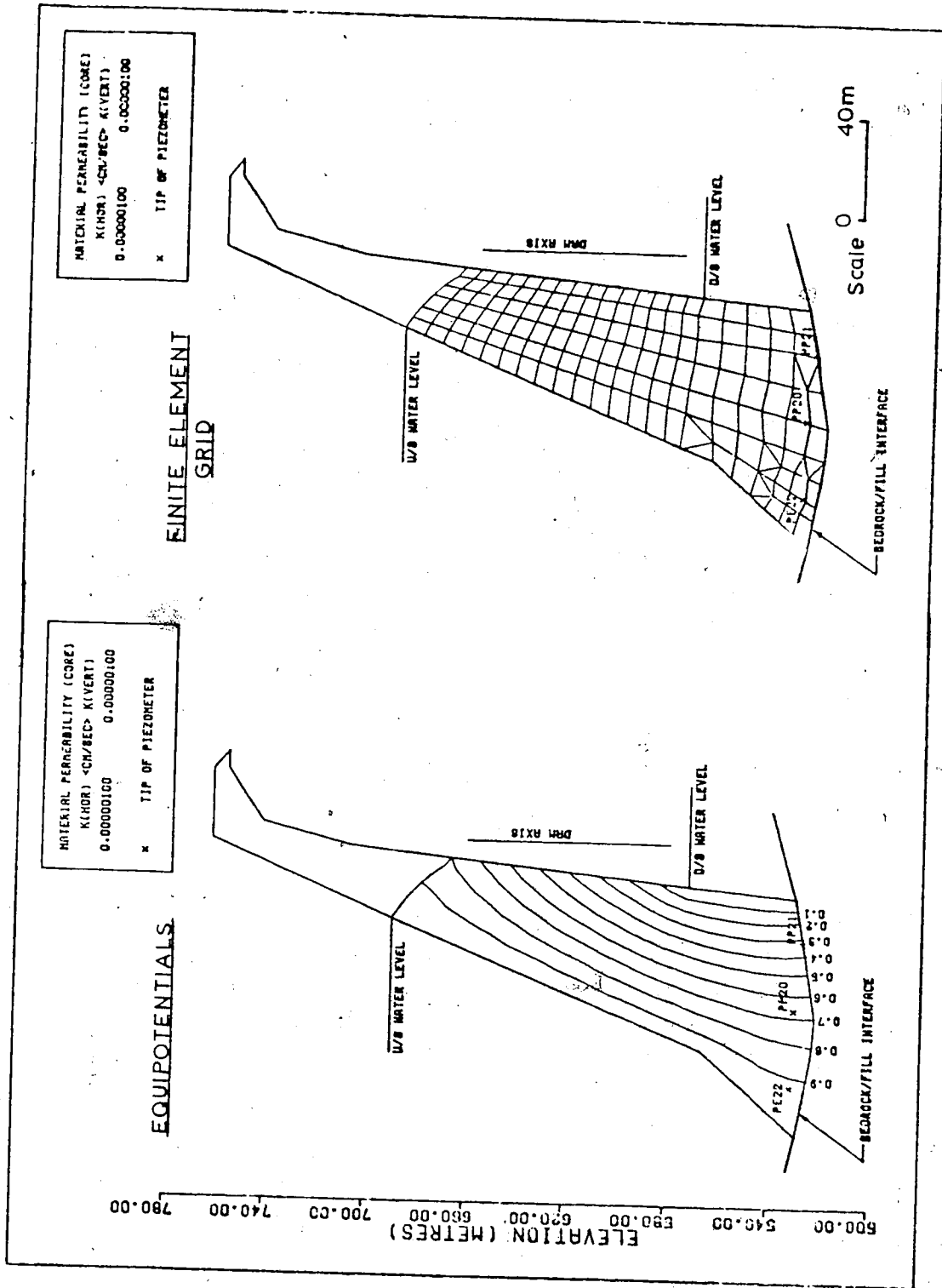
Very little analysis was done on this section because of the proximity of the piezometers to the bedrock, hence, the localized effects of underseepage became important. Results of an analysis are shown on Fig.4.13. But they are probably incorrect near the base of the core due to the uncertain boundary condition.

4.4.3 Section 16+50

This section was analyzed as a homogeneous isotropic section, for various reservoir levels. The section is entirely above elevation 610 m. So there is no abrupt change in core properties. The results are shown on Fig.4.14. And a plot of piezometric level versus elevation was made (Fig.4.8). An anisotropic core was analyzed to investigate the local effect on piezometer PH11. The result is shown in Fig.4.15. There is a moderate local disturbance, the piezometric level is raised by 1.8 m.

4.4.4 Section 30+50

A minimum number of cases were studied, due to the similarity between this section and Section 16+50. The



SECTION 24+50

FIGURE 4.13 Steady State Analysis. Section 24+50

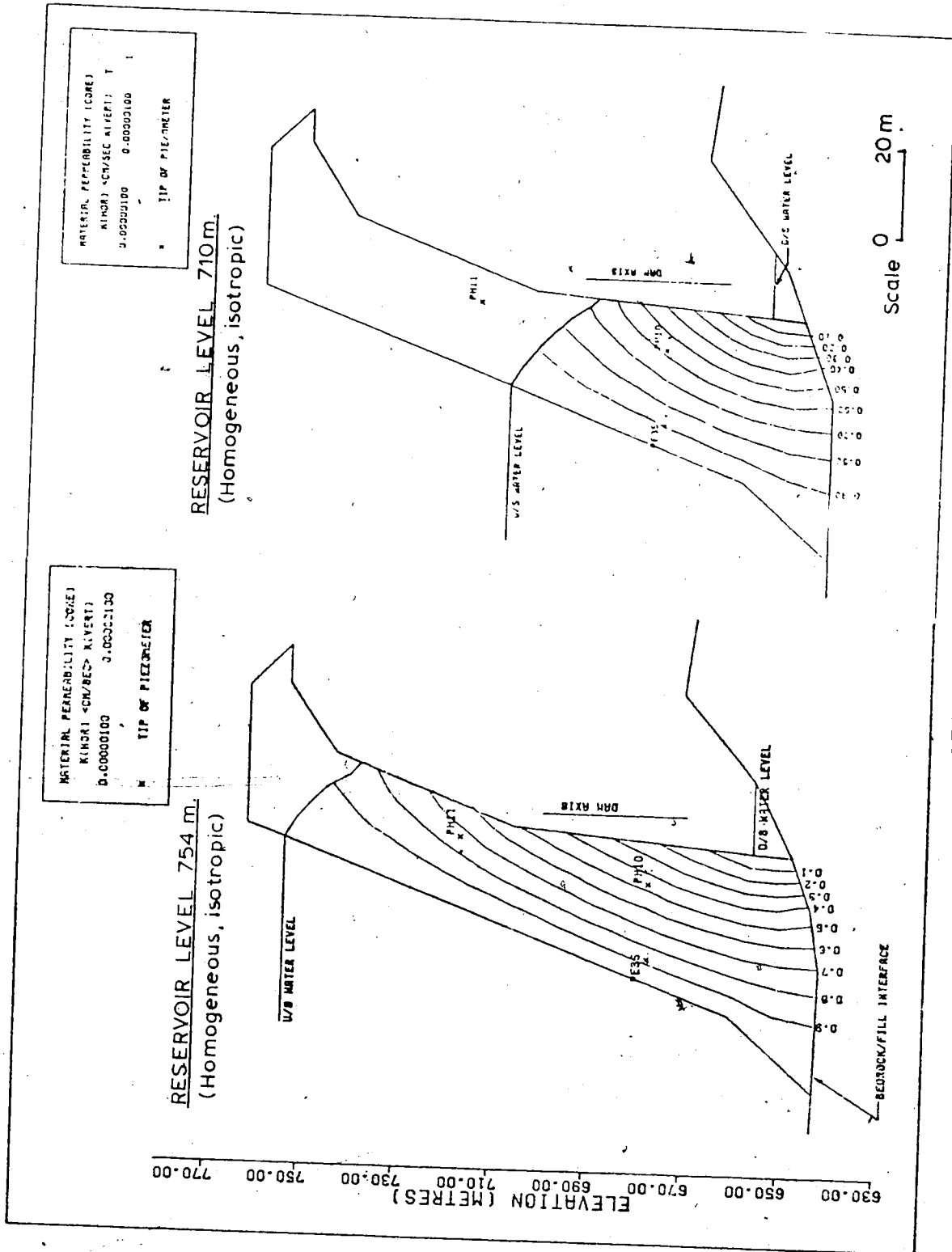
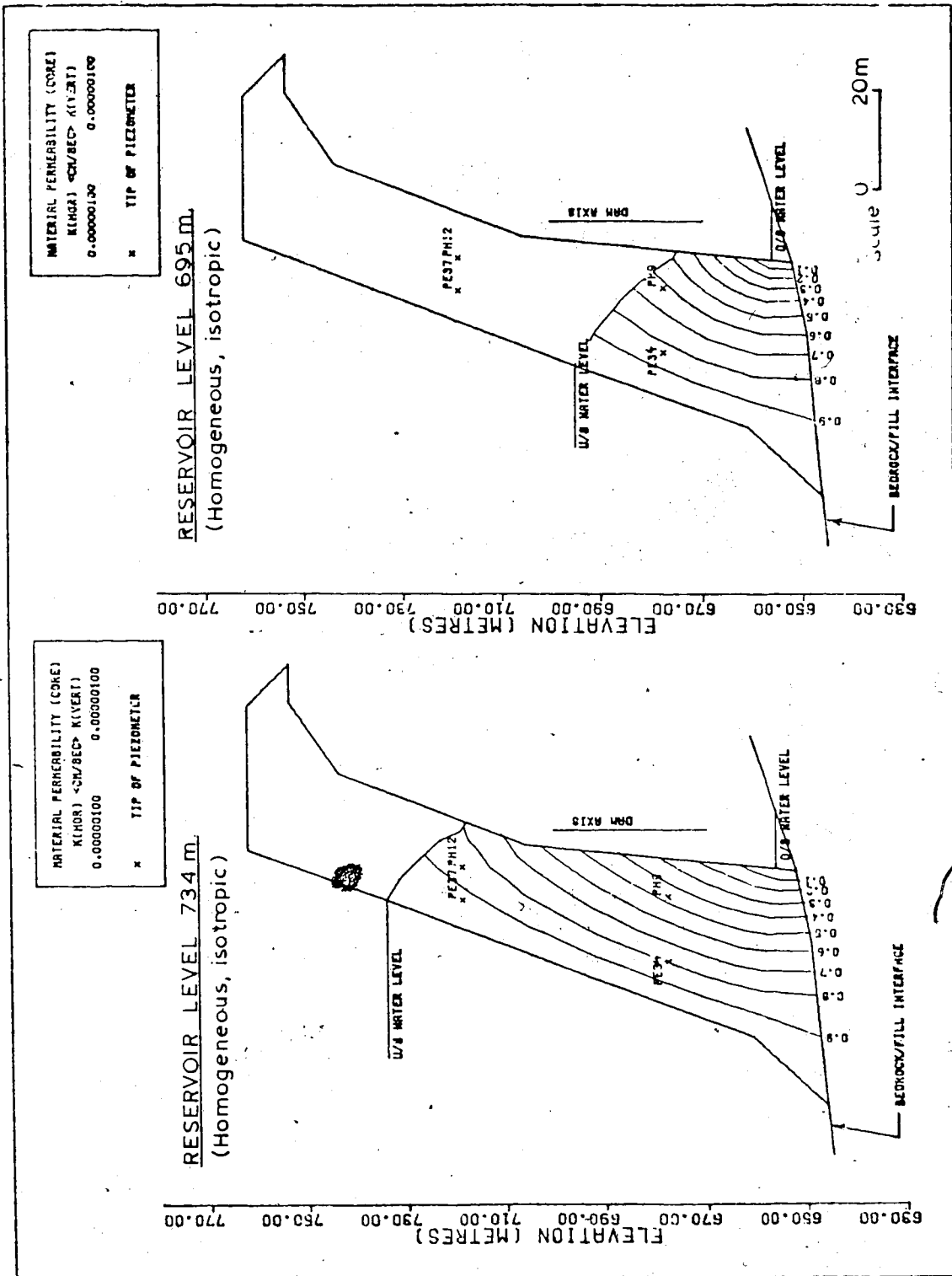


FIGURE 4.14 Steady State Analysis. Section 16+50

results and conclusions were very similar. Results are shown on Figs.4.16.

4.4.5 Conclusions

This analysis has enabled plots of reservoir level versus piezometer level to be drawn for the major instrumentation sections for steady state seepage conditions. Various effects such as anisotropy, non-homogeneity, underseepage were investigated and found only to have localized effects which although generally unimportant should not be ignored in certain cases, for example, when piezometers are located close to geometric boundaries with ill-defined boundary conditions. In order to increase the accuracy of the analysis it would be necessary to have many more specific details on such parameters as construction irregularities and anisotropy which are not readily available. However, it is considered that the results are well within an acceptable degree of accuracy and should, indeed, compare with actual piezometer readings when steady state conditions are reached in the core.



SECTION 30+50

FIGURE 4.16 Steady State Analysis. Section 30+50

CHAPTER V

COMPARISON OF OBSERVED AND PREDICTED PORE WATER PRESSURES

5.1 Introduction

The purpose of this chapter is to compare the actual pore pressure distribution with the theoretical steady state distribution at various times from reservoir filling (early 1973) to the end of 1978. This should indicate whether or not the pore pressure response due to filling and transient flow is converging on the expected steady state conditions.

A number of different methods of comparison were adopted, the purpose being to select the best method to visualize the pore pressure behaviour.

5.2 Comparison of Individual Sections

5.2.1 PE24...PH1

Plots of piezometer locations and of piezometric level versus time are shown on Figs.5.1 to 5.4. These figures include the theoretical steady state response of the piezometers. During transient seepage it would be expected that the actual readings would converge on the steady state readings.

Some trends are immediately apparent. PE24 is reading much below, and does not tend to converge on, the steady

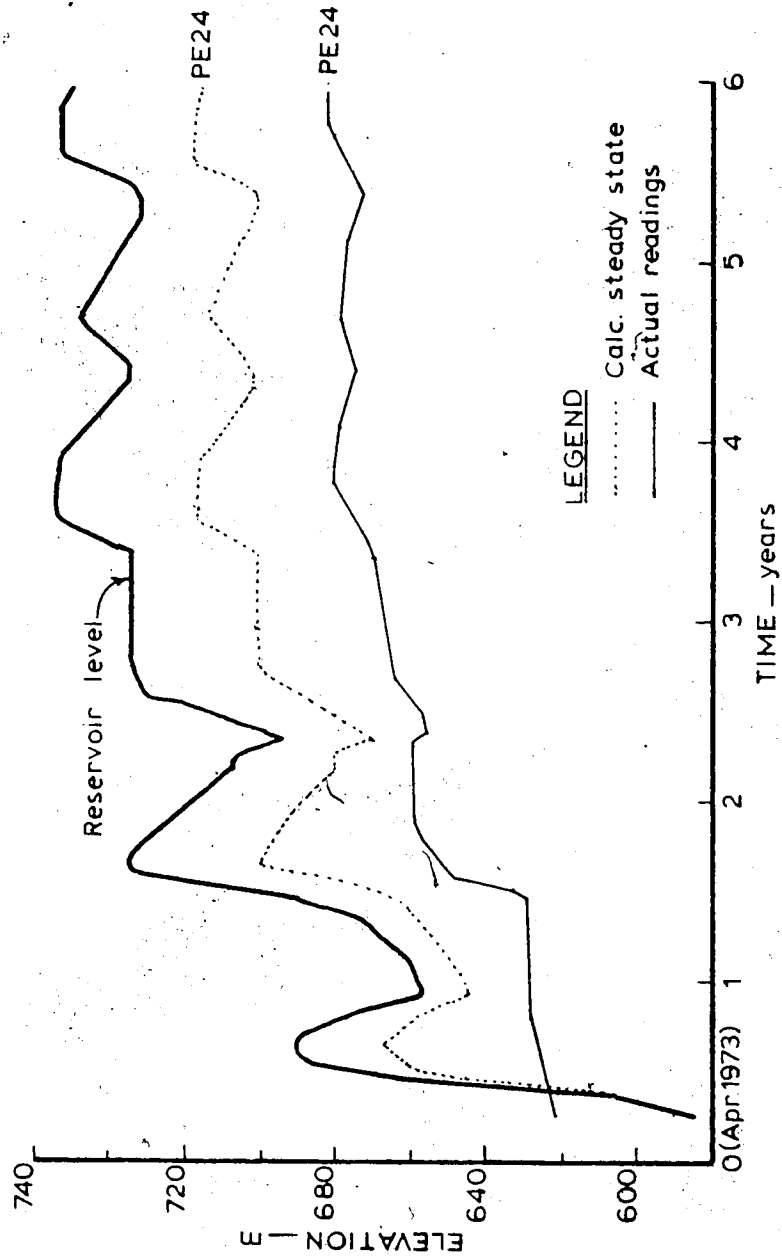


FIGURE 5.1 Piezometric Level (PE24) versus Time

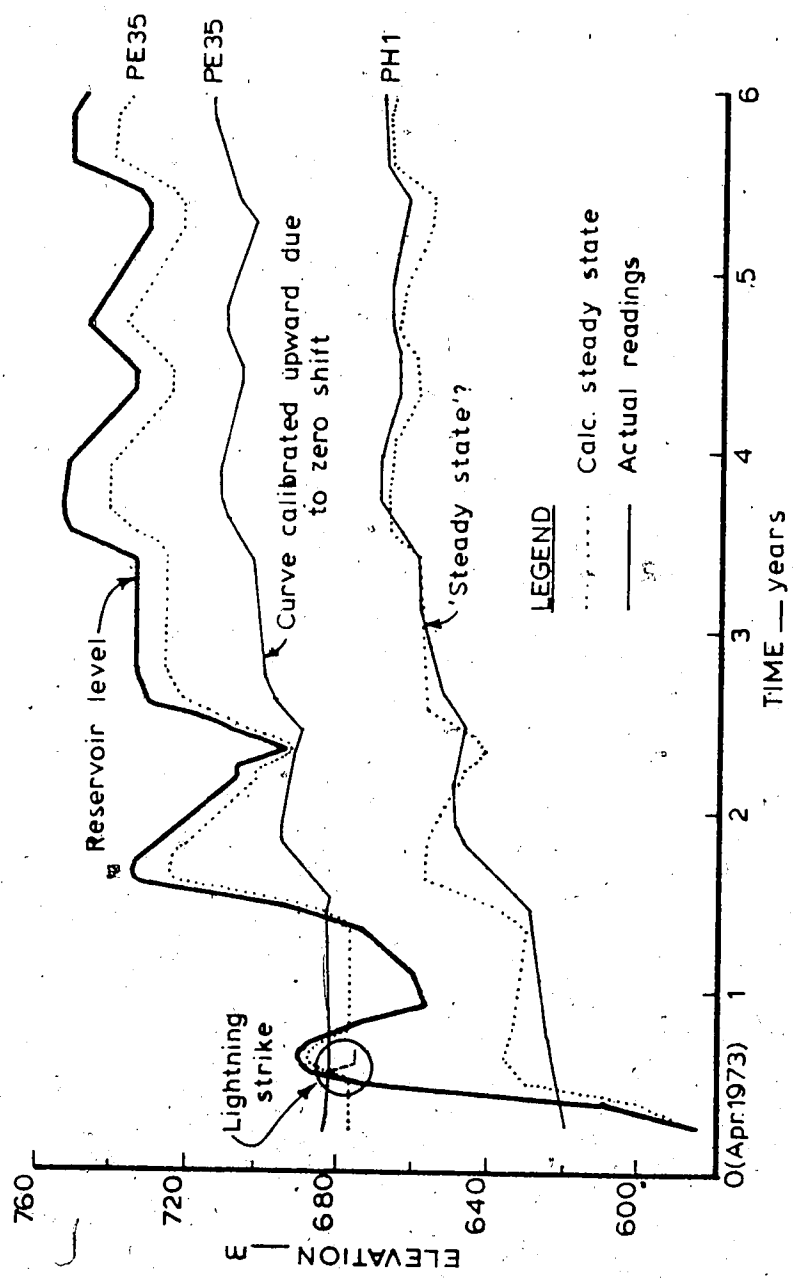


FIGURE 5.2 Piezometric Level (PH1, PE35) versus Time

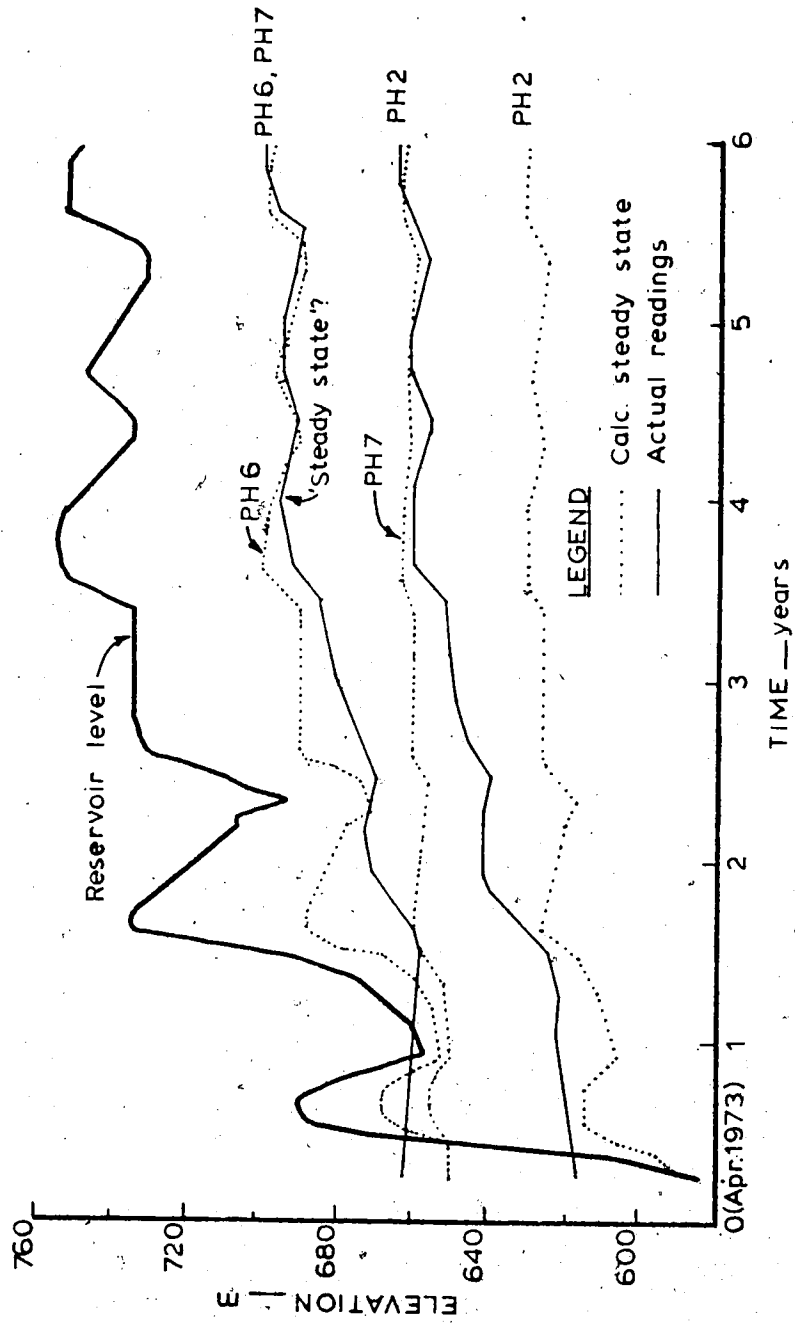


FIGURE 5.3 Piezometric Level (PH2, PH6, PH7) versus Time

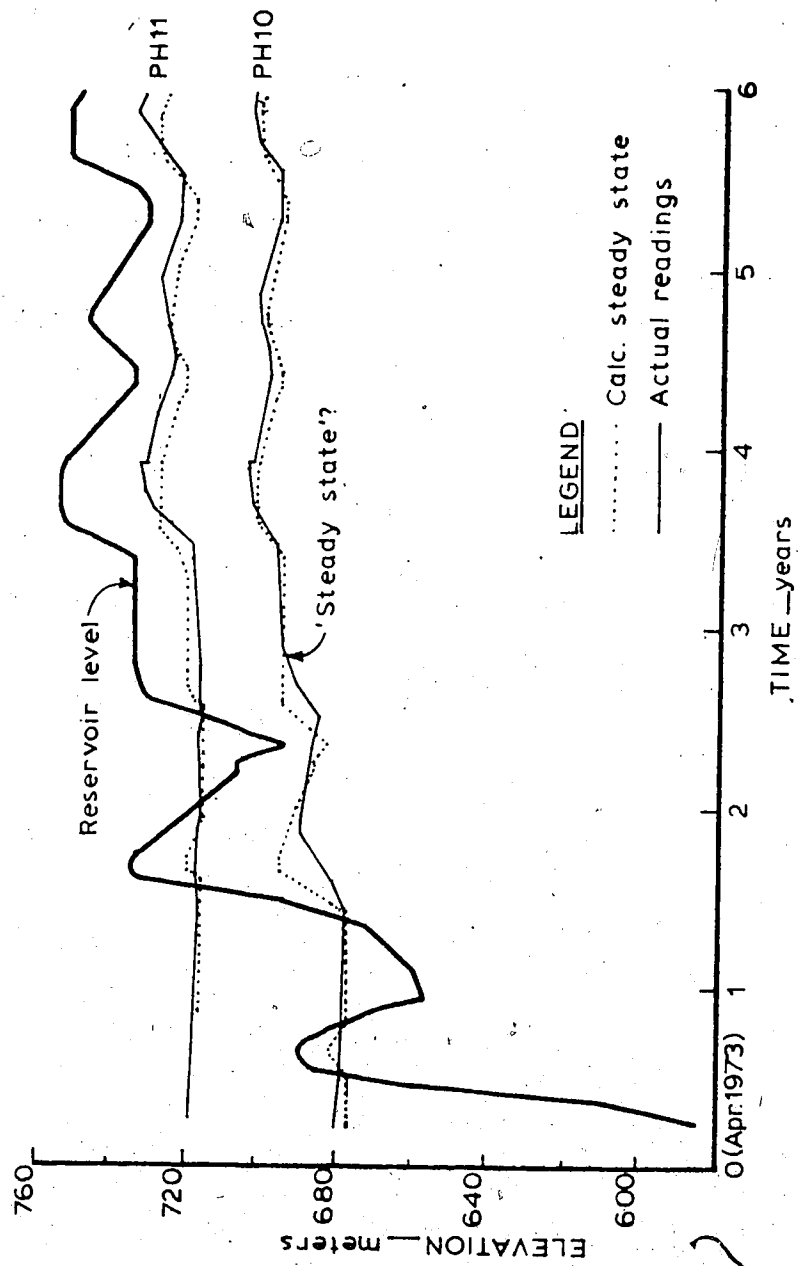


FIGURE 54 Piezometric Level (PH10, PH11) versus Time.

state condition throughout the 5 years shown. PH2 is reading very high at all times and does not converge on the lower steady state values. However, PH1 appears to be reading very close to the steady state conditions from early 1976 onwards. The actual readings are a little high (approx. 5 m) but this is only an error of 6%.

An interesting observation is that if the steady state line is shifted vertically it tends to match the actual conditions in a similar manner to PH1. PH1 suggests that steady state conditions have been reached by mid-1976 and that prior to this time there must be transient seepage. The time lag should be noted as the reservoir is raised to a peak, after the reservoir level drops again the piezometer continues to rise. This behaviour may be explained as transient seepage. Even though the reservoir level is dropping the steady state value for a particular piezometer may still be higher than the actual value, so the piezometer will continue to rise.

The large differences between calculated and observed values for PE24 and PH2 cannot be explained by anisotropy, non-homogeneity nor any other parameter already investigated. Figure 5.5 clearly shows the unusual pore pressure distribution at various time intervals.

5.2.2 PH6...PH7

Plots of piezometric level versus time are shown in Fig.5.3. The steady state case is superimposed on these

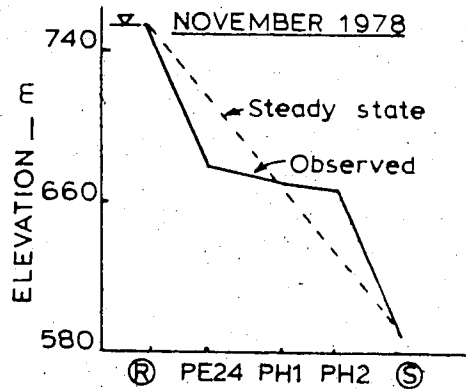
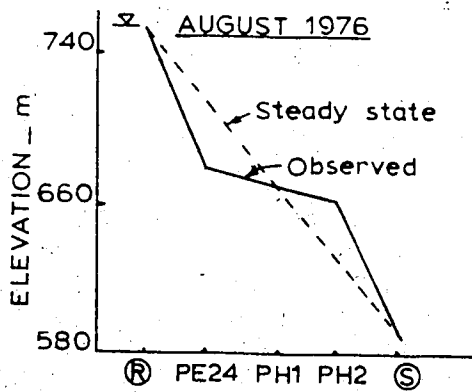
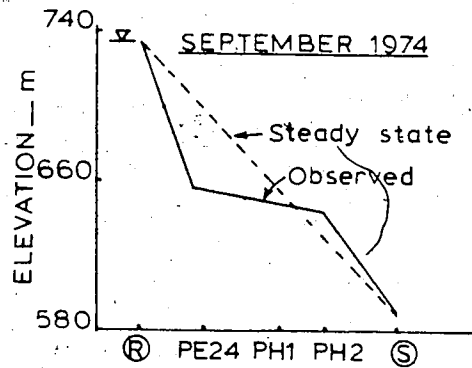
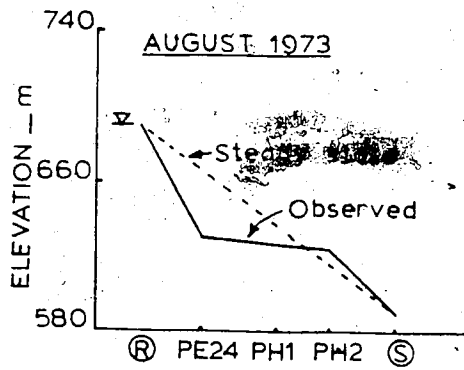
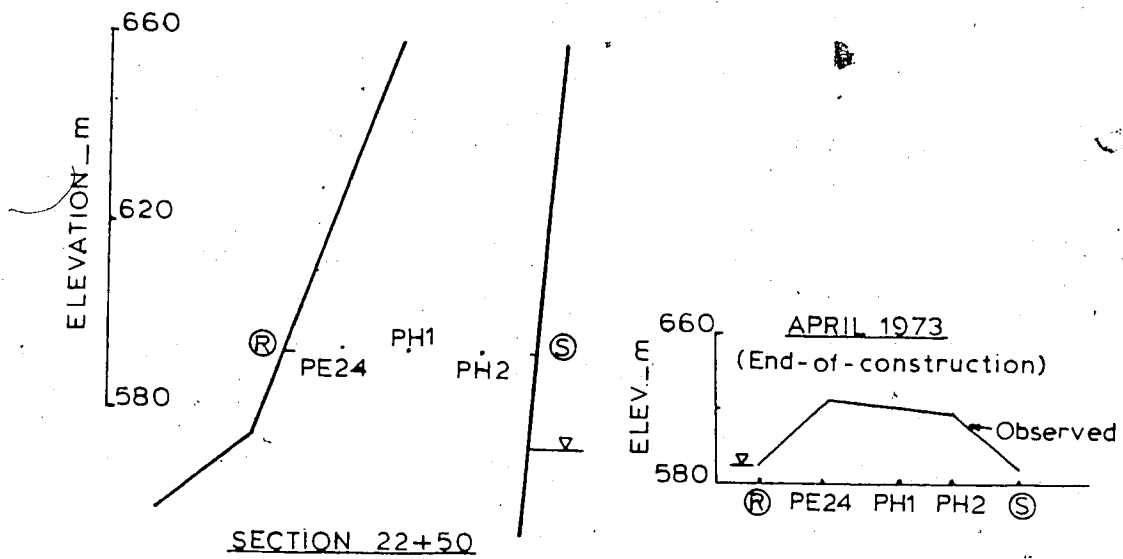


FIGURE 5.5 Pore Pressure Distribution (22+50) across Elev. 590.7 m with Time

figures. It has already been noted that either PH6 or PH7 must be incorrect. A comparison with the theoretical steady state core indicates that PH6 is in fact very close to steady state from 1977 onwards, whereas PH7 is actually reading above steady state. Once again if the steady state line is displaced vertically the behaviour is very similar in nature to PH6. PH6 again illustrates the time lag associated with transient seepage. As for PE24 and PH2 it is impossible to explain why PH7 is reading too high from the parameters previously studied.

5.2.3 PE35...PH10 and PH11

Plots of piezometric level versus time are shown on Figs.5.2 and 5.4. The steady state case is superimposed on these figures. It is apparent that PE35 is reading much lower (47 m) than the predicted steady state values, even though this unit has been recalibrated upwards to account for the zero shift discussed earlier. Both PH10 and PH11 appear to be reading too high by about 6 m and 9 m, respectively. PH10 and PH11 are both perhaps close enough to steady state conditions that the differences noted could be explained by a number of minor effects such as reading pore air pressure rather than pore water pressure as discussed earlier. However, there is no explanation for the behavior of PE35. Once again the piezometers on the downstream side of the core are reading high whereas the piezometers on the upstream side are very low.

Drawings were not prepared for the remaining piezometers. PH12 behaved in a manner very similar to PH11. The other piezometers such as PE38, PP36, PE44, PP44, PP45, PP46, PP47 were not compared because in the case of PE38...PP36 and PE44...PP44 the readings have already been noted as unreliable (Nussbaum 1976). The complicating factors for the piezometers at high elevations such as PP45...PP47 render their response difficult to analyze.

5.3 Conclusions

In an attempt to define a common trend for all the piezometers contour plots of pore pressure were made on a composite section for various reservoir levels. They indicate a definite pore pressure bulge on the downstream side of the core. Although it may not be as conclusive due to the lack of functioning or reliable piezometers on the upstream side, both PE24 and PE35 are considerably below the theoretical steady state value.

This unusual pore pressure distribution does not show any convergence on the theoretical steady state distribution over the 5 years observed to late 1978. However, some individual piezometers such as PH1 and PH6 appear to show that steady state has indeed been reached as early as 1976 and 1977. The other piezometers with a vertical "correction" also show this trend. The obvious disparity from the steady state values cannot be explained by any of the parameters previously studied in the parametric evaluation.

An alternative theory is obviously required to explain the observed pore pressure distribution. This is investigated further in Chapter 6.

CHAPTER VI

INVESTIGATION OF PORE PRESSURE ANOMALIES

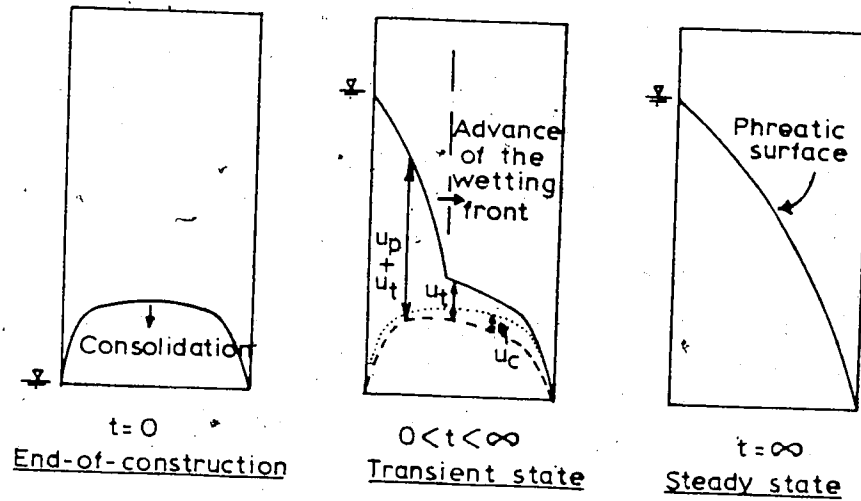
6.1 Introduction

Some observed pore pressures in the core are significantly different to the predicted steady state values. The intent of this chapter is to investigate these pore pressure anomalies in detail.

The pore pressures, upon reservoir impounding, are altered as a result of two processes, these are:

1. Total stress changes.
2. Transient seepage (which includes three sub-processes).
 - a. Consolidation and swelling (void ratio changes)
 - b. Fluid density changes
 - c. Changing degree of saturation

It is very difficult to distinguish between the processes because they may be occurring simultaneously within the core. However by studying the contribution of each process separately it is possible to evaluate the relative importance of each. Figure 6.1 shows schematically the processes occurring in a simple section.



Note

- u_t - Increase in pore pressure due to reservoir load
- u_p - Increase in pore pressure due to advance of wetting front
- u_c - Decrease in pore pressure due to consolidation

FIGURE 6.1 Schematic Diagram of Processes Occurring in core

6.2 Pore Pressures Resulting from Total Stress Changes.

The changes in total stress which are of concern in this section are those resulting from reservoir loading. As the reservoir is raised and lowered there are increments of total stress applied and removed from the core. There will be a reaction of the pore pressures to these increments of total stress. To determine these reactions it is necessary to calculate the magnitude of the stress changes at representative locations within the core. Then with these values and appropriate pore pressure parameters the pore pressure changes within the core for various reservoir increments may be calculated.

6.2.1 Model for Reservoir Filling

The proposed model assumes an impermeable upstream core face. This means that the reservoir load is applied directly to the upstream face of the core, and there is no interference of the pore pressure distribution due to transient seepage.

The reservoir filling does not impose a total stress increment on the core face equivalent to the hydrostatic pressure increment. The reason for this is that the upstream shell is only slightly saturated initially and so the reservoir impounding will cause complete saturation of the shell. The horizontal effective stress increment is related to the vertical effective stress increment by means of the coefficient of earth pressure, K . Hence a calculation of the

change in vertical total stress (due to the change in degree of saturation), coupled with the hydrostatic pore pressure and K will yield a horizontal total stress increment.

As shown in Figure 6.2 the applied horizontal load is approximately 60% of the hydrostatic load for this section. The order of magnitude of this result is substantiated by the field results reported for the Gepatsch dam in Austria (Schober 1967). The increment in vertical stress is calculated to be quite small, which concurs with Nobari and Duncan (1972).

The incremental load is then distributed across the section in proportion to the assumed shear stress distribution. So that on the downstream side of the core the increment of horizontal stress will be smaller than that on the upstream side. This too has been observed on the Gepatsch Dam. By assuming a shear stress distribution it was possible to calculate the horizontal and vertical stress increments at some points across the core. Using these values and an assumed original stress distribution obtained from Simmons (1974) and Law (1975) it was possible to draw the Mohr circles and stress paths followed during reservoir loading. This in turn provides the increments in principal stresses $\Delta\sigma_1$ and $\Delta\sigma_3$ which may be used to determine the pore pressure changes, using Skempton's (1954) equation. The Mohr circles and stress paths are shown on Fig.6.3. and Fig.6.4. An initial assumption was that the major principal stress was vertical.

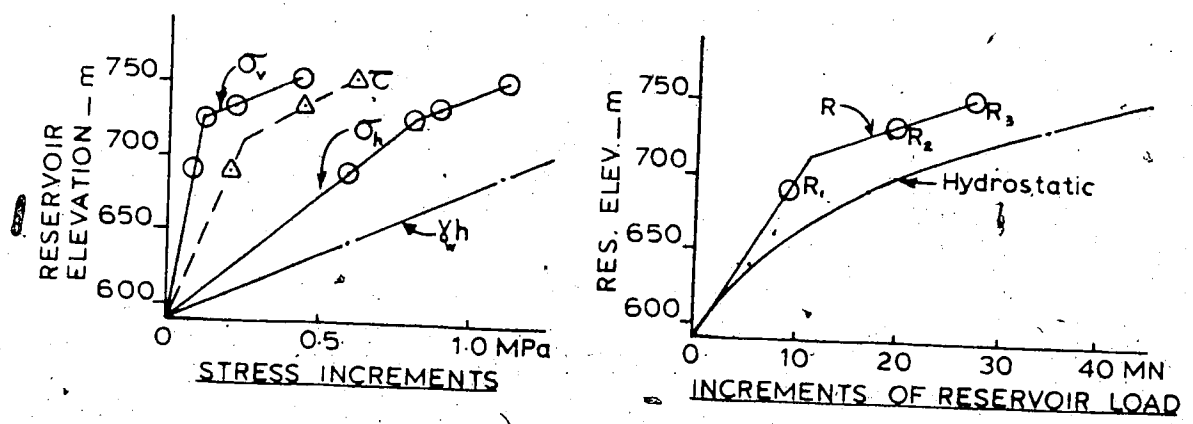
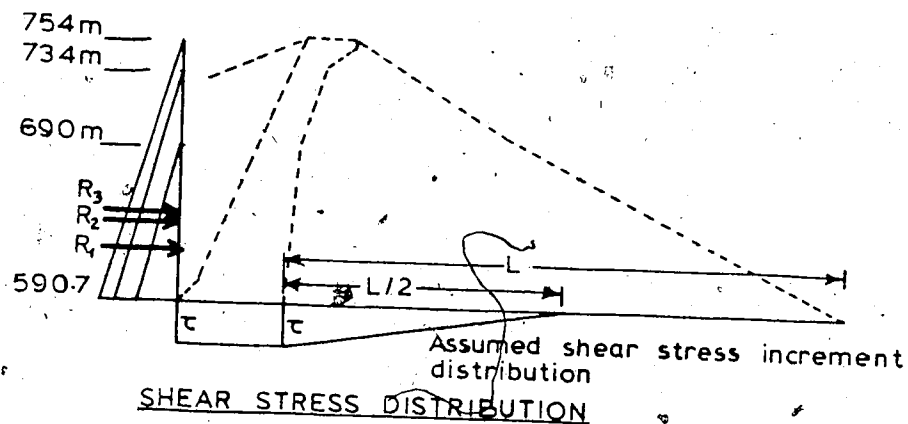
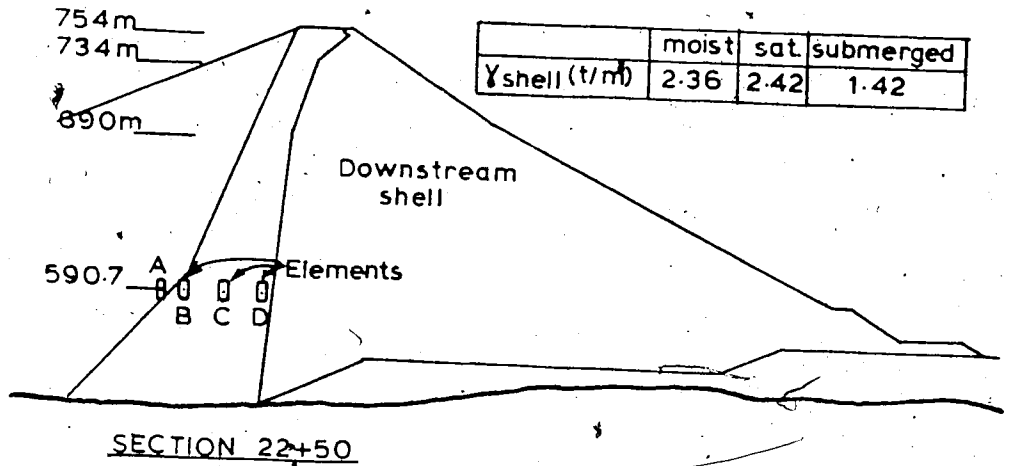


FIGURE 6.2 Reservoir Loading Model and Results

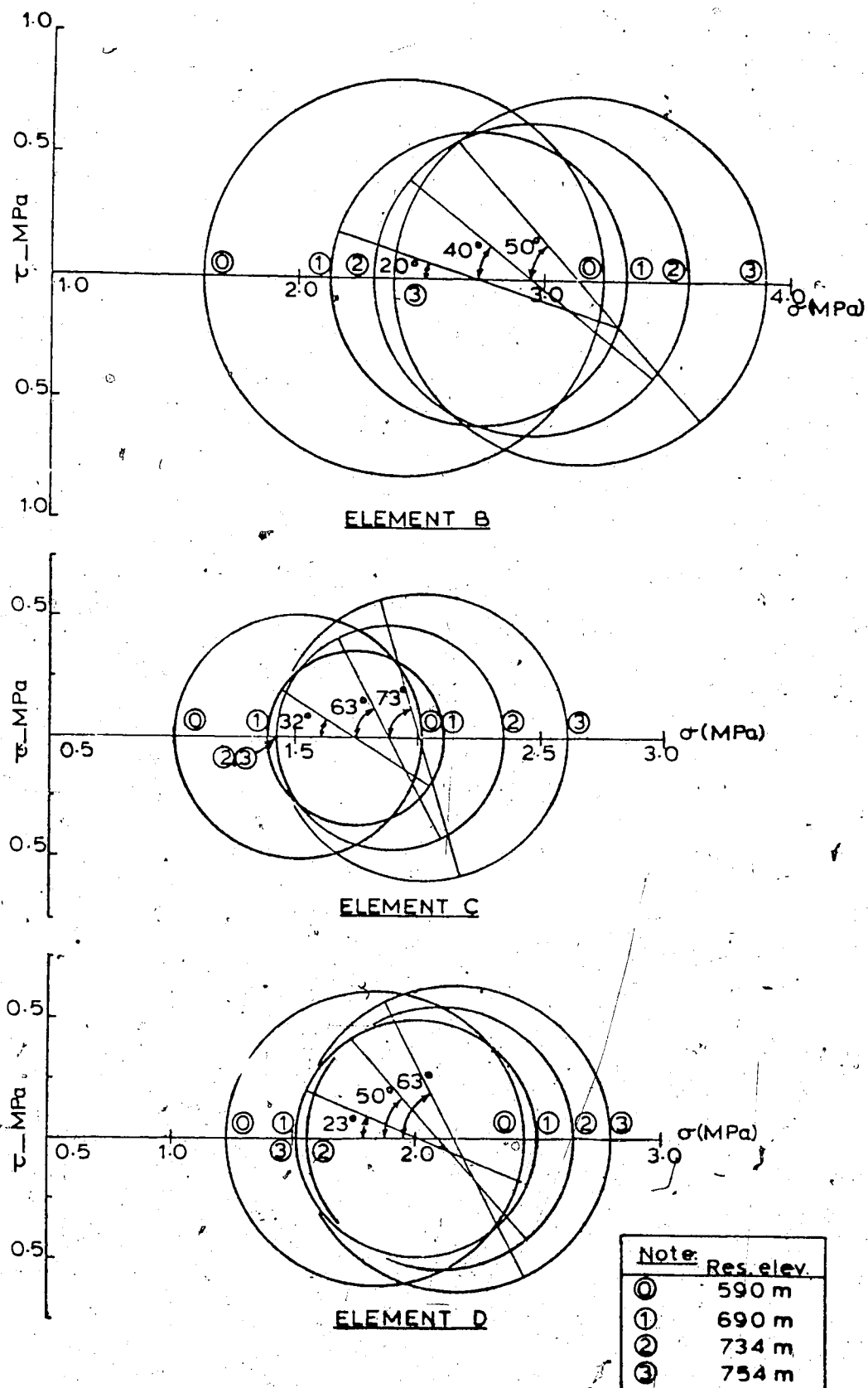
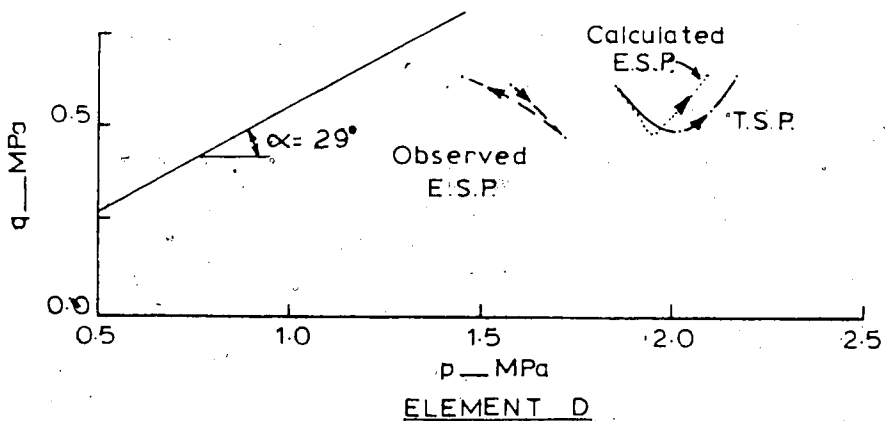
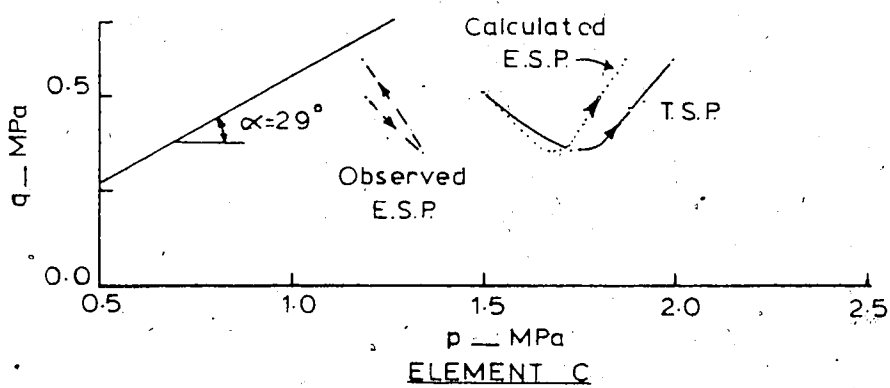
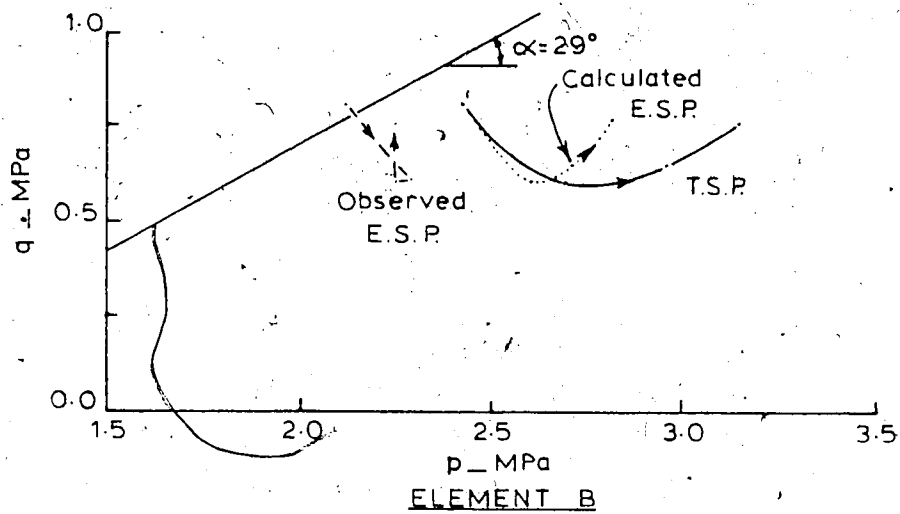


FIGURE 6.3 Mohr Circles for Elements B, C and D



- NOTES: — T.S.P. — Total stress path
 — E.S.P. — Effective stress path
 — The calculated E.S.P. assumes zero excess construction pore water pressure

FIGURE 6.4 Stress Paths

The principal stress increments calculated for this section at elevation 590.7 m are of the same order of magnitude as those calculated for the Oroville Dam by Nobari and Duncan (1972) and as those observed in the Gépatsch dam by Schober (1970). So it is felt that this model provides a reasonable indication of the principal stress increments, and rotation of the principal stresses. A much more refined analysis could be made in a similar manner to that of Nobari and Duncan (1972), taking into account the change in stress-strain characteristics of the upstream shell on wetting and so on. But the pore pressure increments are dependent on the pore pressure parameters, and without more accurate pore pressure parameters, the refined stress increments would be largely wasted effort.

6.2.2 Pore Pressure Parameters

The total stress increments have been calculated due to the reservoir loading. In order to predict pore pressure changes due to these stress increments it is necessary to use a relationship of the form suggested by Bishop (1954), Skempton (1954), Henkel (1960).

Bishop (1954) suggested the use of the parameter B , where

$$\bar{B} = B \left[1 - (1-A) \left(1 - \frac{\Delta\sigma_3}{\Delta\sigma_1} \right) \right]$$

... 6.1

A, B are Skempton's pore pressure parameters.

$\Delta\sigma_3$ is the minor total principal stress increment.

$\Delta\sigma_1$ is the major total principal stress increment.

Then the basic pore pressure equation becomes:

$$\Delta u = \bar{B} \cdot \Delta\sigma_1$$

... 6.2

Δu is the pore pressure increment.

$\Delta\sigma_1$ is the major total principal stress increment.

\bar{B} is the pore pressure parameter.

The advantage of using this parameter \bar{B} is that the pore pressure can be expressed as a direct function of the major principal stress increment. Unfortunately, \bar{B} is a function of the total principal stress increment ratio, in cases where this ratio changes significantly the \bar{B} concept holds no advantage over Skempton's (1954) equation.

The equation suggested by Skempton takes the form:

$$\Delta u = B [\Delta\sigma_3 + A(\Delta\sigma_1 - \Delta\sigma_3)]$$

... 6.3

The pore pressure parameters are determined experimentally, however A is stress dependent and B is a function of the degree of saturation of the soil. This equation makes no allowance for the intermediate principal stress because it has been derived for the special case of the triaxial test where $\sigma_2 = \sigma_3$.

In 1960, Henkel proposed a similar but more general expression, with different experimentally derived pore pressure parameters. Henkel's equation takes the form:

$$\Delta u = \alpha \frac{(\Delta\sigma_1 + \Delta\sigma_2 + \Delta\sigma_3)}{3} + \beta \sqrt{(\Delta\sigma_1 - \Delta\sigma_2)^2 + (\Delta\sigma_2 - \Delta\sigma_3)^2 + (\Delta\sigma_3 - \Delta\sigma_1)^2} \dots 6.4$$

where α is the pore pressure parameter related to the octahedral normal stress increment and β is the parameter related to the incremental octahedral shear stress.

This equation is more suitable than Skempton's (1954) equation in that it better defines the soil behaviour. Particularly for the complicated stress paths followed in a dam core. To use this equation it is necessary to make an assumption about σ_2 . This may be done by assuming plane strain. A value for β is required. β may be evaluated from A obtained from triaxial testing. The major advantage of this approach is that β is not stress path dependent. The α value at high stress levels may not be unity. The value of Poisson's ratio used was 0.35 (Law 1976). The pore

pressure increments calculated by this method are compared to the values calculated using Skempton's equation. A problem arises in the use of Skempton's equation for loading cases other than the standard triaxial compression test. Skempton (1961) discussed the case of extension loading and introduced an absolute value of total principal stress difference; however, an ambiguity still exists in the definition of principal stress increments, especially in the particular case where there is rotation of the principal stresses.

Law and Holtz (1978) suggest an approach to deal with this ambiguity and their approach has been adopted for this analysis. In effect, they redefine $\Delta\sigma_1$ and $\Delta\sigma_3$ as the algebraic maximum principal stress increment and minimum principal stress increment respectively, and the increments have no specific relationship with the principal stresses. This involves a slight redefinition of the A parameter depending on the specific triaxial test under consideration. They note that the A value for an extension test is approximately double that for a compression test, if the material is behaving approximately elastically. They suggest that this system removes the ambiguities which develop when the principal stresses rotate. However, since they give no specific example of this phenomenon their interpretation may need further definition.

The rotation of the principal stresses may be equivalent to an increase in A as reported by Broms and

Casbarian (1965); however, without further evidence and test results for a compacted till this effect is ignored as insignificant due to the very low A values observed during standard testing.

It is necessary to ascertain a value for A . Insley and Hillis (1965) published the results from an extensive series of high pressure triaxial tests carried out on the Mica till. These were undrained axial compression tests. They show a plot of the \bar{A}_f parameter versus σ_3 , where \bar{A} equals AxB (Bishop and Henkel, 1962). This is not what was required, since the core will not even be close to failure during reservoir loading. So some A values were backcalculated from the published data at specific confining pressures. The results are shown on Fig. 6.5. They indicate low but positive values of A at the strains estimated in the core. It would be expected that the A value should be close to 0.5 if the soil is behaving elastically in plane strain. The low observed values are probably a result of incomplete saturation in the samples tested. Some results from a compacted moraine material reported by Bishop and Henkel (1962) indicate a negative \bar{A}_f of the order -0.1. In other words the A_f values reported by Insley and Hillis (1965) for the Mica till are higher than expected and they attribute this behaviour to the rather higher than normal confining pressures.

The A values to be used in this analysis vary between 0.04 and 0.08 for axial compression loading and double these

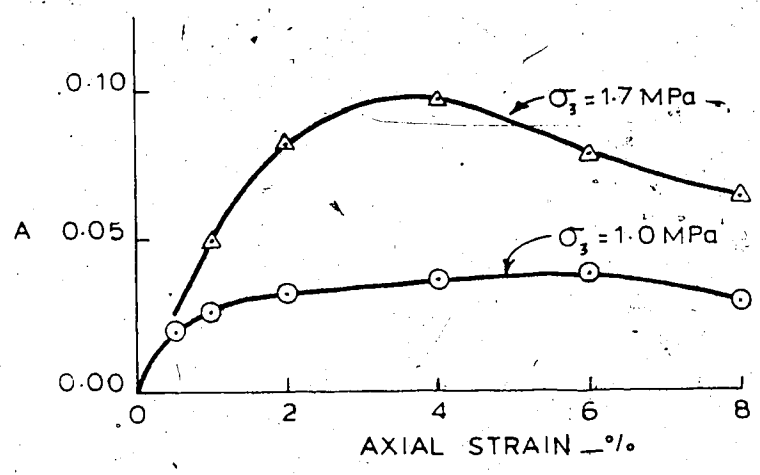
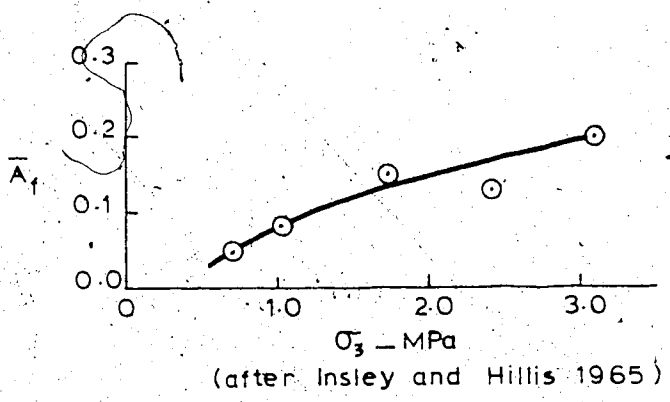


FIGURE 6.5 "A" Values for Mica Till

values for lateral compression values, depending on stress levels at the element being analyzed.

The B parameter is a function of degree of saturation. The degree of saturation of the core at the end-of-construction has been estimated (Section 6.2.3) to be approximately 93% at elevation 590 m. This results in a B value of approximately 0.7 (Lambe and Whitman, 1969 - Boulder clay). This value may be slightly in error, but it will not introduce a significant error. As a simplification, it was assumed that the B value will increase to 0.9 during reservoir filling. This value may be a little high (Lee et al. 1969) however the results are not very sensitive to this variation.

6.2.3 Degree of saturation of core

The degree of saturation of the core till at the time of placement can be calculated knowing the specific gravity, dry density and bulk density. In this manner an average degree of saturation was evaluated for both the lower (below elevation 610 m) and upper zone of the core. Some typical properties are tabulated below:

Property	Unit	1969 Fill	1970-1971 Fill
γ_d	Mg/m ³	2.10	2.27
w.c.	%	8.8	6.3
γ_t	Mg/m ³	2.29	2.41
G _s		2.8	2.8
Sr	%	74	74.5

n

0.250

0.190

The specific gravity of the Mica till was reported as 2.80 (Law 1975). This value appeared high so some specific gravity tests were carried out which confirmed the high values. The degree of saturation will increase with the addition of fill. With some simplifying assumptions it is possible to backcalculate the changing degree of saturation as construction proceeds, using the measured increases in pore pressure. The method is based on that of Hilf (1948) or Bishop (1957).

Calculations for PE24 and PH6 indicate a final degree of saturation in the lower core, before reservoir filling commences, of 94 %.

These values show that the pore pressure parameter B will certainly not be unity. Lambe and Whitman (1969) indicate a value for B at 93 % saturation, for a boulder clay. This value is considered to be reasonably representative for the Mica till.

The increase in pore pressure is caused by a volume change, which is initiated by the increase in total stresses on the unsaturated fill. The high compressibility of the air governs the volume change and the diffusion of the air into the pore water due to the increase in pore pressure. The laws which govern this behaviour are Boyles Law and Henry's Law of Solubility. The volume changes calculated due to the changes in effective stress should be compatible with the volume change calculated by the method outlined above.

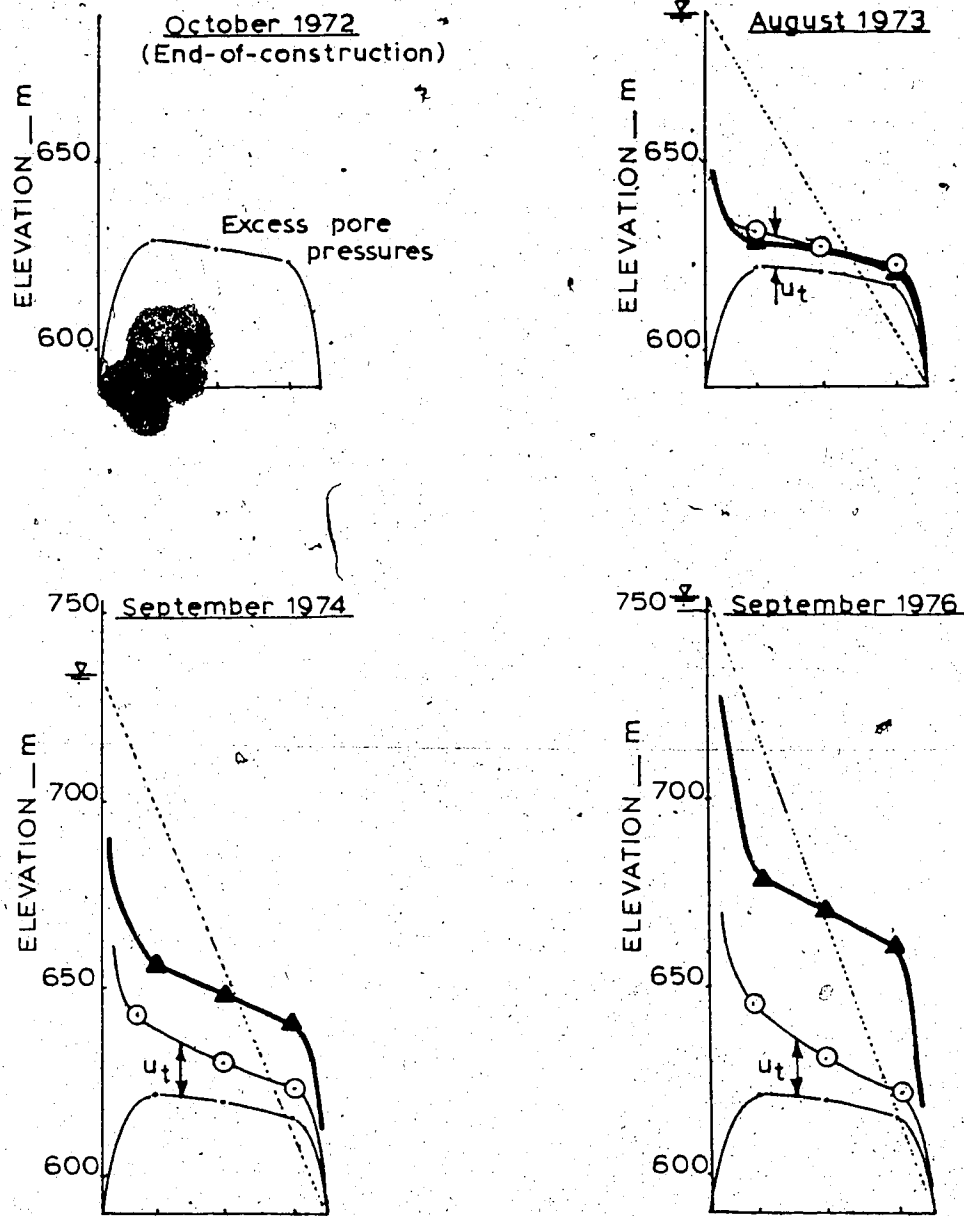
6.2.4 Calculation of pore pressure increments

The principal stress increments have been calculated for various stages of reservoir filling. It was decided to use Skempton (1954) pore pressure equation to evaluate the pore pressure increments. Values for A and B have been assumed. Therefore using the equation:

$$\Delta u = B [\Delta \sigma_3 + A (\Delta \sigma_1 - \Delta \sigma_3)] \quad \dots 6.5$$

the pore pressures may be calculated. As discussed in Section 6.2.2 the approach suggested by Law and Holtz (1978) is adopted here, for determining the maximum and minimum principal stress increments.

The results of this analysis are shown on Figure 6.6. The A value has been altered with each reservoir stage. Some allowance has therefore been made for stress level effects on A, that is, the reduction of stresses in the central core due to arching. The alteration in the A value depending on the stress path has been mentioned previously and this factor is also taken into account. During the early loading the stress path is similar to that of an ordinary triaxial extension (lateral compression) test and later this changes to that of a triaxial compression (axial compression) test. Which is why the A value has been reduced for the second and third loading stages. The final factor is that the A value



ALL SECTIONS THROUGH CORE (22+50) AT ELEV. 590-7 m

LEGEND

- Steady state (calc)
- ▲—▲ Observed distribution
- Pore press. due to total stress increments
- End-of-construction pore pressures
- u_t Increment in pore press. due to reservoir load

FIGURE 6.6 Results of Total Stress Analysis

is dependent on the mobilized strength of the element, and this factor has also been estimated. A combination of these factors result in the selected values for A between 0.05 and 0.10.

The B value has simply been assumed to increase with the increasing loading. This may be an over-simplification and the final value of 0.9 is probably too high, however it has little effect on the results.

6.2.5 Suitability of adopted procedure.

It is possible that doubt may be expressed over the approach taken by Law and Holtz (1978). The deviation from the standard approach only occurs during the first loading stage. The pore pressure increments calculated from this stage were compared with the measured pore pressure increments calculated from Henkel's (1960) equation. These are tabulated below:

Element	Res. Incr.	Henkel(1960)	Skempton(1954)
		Δu -m.	Δu -m.
B	1	8.5	9.8
	2	12.0	14.3
	3	9.3	8.8
	Total	29.8	32.9
C	1	6.6	7.1
	2	4.4	3.2
	3	3.8	1.1
	Total	14.8	11.4

D	1	4.4	6.6
	2	3.9	6.6
	3	-0.2	-2.5
	Total	8.1	7.7

The comparison is excellent considering the assumptions used in the analysis. This appears to confirm that Skempton's (1954) equation may be used provided care is taken in the definition of the principal stress increment. Henkel's (1960) equation is more suitable for complicated stress path problems.

The total stress / pore pressure increments are shown on Figure 6.6. The comparison with the actual pore pressures is excellent at the early stage in filling (August 1973). There is little effect of transient seepage so the comparison is straightforward. If the normal procedure had been adopted for the principal stress increments in Skempton's (1954) equation then the calculated pore pressure increments would have been much higher than the observed values.

Since the results for this early period appear to be confirmed by the observed values, it is felt that the later values of the pore pressure calculated by the same method are also realistic. It is difficult to check these due to the unknown contribution of transient seepage.

Figure 6.6 shows the resulting pore pressure distribution for the final reservoir level, assuming no further consolidation on the downstream side of the core

which is a conservative assumption. The steady state condition and the actual readings are shown. It would appear then that the pore pressures induced due to reservoir filling are not sufficient to explain the observed distribution.

One interesting result of the analysis is that the element close to the downstream face actually exhibits a slight negative pore pressure increment during the final stage of reservoir filling. This phenomenon is also apparent in Chang's (1976) theoretical study of the New Melones Dam (California). Even though he uses a completely different approach for his analysis (Cam-clay model), he shows in some zones of the core a reduction of pore pressure on reservoir loading.

6.3 Hydraulic Fracture Potential

Hydraulic fracturing within embankment dams is a process which has only recently been recognised by Geotechnical Engineers. Kjaernsli and Torblaa (1968) suggested this mechanism as a possible cause of leakage through the Hyttejuvet Dam. Sherard (1973) provides a good review of some notable case histories which exhibited this phenomenon. Since this time the process has been observed in other dams, and has even been purposely initiated from boreholes within a dam core (Penman 1975). A recent paper by Kulhawy and Gurtowski (1976) studied the parameters likely to affect hydraulic fracture potential through a series of

finite element analyses. The volume of discussion arising from this paper indicates the interest presently held in this area. Hydraulic fracturing is now a widely recognised phenomenon and embankment designers must consider this process in their design. To date there is an incomplete understanding of the mechanisms involved and disagreement as to which parameters increase the likelihood of hydraulic fracture (Charles 1976).

This section analyzes the likelihood of hydraulic fracture occurring in the Mica Dam. Use is made of the total stress increments calculated earlier in Section 6.3.

Hydraulic fracturing has allegedly occurred in the Mica core (Simmons 1974, Skermer 1975, Nussbaum and Stevenson 1976) during inflow tests on the vertical movement gauge MV15. The test was carried out when the reservoir was at elevation 676 m., the maximum level to which the water could be raised in the gauge was 666 m. Both Simmons and Skermer show that the hydraulic fracture could have initiated below elevation 590 m. However neither considered the increase in the minor principal stress due to the reservoir filling to elevation 676 m. The total stress change analysis carried out in this thesis indicated a change in minor principal total stress of about 408 kPa (3.8 tsf) which would mean that the hydraulic fracture could not occur above elevation 533 m which is about 5 m above the bedrock. This assumes that the results of Simmons (1974) 3-Dimensional finite element analysis are correct. The condition of raising the

water level in a borehole or vertical movement gauge however is not the same as raising the reservoir. Raising the reservoir causes total stress increments within the core which should not be ignored. If the dam is arched between the abutments the stresses may be redistributed. The effect of wetting the upstream shell may have a further influence on the stresses so it cannot be evaluated with certainty whether hydraulic fracturing is likely on reservoir filling from the results of a simple analysis or from a simple inflow test.

Hydraulic fracture potential must be evaluated on the upstream face of the core. The stress state at this location is difficult to establish accurately due to the large stress gradients across the interface. If it is assumed that the core arching is continuous to the edge of the core, then using Simmons (1974) stress results for elevation 590 m., the minor principal stress is 850 kPa (8 tsf), whereas the hydrostatic pressure at this level is 1800 kPa (17 tsf). However this does not include the increase due to the reservoir loading. This is estimated to be 850 kPa (8 tsf), therefore the minor principal stress is actually about 1700 kPa. This is very similar in magnitude to the reservoir pressure, and if the values are accurate then hydraulic fracture would probably not occur as it seems to initiate at some value between σ_3 and σ_2 (Penman 1972), this may be due to some structural behaviour or simply because the soil has some tensile strength. An added consideration is that

the direction of σ_3 is not conducive to fracture development, and any fractures which develop are likely to form perpendicular to σ_2 (vertical cracks) or in some direction perpendicular to an average of σ_1 and σ_3 (horizontal or sub-horizontal cracks). The major principal total stress calculated (including reservoir load) is 2575 kPa compared to a reservoir pressure of 1800 kPa. Therefore horizontal, or sub-horizontal cracks are not likely to occur in this case.

The results do indicate that if significant arching (60 % or greater) occurs in the core, and this arching is present to the edge of the core, then hydraulic fracture is indeed possible even though the reservoir load does increase the principal stresses in the core.

The use of controlled hydraulic fracture tests in dams may prove very useful in the future to evaluate the likelihood of hydraulic fracture occurring during reservoir filling. This method would allow the designer to evaluate the degree of arching occurring before reservoir filling and hence a more accurate feeling for the fracture potential. However much more research work is required in this area to provide insight into the physical processes involved.

6.4 Transient Seepage

Transient seepage is the second major process occurring in the core during reservoir impounding. A governing equation is required which includes the three sub-processes occurring

within the transient state. This flow equation should provide the pressure head distribution with time for transient flow through an unsaturated porous medium.

6.4.1 Governing Equation

The equation of continuity for transient unsaturated flow is (Freeze and Cherry, 1979) :

$$\frac{\partial(\rho v_x)}{\partial x} + \frac{\partial(\rho v_y)}{\partial y} + \frac{\partial(\rho v_z)}{\partial z} = nS \frac{\partial \rho}{\partial t} + \rho S \frac{\partial n}{\partial t} + n\rho \frac{\partial S}{\partial t} \quad \dots 6.6$$

ρ = Mass density

v = velocity

n = porosity

s = degree of saturation

Following from this the equation of flow is :

$$\frac{\partial}{\partial x} \left[k(\psi) \frac{\partial \psi}{\partial x} \right] + \frac{\partial}{\partial y} \left[k(\psi) \frac{\partial \psi}{\partial y} \right] + \frac{\partial}{\partial z} \left[k(\psi) \left(\frac{\partial \psi}{\partial z} + 1 \right) \right] = C(\psi) \frac{\partial \psi}{\partial t} \quad \dots 6.7$$

ψ = Pressure head

k = Permeability

C = Specific Moisture Capacity

This equation is often known as Richards equation. The solution for (x, y, z, t) describes the pressure head field at any point in a flow field at any time.

The specific moisture capacity in equation 6.7 is further defined as :

$$C(\psi) = \frac{1}{\rho} \frac{\partial \theta}{\partial \psi} = \frac{S}{\rho} \frac{\partial n}{\partial \psi} + S \frac{\partial n}{\partial \psi} + n \frac{\partial S}{\partial \psi} \quad \dots 6.8$$

where θ = Volumetric moisture content

The term $\frac{S}{\rho} \frac{\partial n}{\partial \psi}$ is the term relating fluid density changes.

The term $S \frac{\partial n}{\partial \psi}$ is the term which considers void ratio changes, the last term $n \frac{\partial S}{\partial \psi}$ is the change in degree of saturation.

Normally the fluid density and void ratio change terms are ignored for unsaturated soil problems (Freeze and Cherry, 1979) because they are small with respect to the change in degree of saturation term.

This is usually true for the $\frac{S}{\rho} \frac{\partial n}{\partial \psi}$ term, however the consolidation or swelling term should be investigated further to determine its magnitude for each case.

If the soil considered is near full saturation then the relationship

$$\sigma' = \sigma - u$$

will apply where

σ' = effective stress

σ = total stress

The term may be redefined as

$$\frac{\partial \sigma'}{\partial e} = \frac{\partial \sigma}{\partial e} - \gamma_w \frac{\partial u}{\partial e}$$

... 6.10

and

$$\frac{\partial \sigma'}{\partial e} = - \gamma_w \frac{\partial u}{\partial e}$$

therefore

$$\frac{\partial \sigma'}{\partial e} = - \gamma_w m_v \frac{\partial u}{\partial e}$$

... 6.11

Now $m_v = -\frac{\partial u}{\partial e}$, where m_v is the coefficient of volume change.

$$\frac{\partial u}{\partial e} = \gamma_w m_v$$

... 6.12

Therefore for a soil near full saturation the specific moisture capacity becomes approximately

$$C(\psi) = \gamma_w m_v$$

... 6.13

When this is replaced in eqn. 6.7 then the classical consolidation equation is recovered, assuming that K , the permeability, is unique within the pressure range under consideration.

For the case where there is incomplete saturation then equation 6.7 is not sufficient to describe the behaviour. In order to compare the magnitude of the terms $S \frac{\partial u}{\partial y}$ and $\frac{\partial u}{\partial y}$ it is convenient to use equation 6.9 to give an upper bound value for $S \frac{\partial u}{\partial y}$.

Using this assumption the specific moisture capacity then becomes

$$C(\psi) = S \gamma_w m_v + n \frac{\partial S}{\partial \psi}$$

... 6.14

For practical purposes the situation where equation 6.14 may be of concern is where ψ is increasing and the first term then relates to swelling.

Hence

$$C(\psi) = S \gamma_w m_s + n \frac{\partial S}{\partial \psi} \quad \dots 6.15$$

where m_s coeff. of volume change w.r.t. swelling.

A calculation done on the Mica dam core material indicates an order of magnitude difference between the first and second terms of equation 6.15. Hence it is sufficiently accurate to ignore the swelling term in the governing equation and an analysis considering a rigid skeleton should yield sufficiently accurate results in the zone of the core where the pressure is increasing.

An error may be involved in the downstream zone of the core where consolidation is continuing. To avoid the complication of ascertaining the consolidation / swelling boundary required for an accurate solution of equation 6.7, an assumption was made that there is full saturation across the core and further that m_v approximately equals m_s and the resulting consolidation equation is one dimensional nature.

This results in a specific moisture capacity of

$$C(\psi) = \gamma_w m_v \quad \dots 6.16$$

hence equation 1 becomes

$$C_v \frac{\partial^2 \psi}{\partial x^2} = \frac{\partial \psi}{\partial t} \quad \dots 6.17$$

where C_v = coefficient of consolidation.

This is Terzaghi's one dimensional consolidation equation. It is simply solved by a finite difference explicit scheme, otherwise known as the marching forward technique.

6.4.2 Rigid soil skeleton - Transient seepage

The reservoir impounding causes an increase in pressure head on the upstream face of the core, which is transmitted through the core by the process of transient seepage. The assumption of a rigid soil skeleton is common for transient flow in unsaturated porous media (Freeze and Cherry, 1979). In effect what this means is that both of the terms in the specific moisture capacity equation 6.8, relating to void ratio changes and fluid density changes are negligible in comparison to the the saturation term. In other words

$$\frac{S_n}{\rho} \frac{\partial \rho}{\partial e} < S_{\gamma_w} m_s \ll n \frac{\partial S}{\partial \psi} \quad \dots 6.18$$

or in an alternative form

$$\frac{S_n}{\rho} \frac{\partial \rho}{\partial \psi} < S_{\gamma_w} m_s \ll n \frac{\partial S}{\partial \psi} \quad \dots 6.19$$

This validity of this assumption was checked for the Mica till using an m_s value equivalent to one fifth the value. This resulted in an order of magnitude difference between $ST_w m_s$ and $n \frac{\partial S}{\partial y}$ which supports the assumption of a rigid soil skeleton.

A review of the literature provided a number of solutions to the transient flow problem, with the assumption of a rigid soil skeleton. These were by Brahma and Harr(1962), Desai and Sherman (1971), Dvinoff(1970), Dvinoff and Harr(1971), and Stephenson(1978). For this thesis the approach suggested by Dvinoff(1970) was followed.

Dvinoff uses the linearized governing equation:

$$\frac{\partial h}{\partial t} = \frac{H}{N} \left[k_x \frac{\partial^2 h}{\partial x^2} + k_y \frac{\partial^2 h}{\partial y^2} \right] \dots 6.20$$

h = total head at a point

H = mean height of reservoir

N = Specific moisture capacity x H

k = horizontal permeability

k = vertical permeability

x = horizontal coordinate direction

y = vertical coordinate direction

t = time

The assumptions inherent in this solution are:

- flow is two dimensional
- inertia forces are insignificant
- fluid is continuous
- air escapes freely from pore spaces
- soil is rigid, n, k are constant with time
- Darcys law is valid
- Dupuit's assumptions are valid

In order to use the charts provided by Dvinoff (1970), some simplifying assumptions were made regarding the reservoir raising. The assumptions are shown on Figure 6.7. The solution is sensitive to the value of k/N . k is assumed to be 10^{-7} cm/sec. throughout the dam. The value of N , which is a 'storage' coefficient, is more difficult to evaluate. None of the aforementioned authors has compared their analyses to actual case histories, and so have not indicated typical values for this 'storage' coefficient, save for their model tests where N is simply the total porosity.

It is assumed for this study that N may be evaluated from the degree of saturation existing at the end of construction. That is, assuming a rigid soil structure calculate the change in degree of saturation required to achieve a steady state pore pressure distribution, this coupled with the actual porosity will give the required volume of inflow per unit volume (storage coefficient). This value will not be the same under drawdown conditions because of capillary effects. However the reservoir-time curve assumed does not include any drawdown. The storage

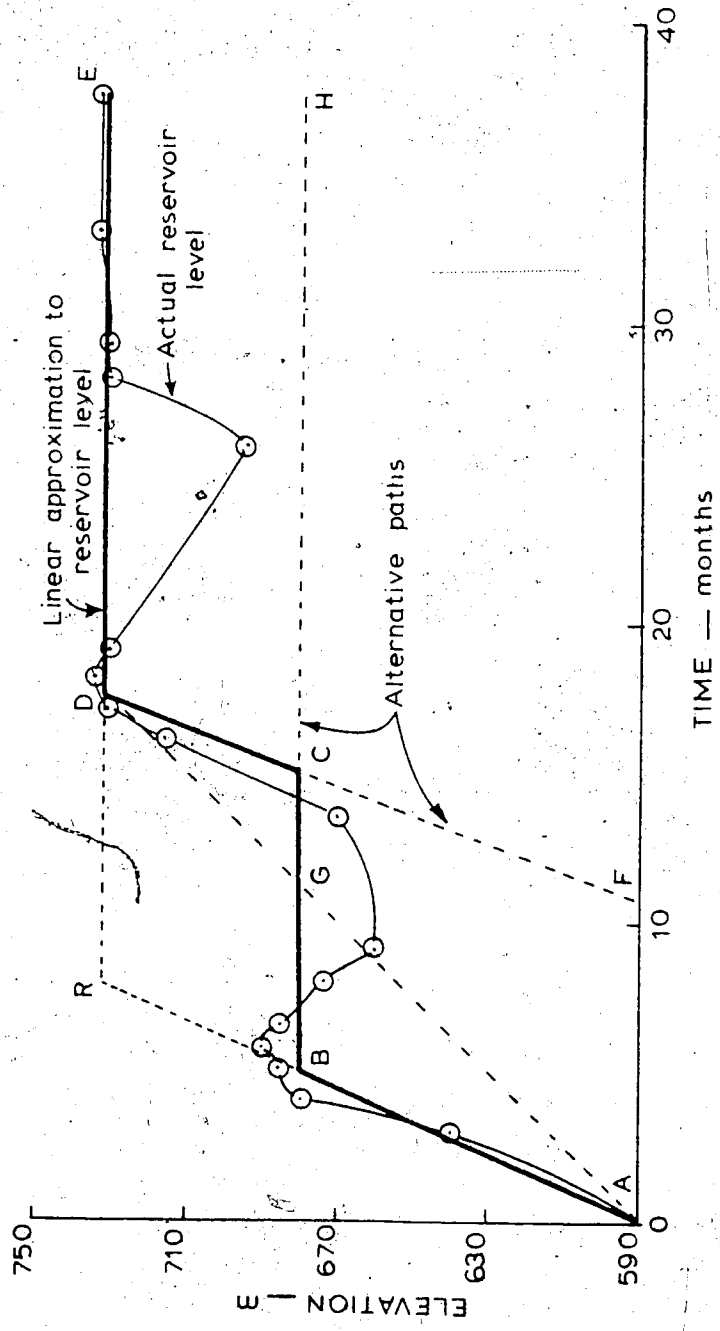


FIGURE 6.7 Reservoir Filling Curve and Approximations

coefficient will not necessarily be constant across the dam so an average value has been chosen from the central core zone.

The approach adopted for solution of the composite reservoir-time curve is similar to that of Dvinoff (1970). That is, simplified paths are assumed as upper and lower bounding conditions, each of which may be solved using the charts and tables provided. Then the composite solution is approximated between these limiting solutions. The results are shown on Figure 6.8 for the time intervals of 1, 2 and 3 years after reservoir filling commences.

The piezometers were plotted on these figures and the calculated piezometric levels were then plotted versus time. Superimposed on these plots are the actual piezometer readings and the steady state values. These results make no allowance for pore pressure changes due to the reservoir loading. These effects have been shown to be relatively small and so their contribution would be to speed up the advance of the phreatic surface by a small amount (the storage coefficient is slightly reduced).

6.4.3 Discussion of results from transient seepage analysis

The results of this analysis show that the phreatic surface proceeds rapidly through the core, even though the permeability is very low. This is because the advance is not a function of permeability alone, but of the square root of permeability divided by a storage coefficient which is

SECTION 22+50

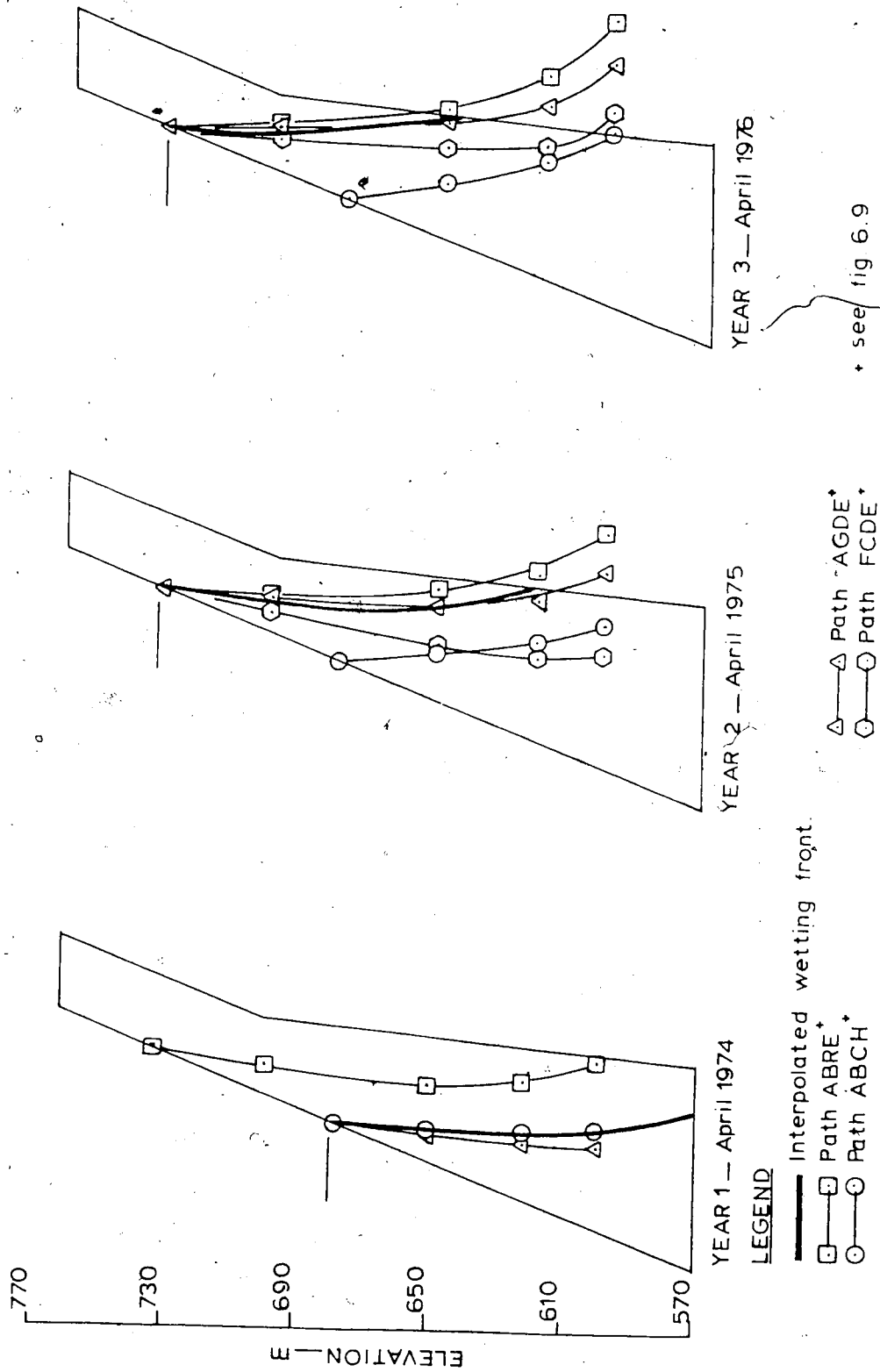


FIGURE 6.8 Wetting Fronts for Various Reservoir Paths

related to the specific moisture capacity. Errors in this function are reduced by virtue of the square root term. The value for the specific moisture capacity used in this analysis was 0.0002 m^{-1} .

Evidence to support the theoretical movement of the wetting surface may be seen in the observed water levels in the vertical and near-vertical movement gauges. These values are shown in Figure 6.9 and compared with the phreatic surface. The comparison is good for MV8 and MV15, however the results for MV9 are unusual. The water level begins to raise after one year which corresponds well with the calculated data. However the value at the end of 2 years appears rather low. This could be due to inaccuracies in the solution towards the base of the core, but the gauge rises only marginally over the next 3 years. This behaviour makes the readings of MV9 suspect. The cause could be some irregularity in construction procedure allowing preferred seepage path to the downstream shell. An alternative solution is proposed by Freeze (1971) who suggests that present steady state analyses which only consider flow within the saturated zone result in an erroneous phreatic surface. The complex problem of assuming flow within the unsaturated zone above the phreatic surface cannot be modelled by the simplified transient flow analysis used here. Hence an error in the solution close to the downstream boundary is possible.

The values indicated by MV's 4 and 14 show a more rapid

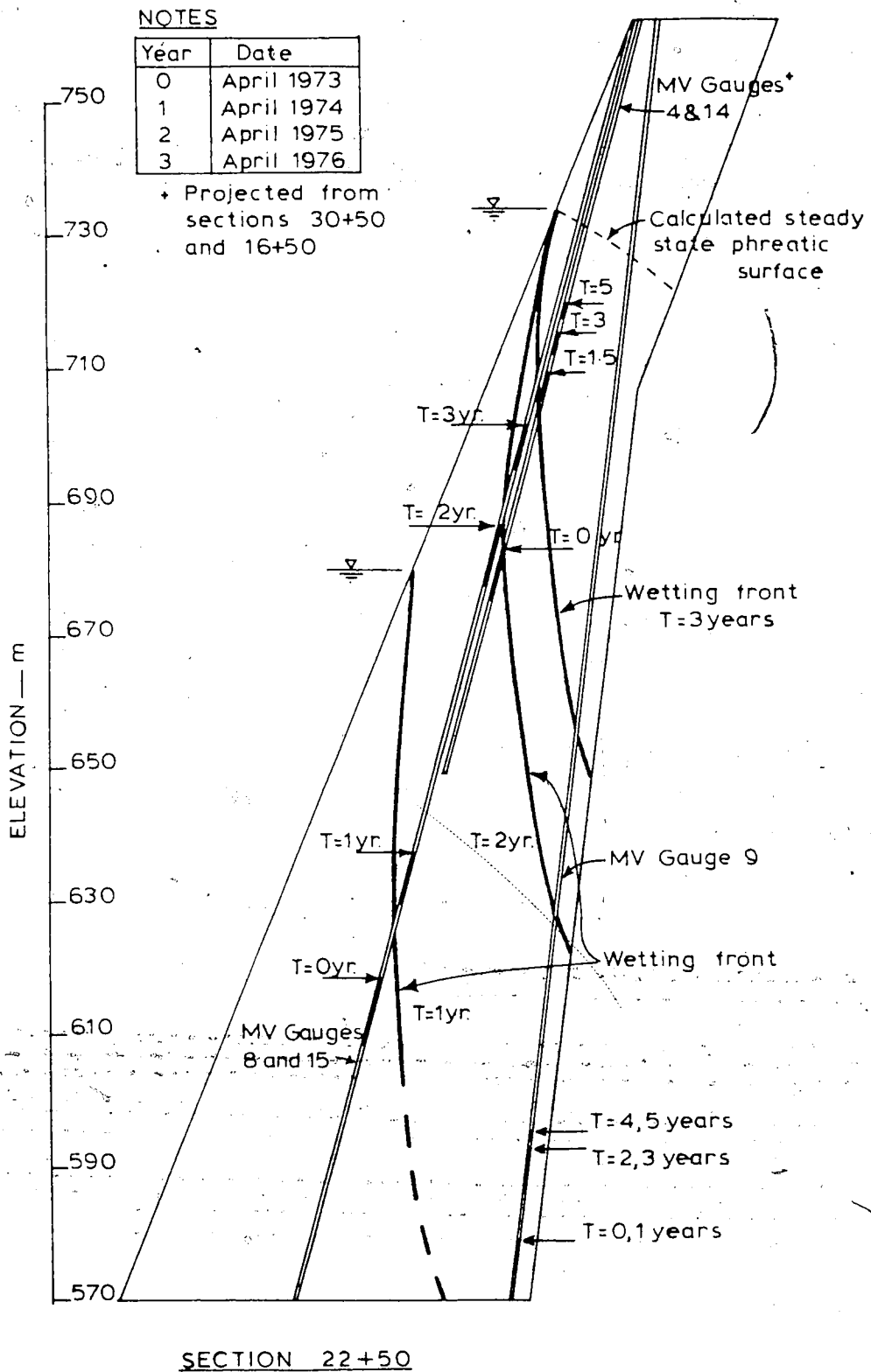
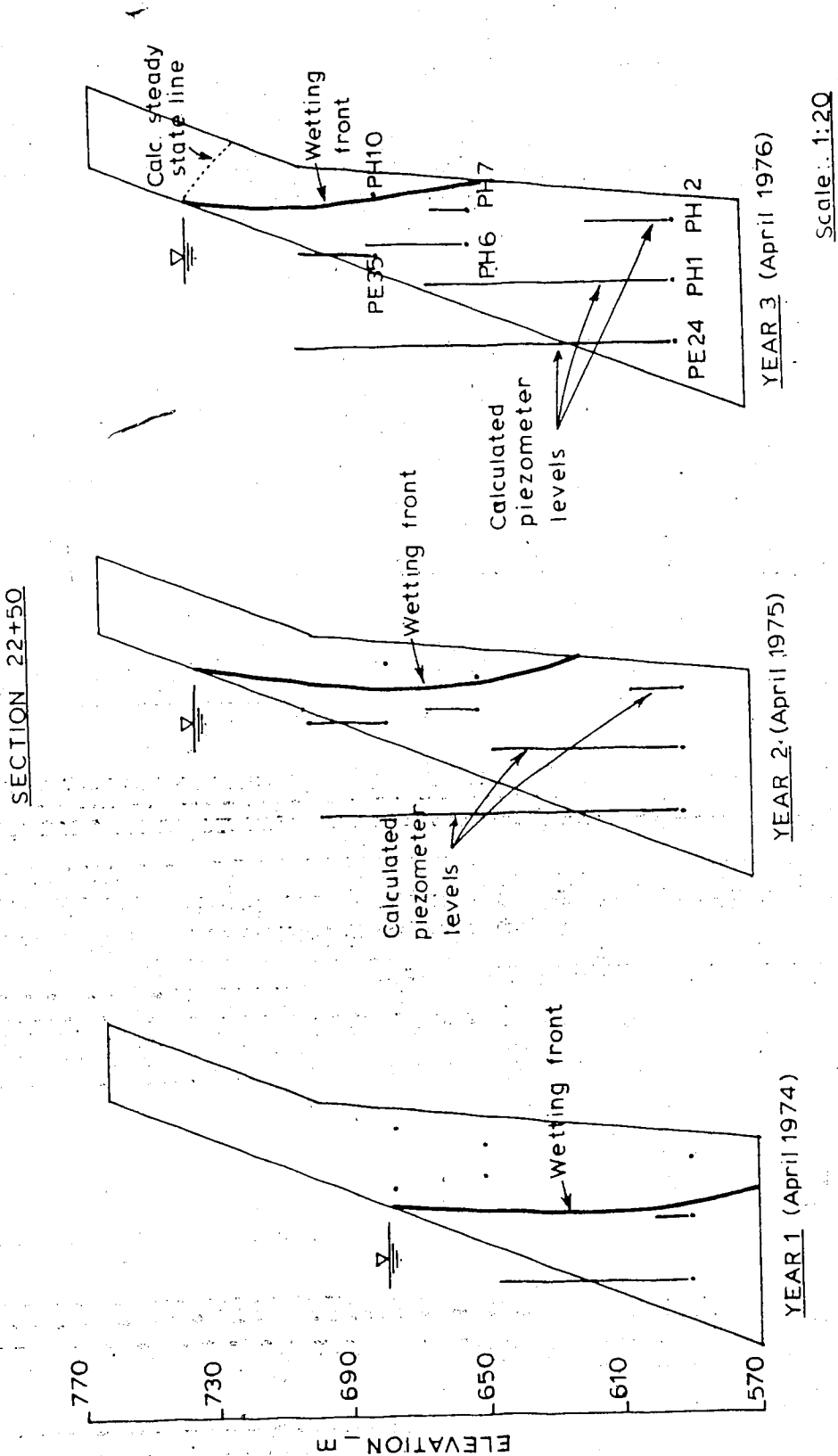


FIGURE 6.9 Wetting Front Compared with Movement Gauge Readings

movement of the phreatic surface, however these movement gauges are located in much shallower sections closer to the abutments and so their behaviour may not necessarily be the same as for the deeper section.

More interesting are the plots of the piezometric levels versus time, Figs. 6.10 and 6.11. These show quite clearly the rapid development of 'approximate' steady state conditions. A comparison of the theoretical values with the observed values may be made. The agreement between PH1, PH6 and PE35 are remarkably good considering the simplifications necessary for the analysis. The earlier observed reactions of these piezometers could be due to the assumption of no pore pressure change due to reservoir filling. The general shape of the reaction and the convergence on steady state values is excellent. However large inconsistencies exist in the remaining piezometers PE24, PH2, PH7 and PH10. In order to evaluate their responses it is necessary to consider their respective locations (Figure 2.3).

In the case of PE24 (upstream), PH1 (central) and PH2 (downstream), PE24 reacts at the correct time but its response is much too subdued. PH1 reacts early and its response is correct. PH2 reacts much earlier than the theory suggests and its reaction is above the theoretical values for steady state. Similar behaviour is noted for PH6 (central) and PH7 (downstream), and again for PE35 (upstream) and PH10 (downstream). In general it could be stated that the upstream piezometers react at the correct



Scale: 1:20

FIGURE 610 Advance of Wetting Front and Calculated Piezometer Readings

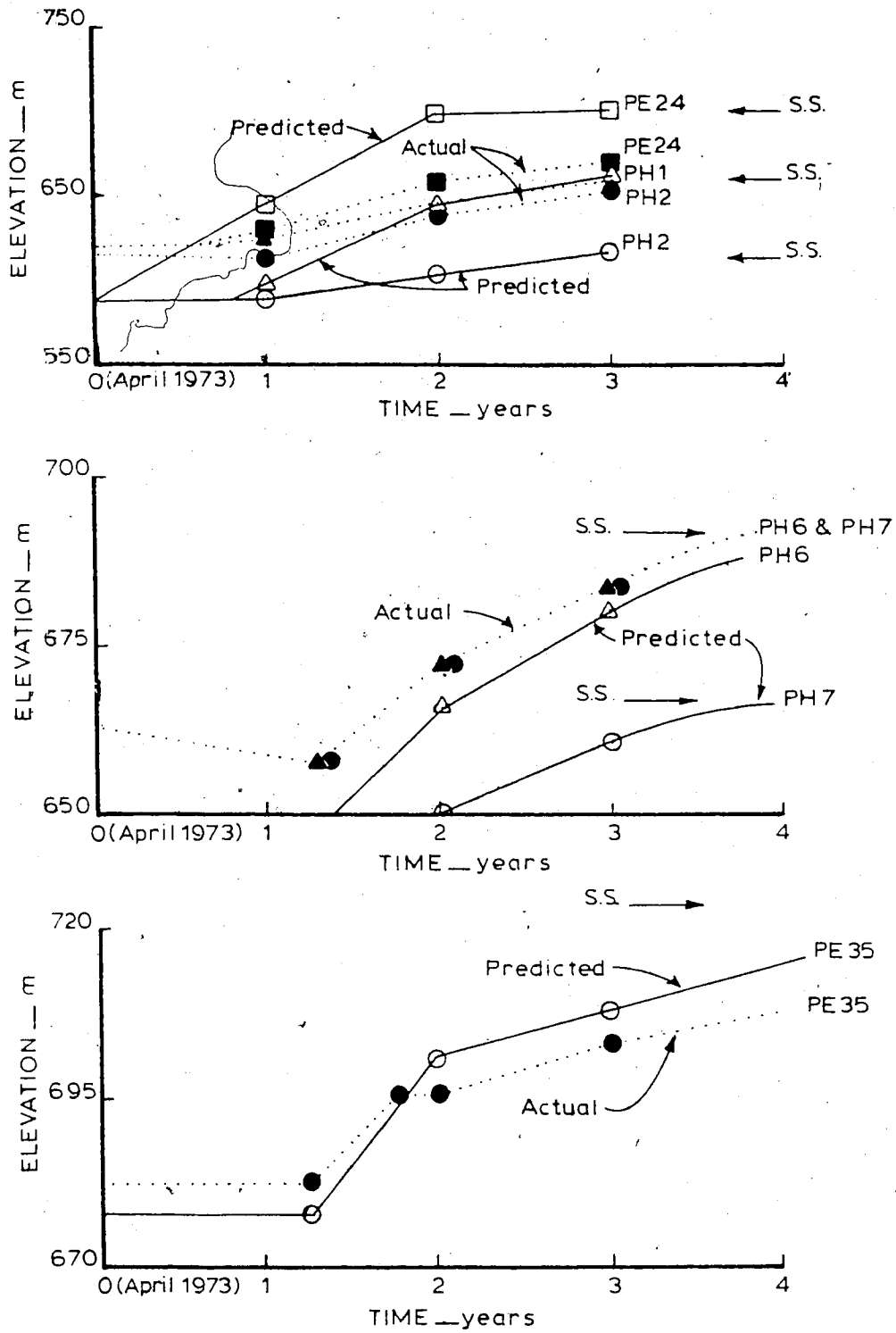


FIGURE 6.11 Predicted Piezometric Levels during Transient Seepage

time (approximately) but their response is low. The central piezometers react a little too soon and their response is correct. The downstream piezometers react much too soon and their response is too high (compared to steady state theoretical values).

In general it is considered that this analysis provides a fairly accurate description of the advance of the phreatic surface within the Mica Dam core. The advance is rapid and is substantiated to some extent by the pore pressure readings taken in the vertical and near-vertical movement gauges.

6.4.4 Consolidation -- Transient Seepage.

The assumption that the consolidation term $S \frac{\partial u}{\partial y}$ in equation 6.8 is negligible compared to the saturation term $n \frac{\partial S}{\partial y}$ may not be valid in the core zone where the pressure head is continually reducing. Particularly if the degree of saturation is high.

In order to investigate the rapidity of dissipation of the pore pressures in the consolidating downstream zone the term $n \frac{\partial S}{\partial y}$ was assumed to be zero. This is true if $S=1$ and is not an unreasonable assumption for this material at approximately 95% saturation.

To simplify the calculations the upstream 'swelling' zone of increasing pressure head was assumed to have a coefficient similar in magnitude to that in the consolidating zone. The errors inherent in this solution

will occur in the time rate of advance of the phreatic surface in the upstream zone. However the indicated rate of consolidation should be reasonably accurate for the downstream zone.

The coefficient of consolidation was assumed to be $14 \text{ m}^2/\text{mo.}$ (Law 1976). The equation was solved using a simple finite difference (marching forward) explicit 1-Dimensional scheme. The reservoir impounding was modelled by a moving upstream boundary condition. The reservoir level was held constant at elevation 734m between the 2nd and 10th years.

The solution is shown on Figure 6.12 . The results show rapid dissipation close to the downstream face of the core (PH2), with only minor fluctuations in pore pressure as the reservoir rises. Similarly in the central core (PH1) there is little decrease in pore water pressure due to consolidation. It can clearly be seen that the behaviour of PH2 is very dissimilar in magnitude to the theoretical behaviour. During the early stages of consolidation however the comparison is not unreasonable (PH2). It is not expected that the upstream side of the core (PE24) will match well because of the simplifications introduced into the governing equation.

6.5 Conclusions

This chapter reviews the physical processes occurring in the core of the Mica dam prior to the establishment of steady state seepage. The processes studied separately were:

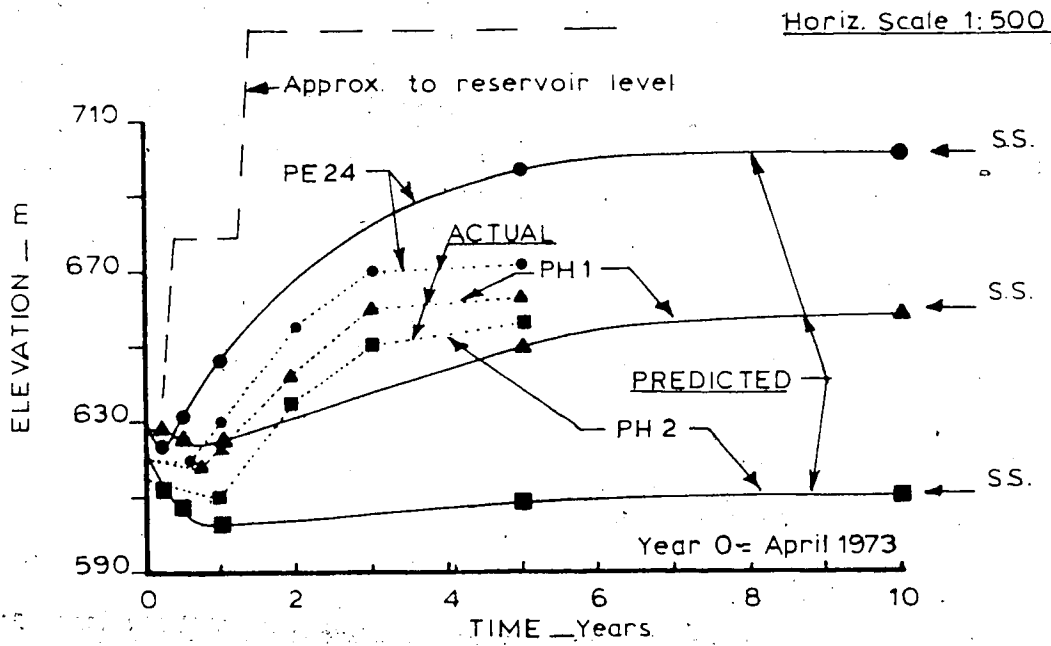
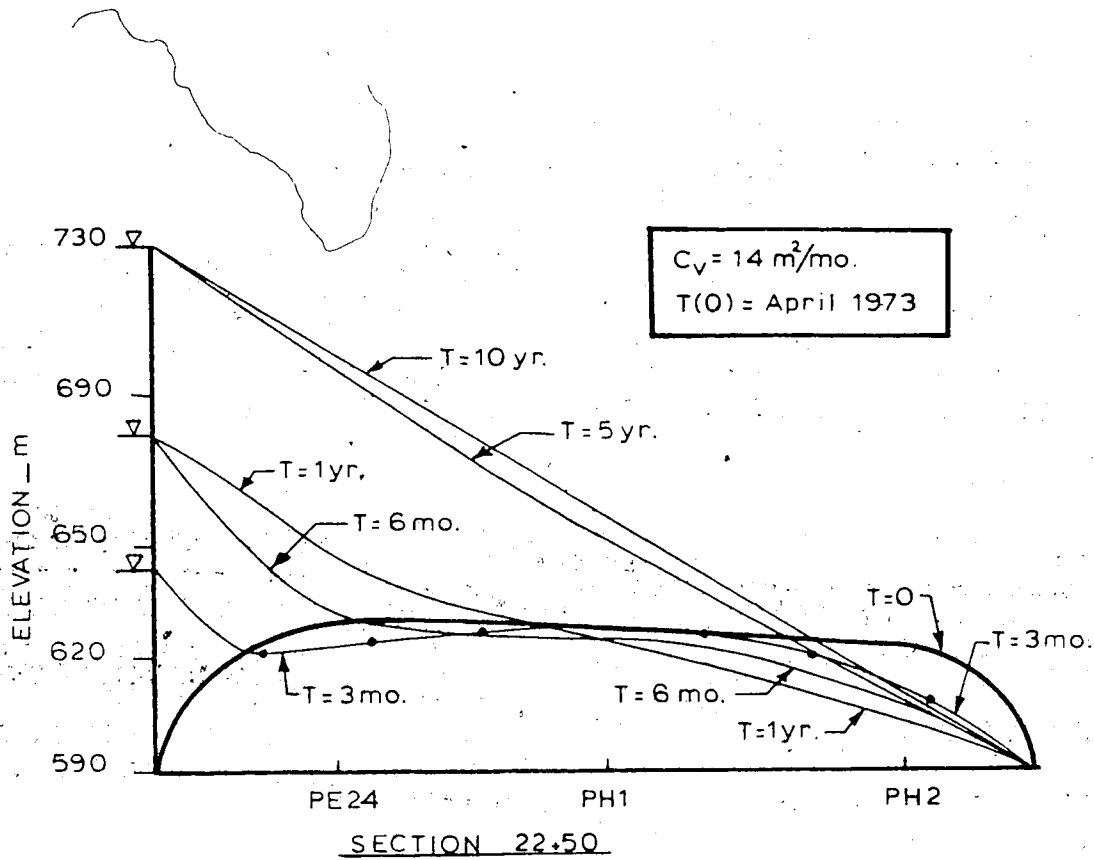


FIGURE 6.12 Pressure Head Versus Time

- total stress changes due to reservoir filling
- transient seepage

The most significant contribution to the pore pressure increments was found to occur from the transient flow. The advance of the phreatic surface is rapid, approximately 3 to 4 years to develop steady state. Because this surface is nearly vertical the response of the piezometers is also rapid. The most significant contribution to the transient process is from the changing degree of saturation for unsaturated soils and so it is reasonable to assume a rigid soil skeleton. However the consolidating portion of the core is more affected by the changing void ratio. Whereas the fluid density changes are not normally significant and may be ignored.

The contribution from the total stress changes due to undrained reservoir loading was calculated to be small but not negligible. If this effect was to be superimposed on the development of the phreatic surface it would reduce the 'storage' coefficient slightly and so increase the rate of advance of the phreatic surface. These processes are not sufficient to explain the observed pore pressure distribution in this embankment core.

A comparison of the observed and predicted pore pressure distributions during transient seepage or steady state infers some irregularity within the core. A possible explanation would be the existence of hydraulic fractures in the core. The likelihood of fracturing has been investigated.

and the results indicate that hydraulic fracture is unlikely in the upstream zone of the core, but would be possible in the central and downstream core zones if the full reservoir pressure could be transmitted in some manner to these zones. However because the unusual pore pressure distribution is similar through various sections and levels in the core it could be argued that hydraulic fractures, if they did occur, would not appear as uniformly, nor in sufficient quantity, to create this distribution. An alternative explanation could be that some material non-homogeneity in the core construction, yielding much more impermeable strips parallel to the upstream and downstream faces of the core. There is no justifiable reason to assume this condition would be regularly repeated throughout the core, and there is no evidence to support this theory.

None of the theories investigated yield results even close to the piezometric values observed. Therefore consideration must be given to the fact that the general pore pressure distribution in the core could be quite similar to the theoretical values postulated, but for some reason there are some local anomalies in the pore pressure distribution close to the piezometers and so these piezometric readings are only reflecting local perturbations.

In light of this argument the reaction of piezometers PE38, PP36 and PE44 are considered. These piezometers are located in the upper core and are noted to respond almost

instantly to the reservoir fluctuations, and to follow this level very closely. This behaviour has been noted previously by Nussbaum (1976). The reason for this unexpected response is because the instrument lead trenches in this area proceed directly into the upstream shell. This suggests that although the remaining trenches do not enter the upstream shell they may have a local influence on the pore pressure distribution. This theory is investigated in detail in Chapter 7.

CHAPTER 7

EFFECT OF PIEZOMETER INSTALLATION METHOD ON PORE PRESSURE DISTRIBUTION

7.1 Introduction

In recent years monitoring of embankment performance has become an integral component of the design procedure. The reasons for this are twofold. In order that the observed behaviour can be compared with the predicted behaviour and so that insight into the physical processes occurring during various phases in the life of the embankment may be developed.

The role played by piezometers is extremely important because without them the actual pore pressure magnitude and distribution would be unknown, excluding the possibility of carrying out an accurate effective stress analysis.

Three basic types of piezometer are in common use today, each having distinct advantages over the others in particular situations. However no matter how sophisticated the instrument the readings will be valueless if the installation procedure is unsatisfactory. The one common weakness with any piezometric system is the link between

measuring unit and readout unit. Concern has been expressed by authors that these lead trenches may act as preferential seepage paths (Sherard et al. 1963). He states:

"... But regardless of the location of the measuring point, the tubing must be carefully backfilled with impervious soil to prevent seepage along the line of the tubes which could change the pore water pressure at the piezometer tip. "

In particular Blight (1970) noted that narrow cores accentuate this danger, and considerable attention should be given to design and installation in these cases, for example he quotes the Bridle Drift dam (S. Africa) and the Manjirenji dam (Rhodesia).

If piezometers are installed in an inadequate manner the observed values of pore pressure may be misleading, and in certain cases lead to an overestimation of the factor of safety. Indeed it may be very difficult to ascertain whether or not the readings are reliable, so the installation should be carried out at all times by experienced and reliable personnel, with a high degree of quality control.

7.2 Design of Instrumentation Lead Trenches for Mica Dam

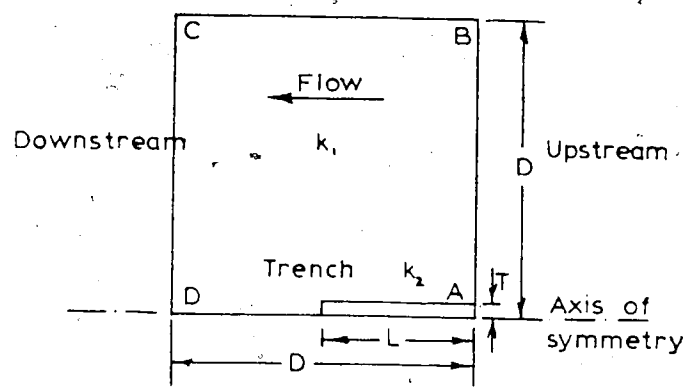
During the early stages of design and construction, attention was paid to this problem of seepage along lead trenches. As a precaution against this the addition of bentonite to the backfill was specified and cut-offs were required every 15 m or between adjacent piezometers, whichever was less. The details of the actual trench installations are given in Section 2.3. These precautions

may not have been adequate, as evidenced by the behaviour of piezometers PE38, PP36, and PE44, discussed previously in Section 6.6. Although it is unusual practise to bring lead trenches into the upstream shell, perhaps in this case it was rather fortunate as it provides conclusive evidence of the unsatisfactory trench behaviour. With this in mind it was decided to analyse the sensitivity of the local pore pressure distributions to varying trench-fill permeability ratios.

7.3 General Model for Piezometer Lead Trenches

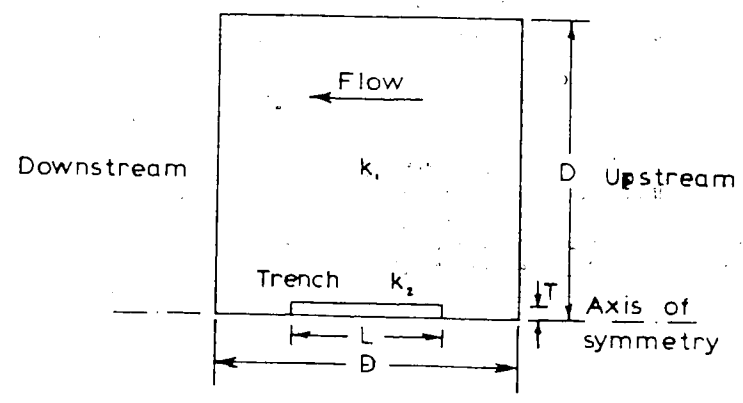
Vaughan (1965) provided an approximate solution for the problem of leakage through backfill around a vertical standpipe piezometer. Unfortunately this analysis could not conveniently be applied to this case of a horizontal pipe in a specific flow domain. It was decided to model the situation using finite element techniques.

The FPM5 computer program was used for this analysis. The model assumed must be axisymmetric, which presents problems in reproducing the asymmetric boundary conditions due to non-horizontal flow. The problem is really three dimensional but because the core is thin an assumption of horizontal flow is not unreasonable. The cross-sectional area of the rectangular trench was approximated by an equivalent area circle. The general model is shown in Figure 7.1.

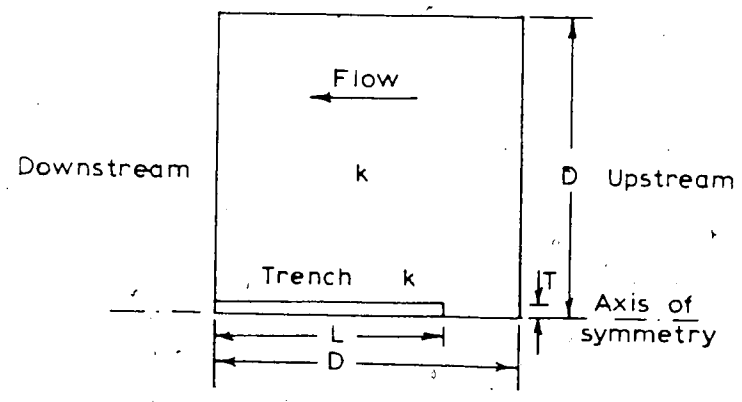


CASE 1

Note: Total head along AB = H
Total head along DC = 0



CASE 2



CASE 3

FIGURE 7.1 Instrument-Lead Trench Model

Three basic cases were studied:

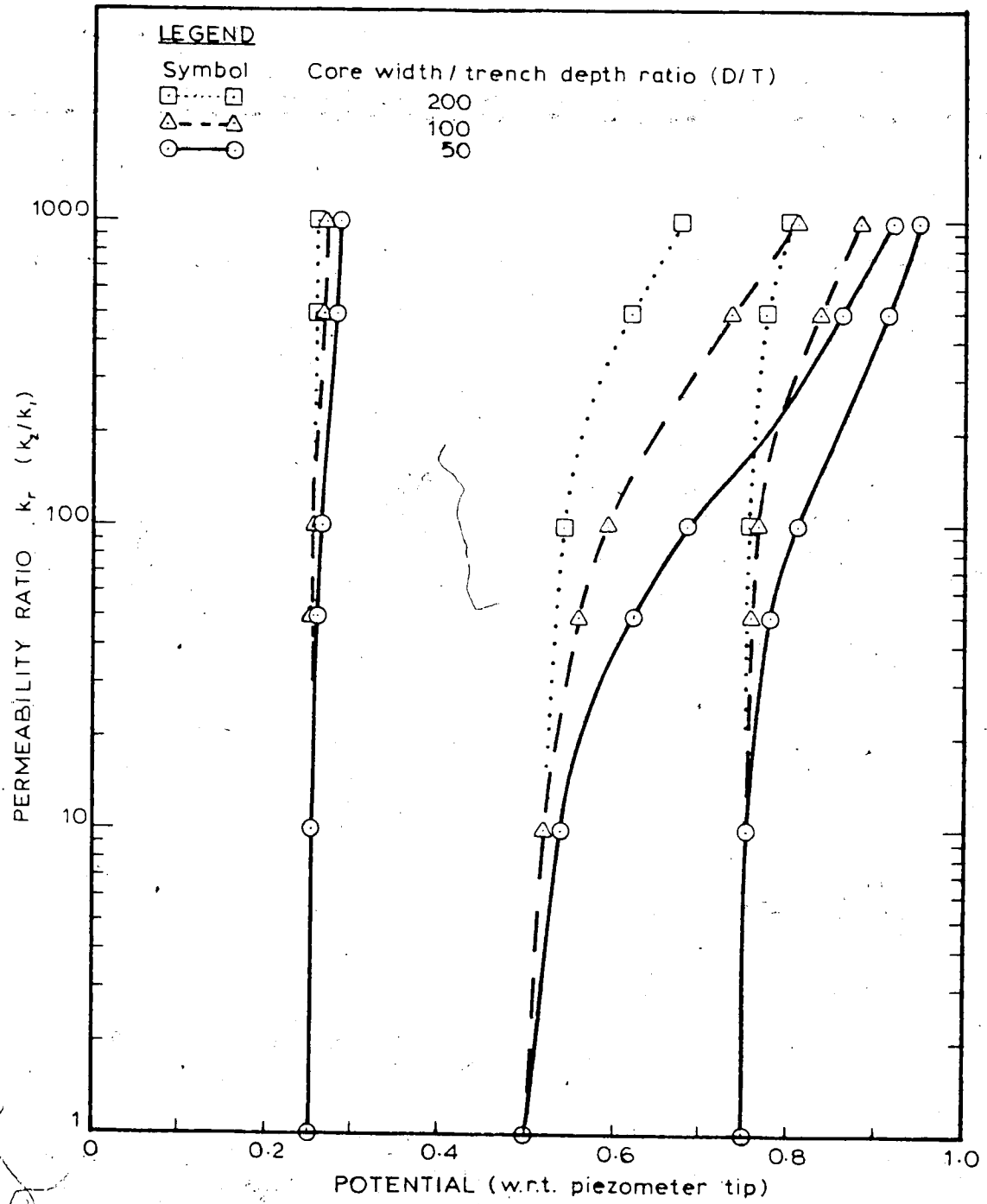
1. The trench connected to the upstream shell (CASE 1)
2. The trench confined in the central core (CASE 2)
3. The trench connected to the downstream shell (CASE 3)

Various permeability and trench depth/core width ratios were considered for each case. The results are plotted as permeability ratio versus potential values at specific locations across the core. The effect of trench diameter is superimposed on the charts (Figures 7.2 to 7.4). Examples of the local changes in pore pressure distribution are shown on Figures 7.5 to 7.7.

The result of this analysis is to show that for each case studied there could be significant alteration to the readings of piezometers located in certain critical positions. The position is aggravated by increasing the trench depth or permeability ratio. Permeability ratios as low as 100 may cause significant disturbances to the pore pressure regime. This is consistent with Vaughan's (1965) conclusion that a grout to soil permeability ratio of 50 is satisfactory for very low permeability soils (standpipe installation).

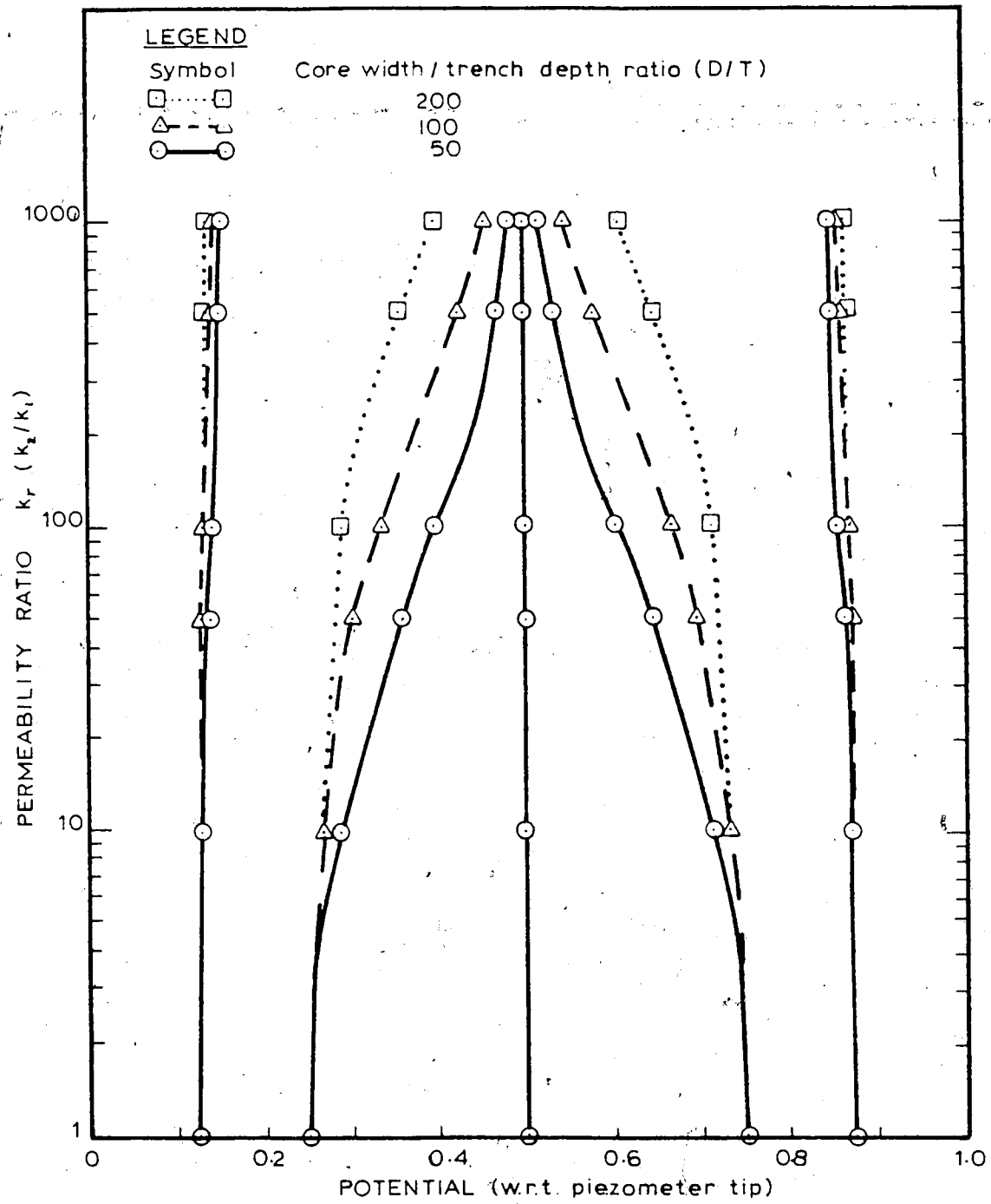
These results are interesting because as shown by Mitchell et al. (1965) (for a silty clay) it is relatively easy to get a variation of two or three orders of magnitude in permeability in the same material by simply varying the compaction moisture content or compactive effort.

This analysis shows that it is possible to get



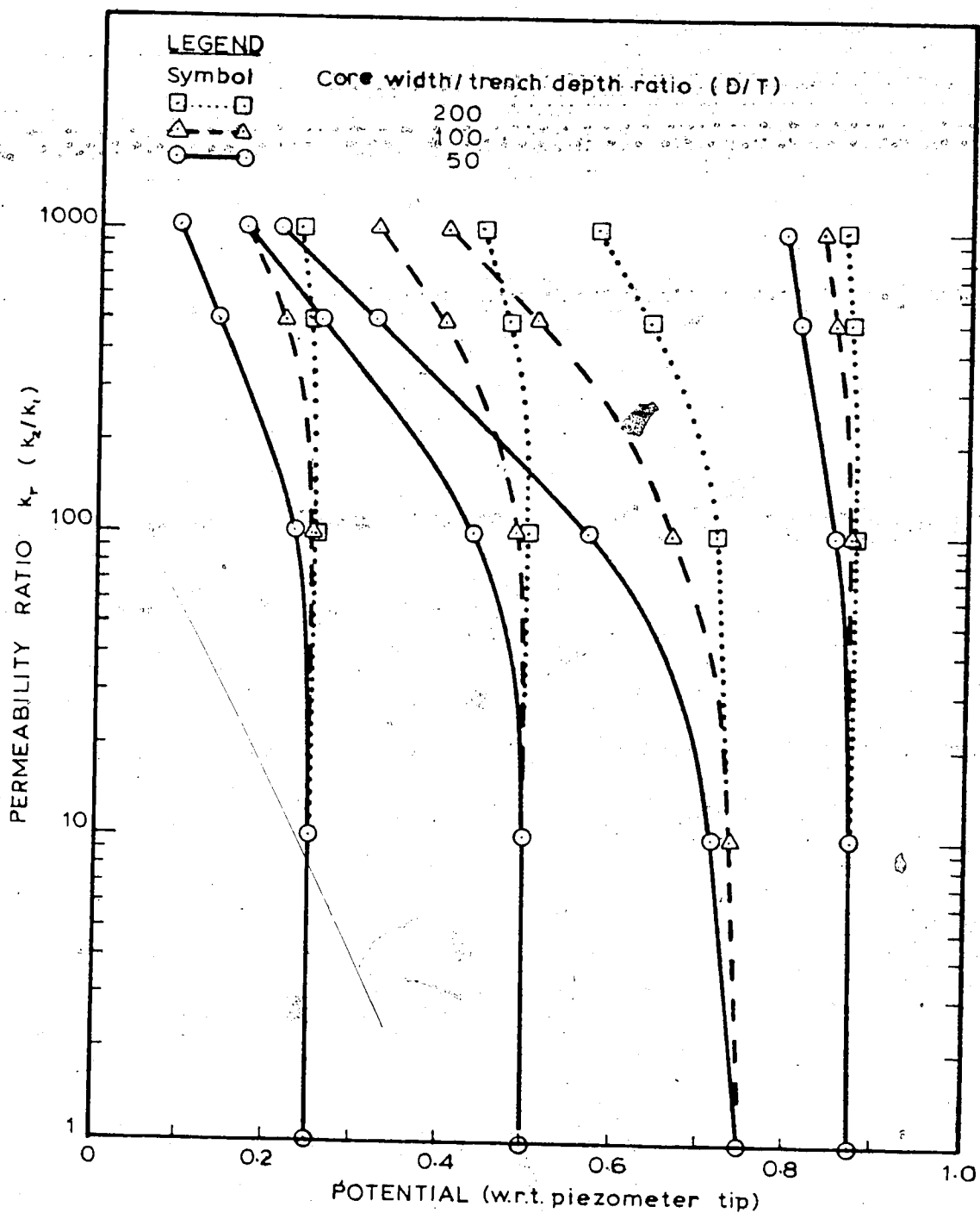
CASE 1. L/D=0.5 (Trench connecting to u/s shell—see fig.7.1)

FIGURE 7.2 Design Chart for Trench Connected to Upstream Shell



CASE 2. L/D = 0.5 (Central trench — see fig. 7.1)

FIGURE 7.3 Design Chart for Centrally Located Trench

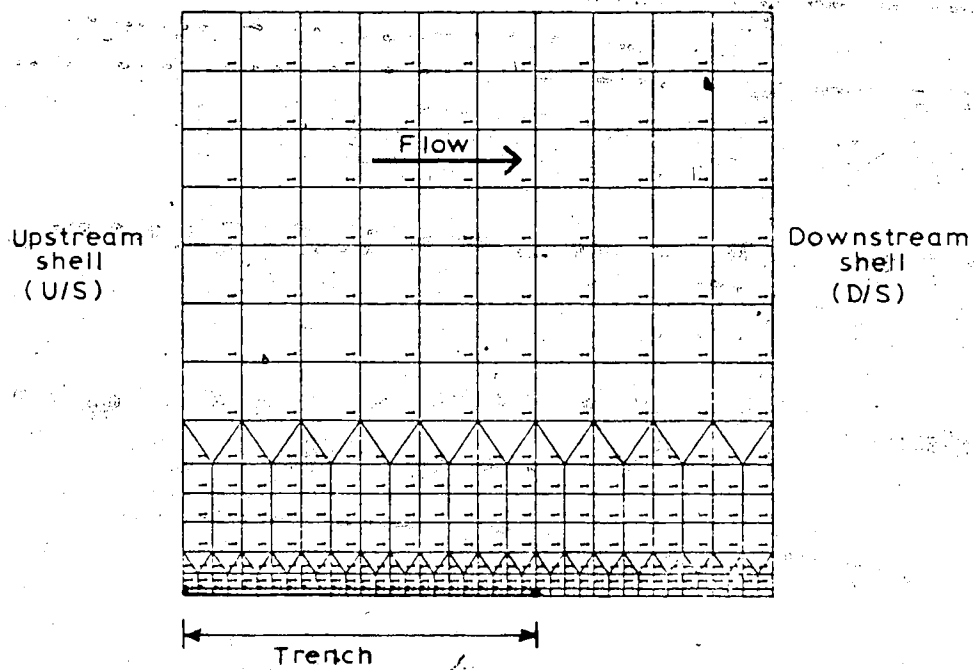


CASE 3. L/D=0.75 (Trench connects to d/s shell—see fig. 71)

FIGURE 7.4 Design Chart for Trench Connected to Downstream Shell

MATERIAL PERMEABILITY (CODE)		
K (HORIZ) <CH/SEC K (VERT)		TYPE
0.00000100	0.00000100	1
0.00000000	0.00000000	2

* TIP OF PIEZOMETER



Note:

Trench backfill — material type 2

Core fill — material type 1

Permeability ratio — $k_r = k_2 / k_1$ where subscripts refer to material type.

FIGURE 7.5 Typical Finite Element mesh for Trench Model

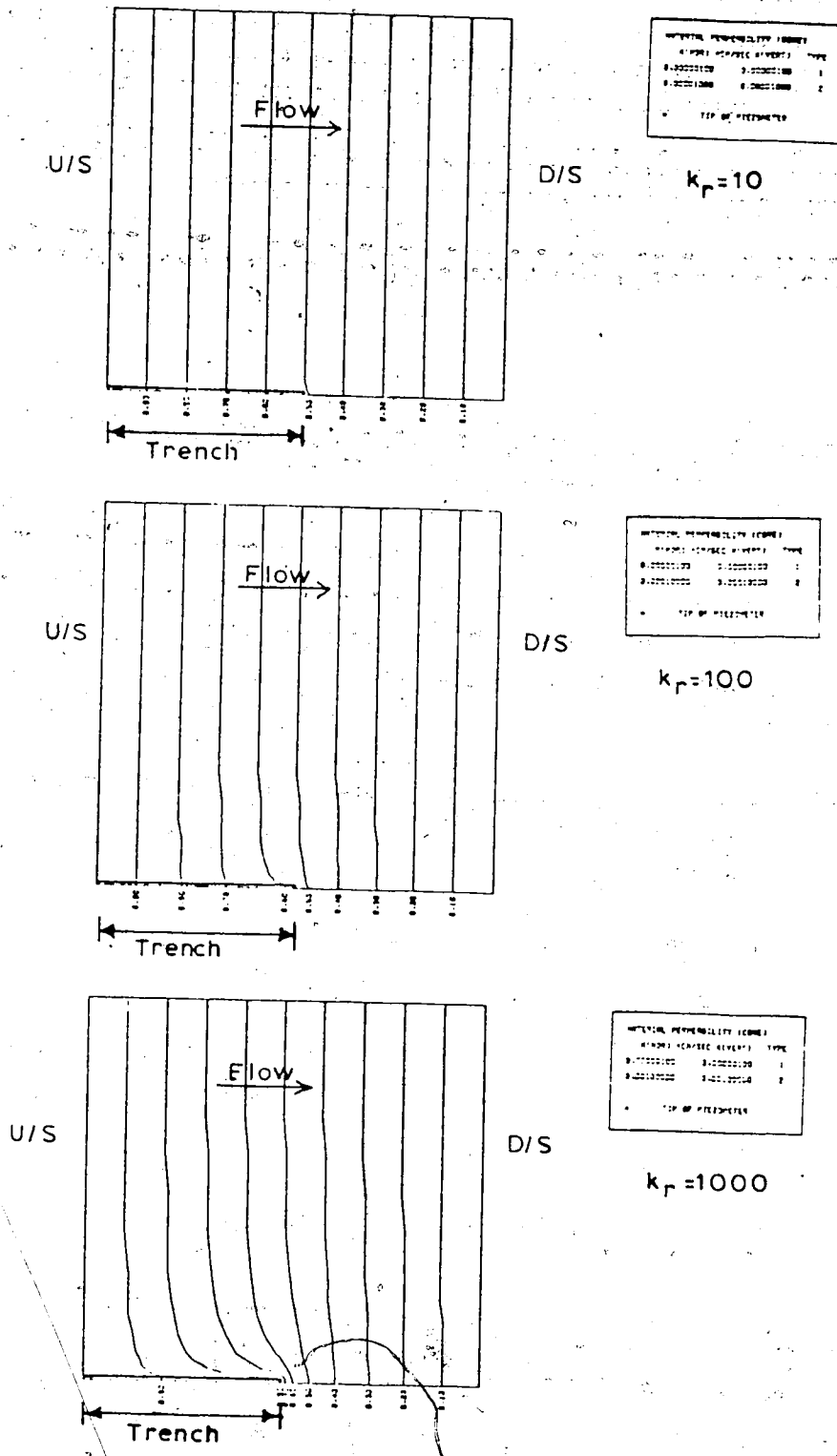


FIGURE 7.6 Typical Results of Trench (Upstream) Analysis

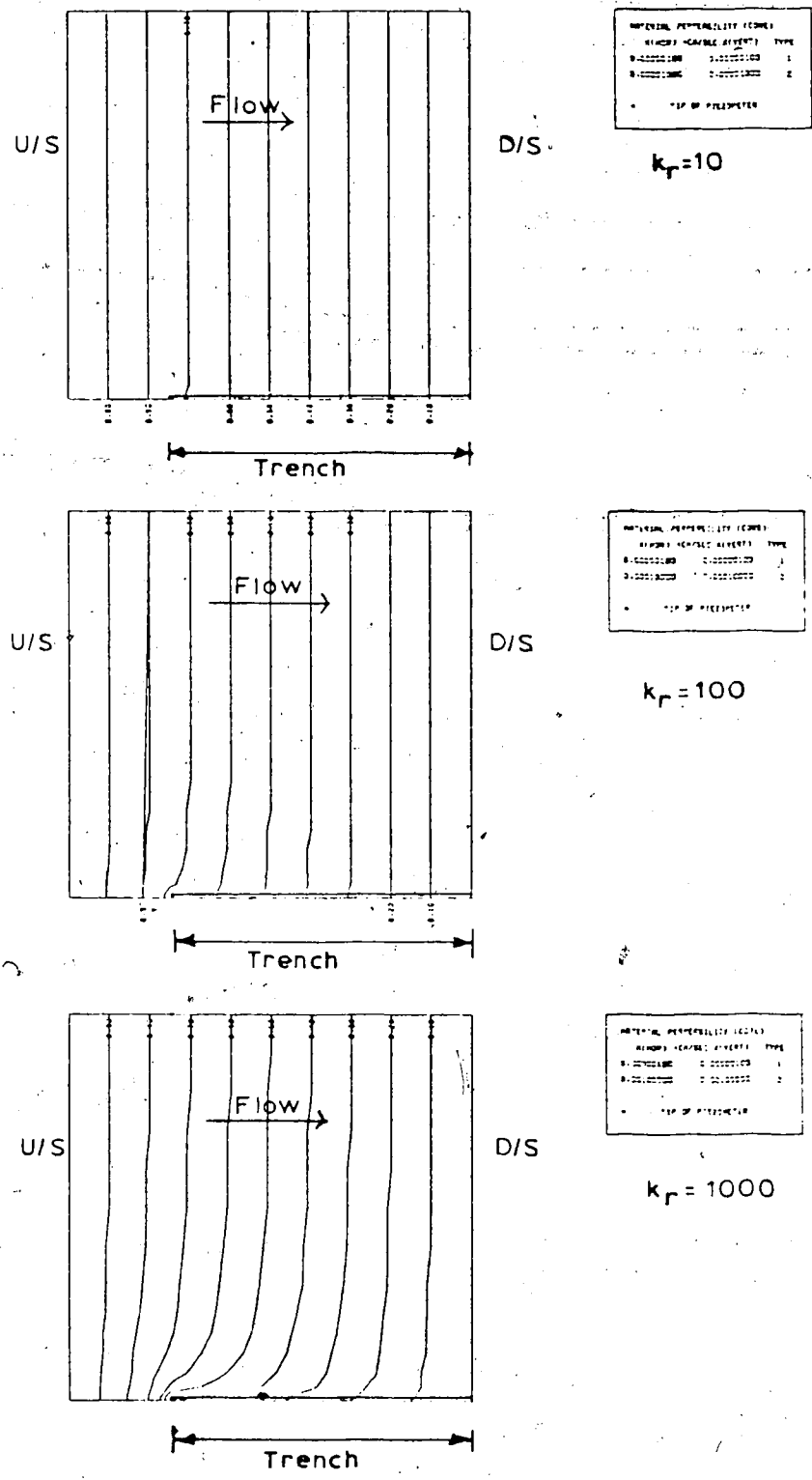


FIGURE 7.7 Typical Results of Trench (Downstream) Model

significant local deviations from the general pore pressure distribution within a core, caused by the instrument lead trenches. Therefore it is necessary to study individual trenches in the Mica dam core more carefully.

7.4 Model Specifically Applied to Mica Dam Core

In order to analyse specific trenches within the dam core, an accurate record of the installation method and locations of the lead trenches was required. This proved difficult to obtain, because some of the records are now more than 10 years old. However some details were obtained from some unpublished 'Dam Instrumentation Construction Notes' (Mica dam) from the years 1969 to 1972 (Caseco Consultants Ltd. 1969-1972). The installation procedure was discussed in detail in Section 2.3, and layouts of the trenches and risers are shown on Figure 2.5.

The observed behaviour of piezometers PE38 and PP36 were analyzed first. The results indicated that a permeability ratio of about 800 is required to model the observed behaviour. The result for PE38 is higher but this piezometer reads erratically later on so it has been rejected as unreliable. Next the model was applied to piezometer PE44, once again the result indicated a permeability ratio of 600. This is very similar to the previous result so an average value of 700 was taken for further analyses. This infers a trench permeability of 7×10^{-4} cm/sec. See Figure 7.8.

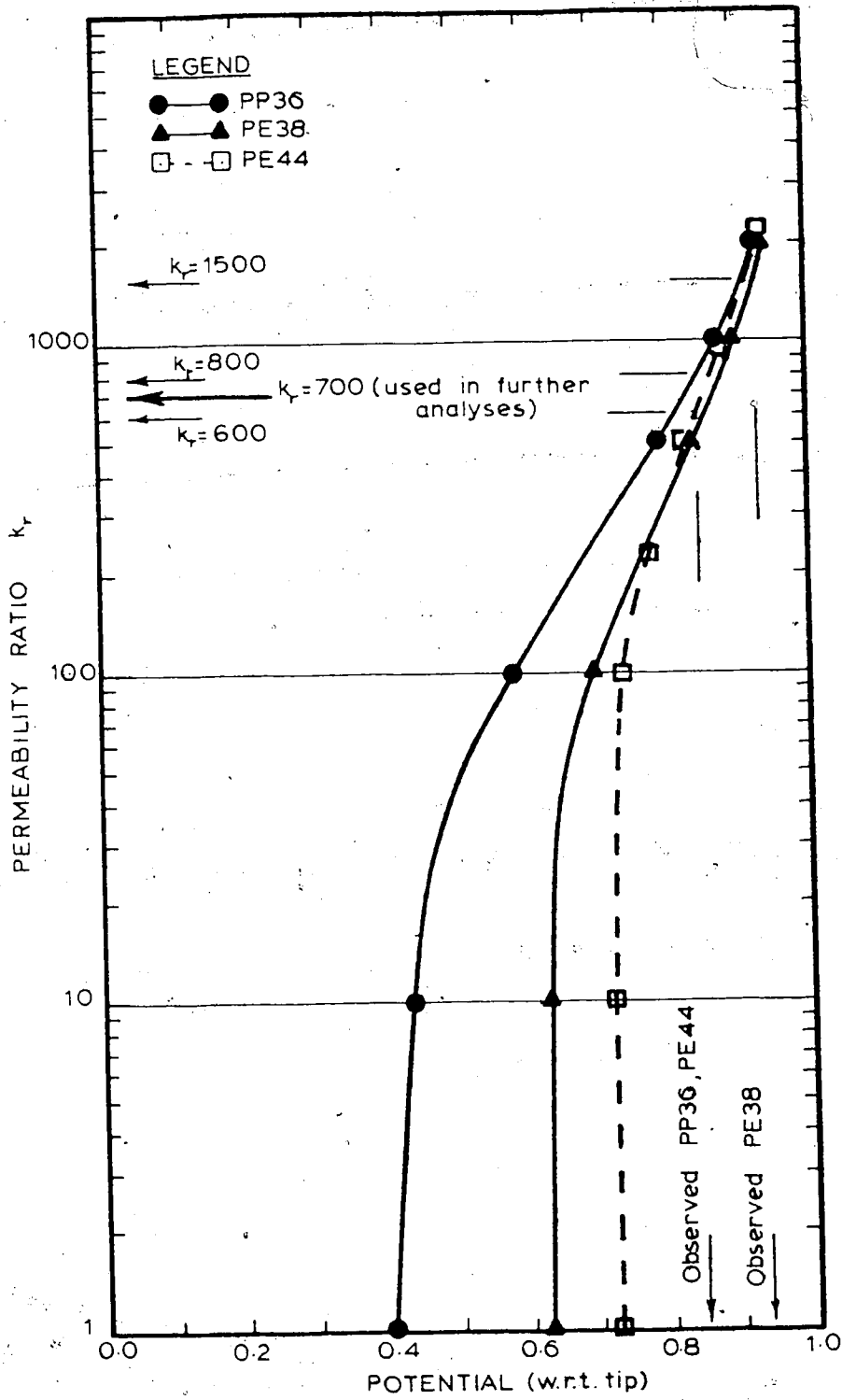


FIGURE 7.8 Results of Trench Analysis on PE38... PP36 and PE44... PP44

The trench backfill was sand-bentonite-cement as discussed previously (Section 2.3). In the upper trenches the complete trench was filled with this material, including cut-offs. From the limited data available it appears that in many cases the fill was compacted very dry of optimum, and the sand used was likely screened shell material. It is quite possible under these conditions that the bentonite did not work as anticipated. Rollins and Dylla (1970) and Middlebrooks et al. (1978) both indicate that bentonite may either lose its sealing power or simply be subject to piping under certain conditions. Neither paper deals specifically with instrumentation trenches but the mechanism may still be possible. In view of the discussion above it is quite feasible for the trenches to have this high permeability. It should be remembered too that if the core material should have a lower permeability than that assumed then the trench permeability need not be so high, because the disturbance is caused only by the ratio of permeabilities.

Next the lower trenches were analyzed, assuming a trench permeability of 7×10^{-4} cm/sec. It was immediately evident that the correct pore pressure trend was resulting. Particularly for the cases where the trenches were truncated within the core (PE25 ... PH7; PE36 ... PH11; PE37 ... PH12). For the cases where the trench continued into the downstream shell (PE35 ... PH10; PE24 ... PH2) the distribution was an improvement, particularly on the upstream side, however the downstream results were too low.

The trench PE24 ... PH2 is a special case because the permeability of this material is assumed to be lower due to the higher compaction moisture content. Therefore the permeability ratio is 7000 in this example. The trench depth is also smaller because of different installation procedure in this zone. Some typical equipotential distributions resulting from the analysis for various trenches are shown on Figures 7.9 to 7.11.

A careful study of the results, Figures 7.12 and 7.13, show a consistent trend. In the cases where a riser exists below the trench (PE25 ... PH7; PE36 ... PH 11; PE37 ... PH12) the predicted readings were all a little high. Where a riser is above the trench (PE24 ... PH2; PE35 ... PH10) the predicted readings in the downstream zone are all much too low, but the upstream zones are good. So perhaps the risers are influencing the results also. The higher permeability being caused by the construction technique (Section 2.3) noted around the risers. This was much more difficult to analyze.

Specific inflow values were specified at the nodes where risers were located. The results were improved in all cases. The required permeability ratio of the annulus around the risers was backcalculated from the flow value, the area, and the known potentials at each end of the riser, this yielded reasonable ratios of about 300. These results are also shown on Figures 7.12 and 7.13.

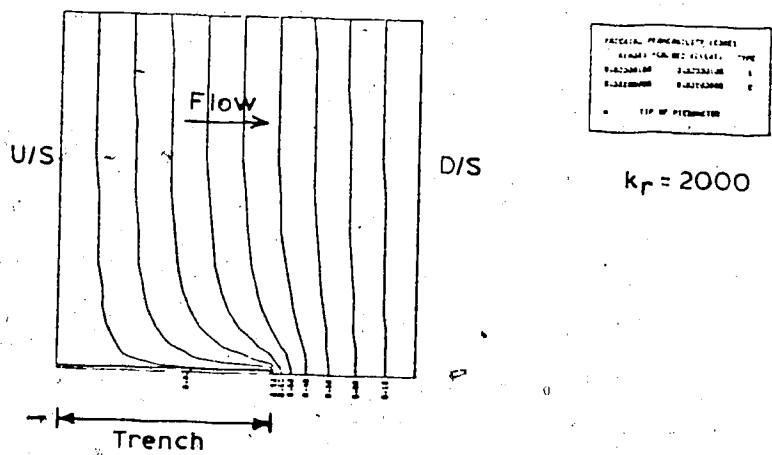
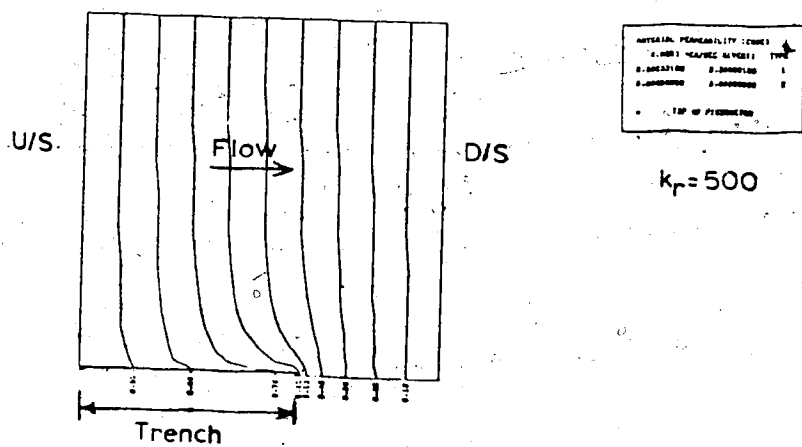


FIGURE 7.9 Equipotential Distribution around Trench PE38...PP36

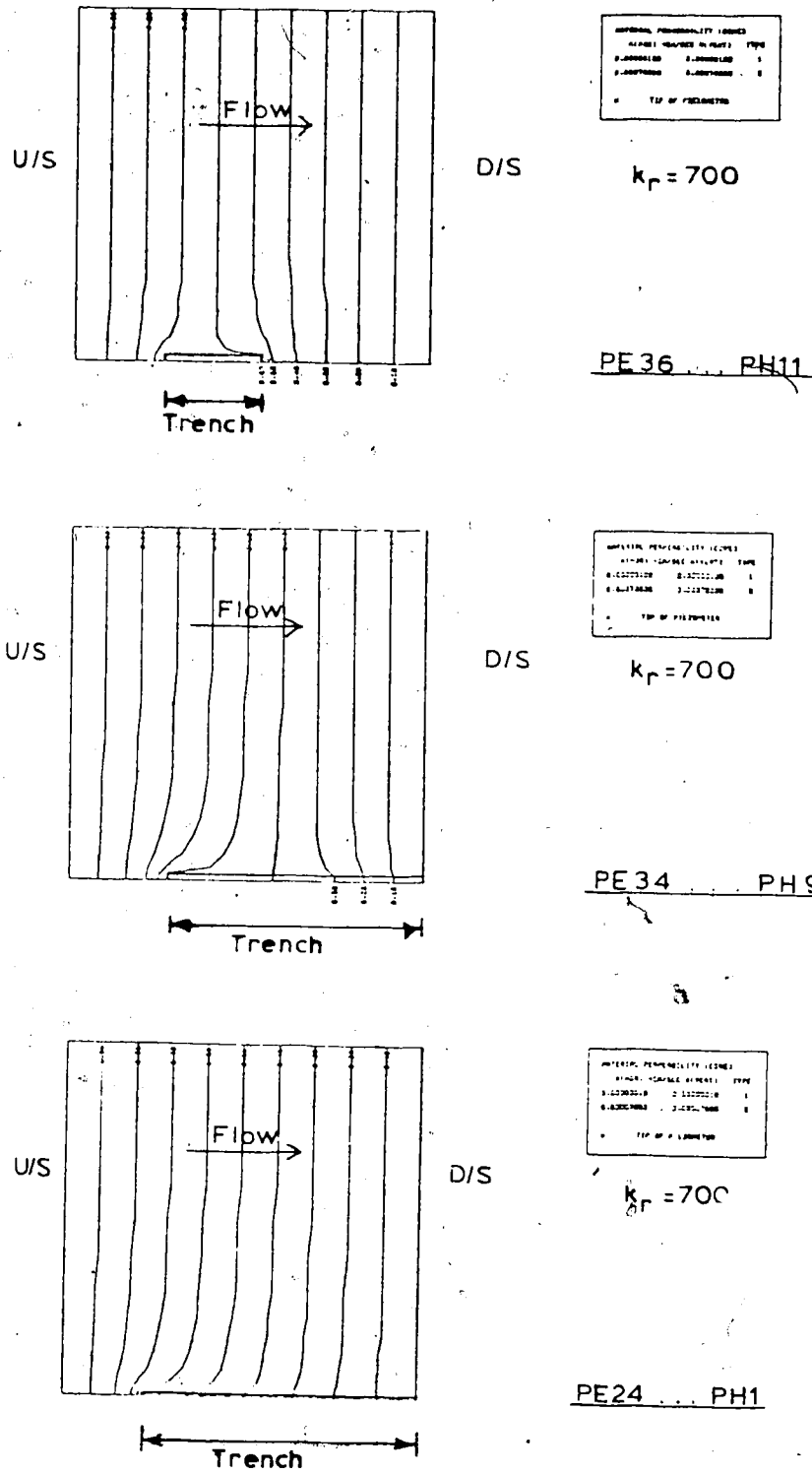


FIGURE 7.10 Equipotential Distributions around Trenches PE36...PH11, PE34...PH9, PE24...PH1

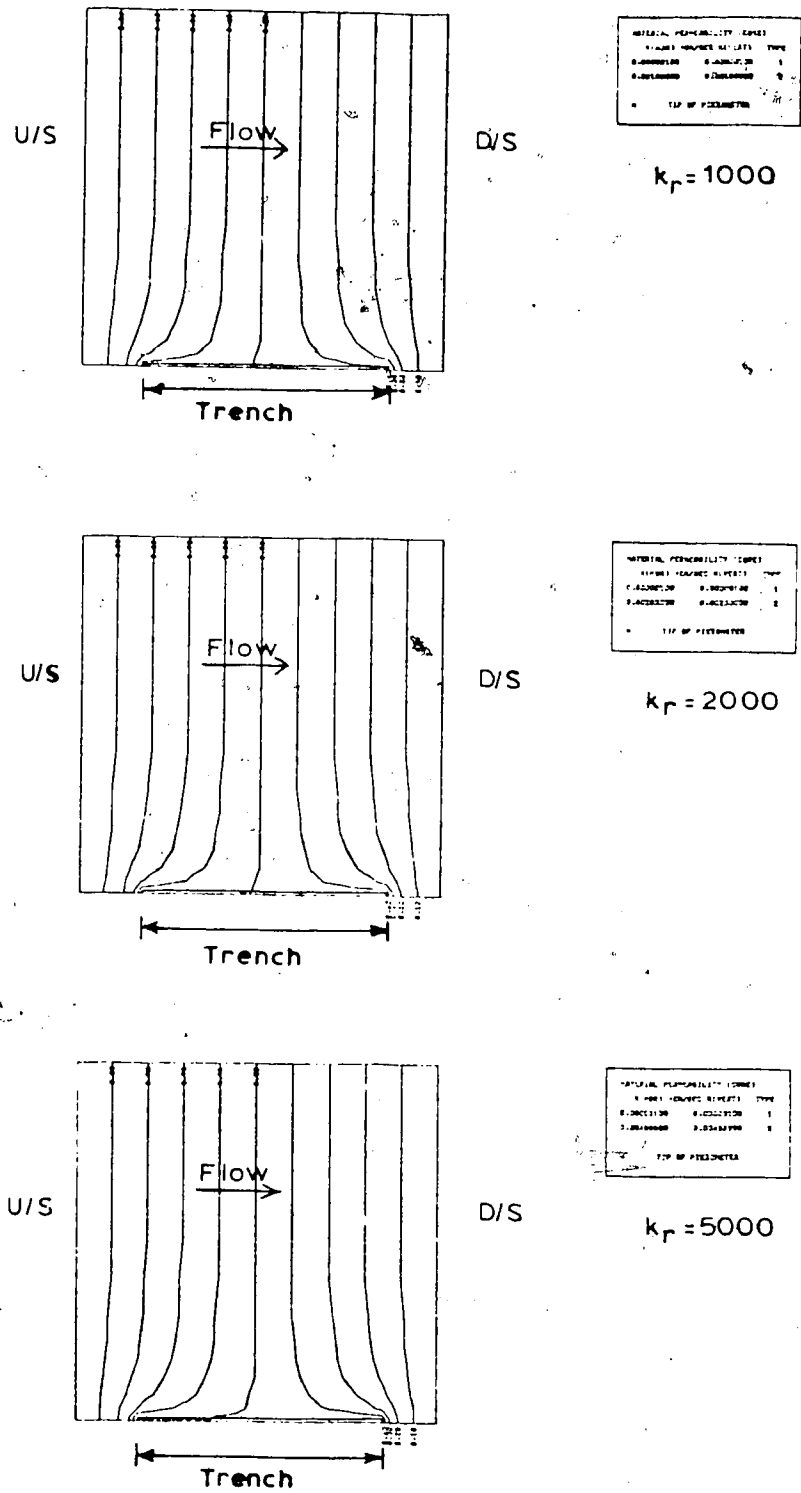


FIGURE 7.11 Equipotential Distribution around Trench PE25... PH7

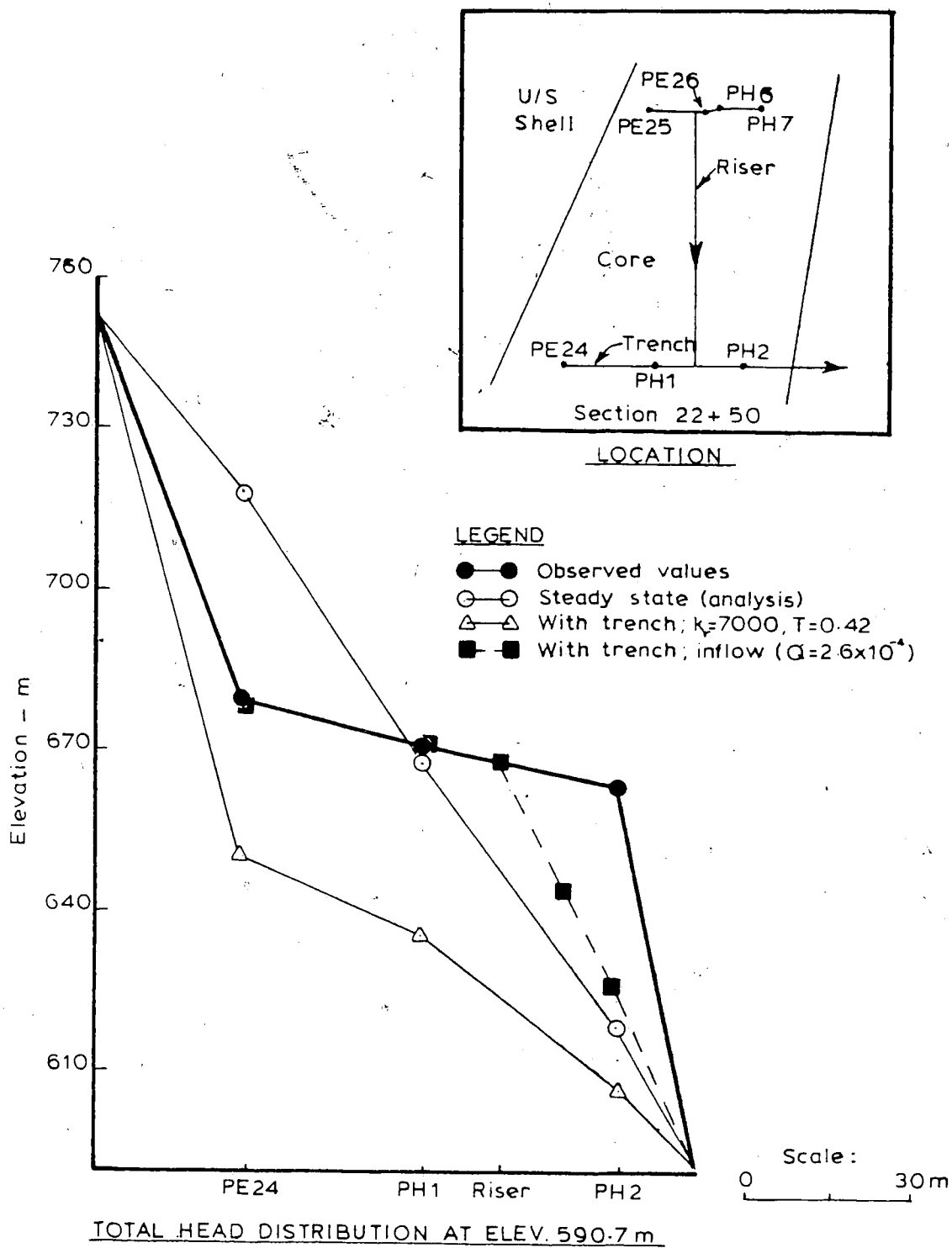
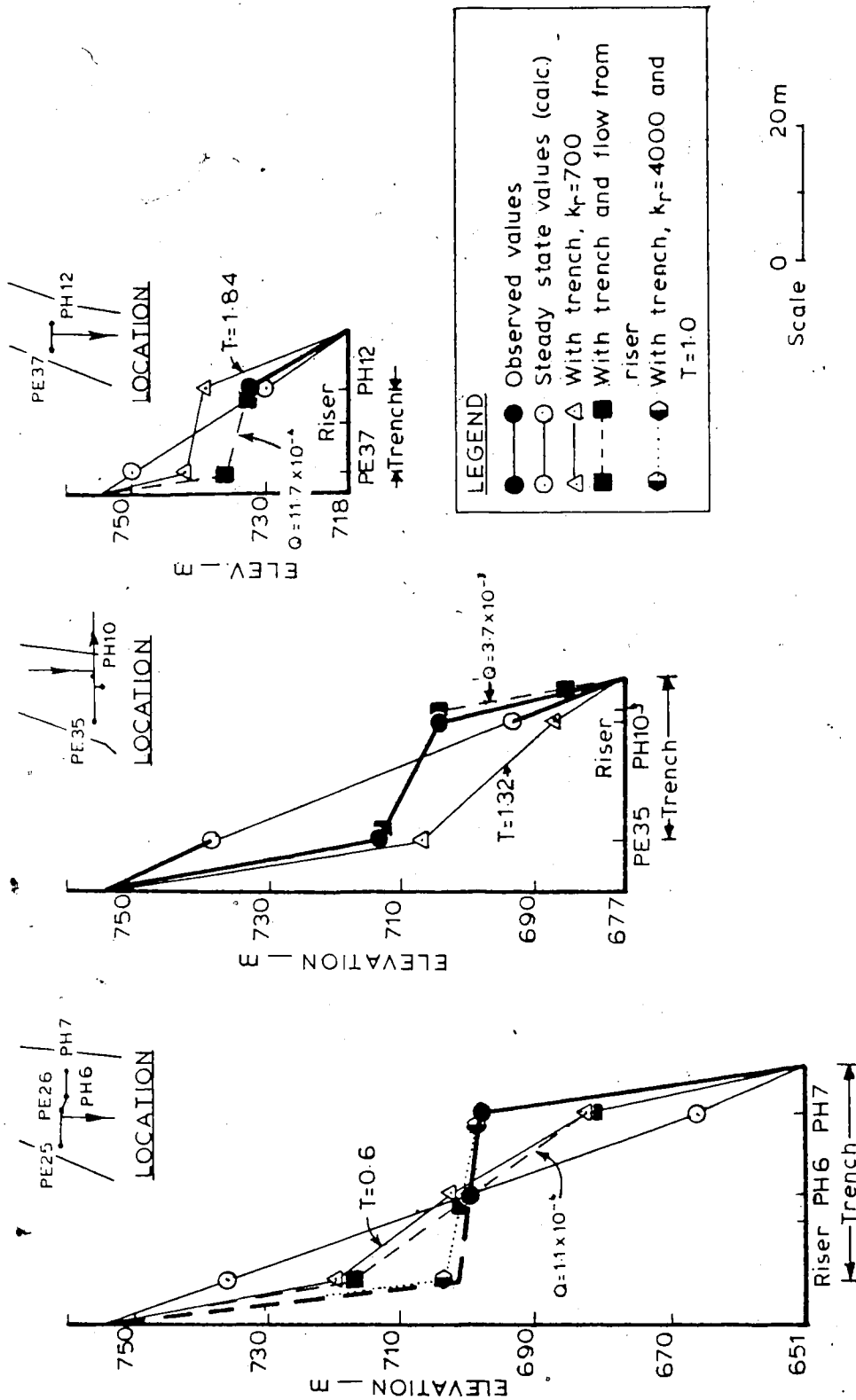


FIGURE 7.12 Theoretical Pore Pressure Distribution Compared to Actual, PE24... PH2



TOTAL HEAD DISTRIBUTION

FIGURE 7.13 Theoretical Pore Pressure Distribution Compared to Actual, PE25... PH7, PE35... PH10, PE37... PH12.

7.5 Conclusions

Whereas none of the previous analyses predicted the observed pore pressure distribution in the core, this analysis assuming the instrument lead trenches to have a higher permeability than the surrounding core, provides a pore pressure distribution similar to the observed values.

The differences are reduced by including some effect from the risers. It is virtually impossible to refine the analysis further, because of the sensitivity of the results to actual construction methods and variations, details of which are not available. PH2 is the only piezometer which does not fit this model well. A way to explain its high readings is by virtue of some constructional deviation which may not have appeared significant enough to report, such as backfilling downstream of PH2 with a slightly more impermeable material.

Additional effects such as pore pressure increases due to reservoir loading are not simple to evaluate in the vicinity of the trenches, except that their magnitude will probably be reduced. The anomalies noted in the transient seepage analysis (the very rapid response of the downstream piezometers) could very likely be due to these trenches with a much higher k/N ratio. The apparent rapid dissipation of the end of construction pore pressures in the central core zone (compared to the edge zones) may also be explained by the proximity to the zones of higher permeability.

It is rather difficult to provide more than a qualitative assessment on the influence of the instrument trenches and risers. Quantitative results are too sensitive to local construction methods and variations. However it has been adequately demonstrated that the instrumentation trenches installed in the Mica dam core may to a large extent be responsible for the unusual piezometric readings. It is therefore likely that the general pore pressure distribution within the core is considerably different than that suggested by the piezometers and, in fact, may be very similar to the distribution suggested by the steady state analysis.

Several solutions are possible to reduce the likelihood of preferential seepage paths along the instrument-lead trenches.

- The backfill material for the trenches should be the same as the surrounding core material, with the larger soil sizes removed. The compaction moisture content and density should be maintained as close as possible to the surrounding core material. This will aid in reducing hydraulic property differences.

Strict construction supervision is required at all times and deviation from the specifications should not be allowed without careful consideration of the possible consequences.

- In very narrow cores of low permeability special precautions may be necessary to ensure instrument

reliability. Procedures such as those suggested by Blight (1970) may be satisfactory.

- For cases where instrumented sections are not far apart along the crest, the instrument-lead trenches could run parallel to the crest. Special attention to detail would be required where the leads turn perpendicular to the crest and exit into the downstream shell. This alternative is controlled by the economics of the situation.

Chapter 8

Conclusions

This thesis has investigated the response of the pore pressures in the Mica Dam to reservoir impounding and transient seepage. It compares theoretical results to the observed behaviour and provides explanations for the differences between them. The process involved during the period between the end-of-construction and steady state seepage are described and analysed separately to gain insight into their relative contributions. The likelihood of hydraulic fracture has been evaluated.

The method of instrument installation has been found to have a significant influence on the observed pore pressure distribution. The general pressure field is locally perturbed by the contrast in hydraulic properties between original compacted material and backfill around instruments. This is both unfortunate and a serious technical problem since satisfactory comparison between theoretical analysis, design assumptions and field performance cannot be easily undertaken.

8.1 Significance of the Processes Involved during Reservoir Impoundment and Transient Seepage.

8.1.1 Total stress changes.

The total stress changes along the upstream face of the core caused by reservoir filling will be less than hydrostatic values. These stress increments will cause a change in pore pressure distribution throughout the core which is significant but apparently does not dominate the observed pore pressure distribution. The estimated values are functions of the induced shear stress distribution assumed across the core. In this thesis the assumed distribution was compared to the analysed case of the Orville Dam and the measured case of the Gessertsch Dam.

8.1.2 Transient seepage.

The transient seepage phase was estimated to be relatively rapid in the Mica dam case, taking approximately 3 years despite the low permeability of the core (10^{-7} cm/sec). The advance of the phreatic surface corresponds reasonably closely to the observed water levels in the movement gauges. The estimated steady state phreatic surface by conventional analysis is very much higher in the downstream zone of the core when compared to an analysis which considers flow within the capillary fringe (Freeze 1971). This anomaly is most pronounced in a dam configuration similar to the Mica dam. The downstream movement gauge appears to substantiate the argument for a

lower phreatic surface and therefore the transient analysis must be considered inaccurate near the downstream core face.

8.1.3 Hydraulic fracturing.

It has been estimated that although hydraulic fracturing is feasible upon reservoir filling, the increase in total stresses are of sufficient magnitude to make this phenomenon unlikely. Hydraulic fracture potential is very sensitive to the degree of arching present in the core. The mechanism of initiating hydraulic fracture from inflow tests in standpipes is completely different from that of reservoir filling and so hydraulic fracture resulting from inflow testing does not necessarily imply a high risk of hydraulic fracture occurring during reservoir filling.

8.1.4 Justification for simplified analysis.

For the purposes of this study the processes leading to pore pressure changes during reservoir filling and transient flow were separated and analyzed individually with simplifications. There are many ill-defined parameters such as the storage coefficient, path dependent pore pressure parameters, which preclude the use of more refined finite element analysis. It would be of limited benefit to refine the analysis until the significant mechanisms and parameters are better defined and understood. It may be very difficult to model the behaviour of a core in the laboratory in order to better determine the relevant parameters because the

results are very sensitive to in-situ conditions such as compaction effort, compaction moisture content, permeability, porosity and compressability, some of which change with time depending on construction history and location in the embankment.

Suitable, well placed instrumentation would help to provide further insight into the contributions of each separate mechanism.

8.2 Comparison with Observed Behaviour

It is apparent that the observed pore pressure distribution within the Mica dam core is at variance with the calculated steady state distribution, even though the evidence suggests that essentially steady state conditions have been achieved after about 3 years.

The observed distribution is not reflected by the reservoir loading nor the transient seepage analysis. It must be concluded that some alternative phenomenon was producing the observed distribution. A study was completed which indicates the sensitivity of local pore pressures to non-homogeneities present in the form of instrument-lead trenches. The evidence from the piezometers connected to the upstream shell shows that these trenches must provide a preferential seepage path. This model when applied to specific trenches within the till core readily reflected the observed trend. The magnitudes are sensitive to permeability ratios and specific trench sizes, accurate details of which

are very difficult to obtain.

Similarly if the risers are considered to behave as preferential seepage paths the agreement between the calculated steady state pore pressure distribution and the measured distribution is improved. It would be useless to refine the analysis further because the specific construction details required for input are not available. The analysis indicates in a quantitative manner that the piezometers placed in the Mica dam core are not reflecting the general pore pressure distribution during impounding. The non-homogeneities caused by the instrument-lead trenches are sufficient to create a local pore pressure disturbance, which is being monitored by the piezometers. It is concluded that the average pore pressure distribution within the core is probably similar to that proposed by steady state theory, with possible errors in the downstream core zone depending on whether the flow in the capillary fringe is being considered.

This emphasizes the very considerable care required when installing piezometers in a narrow core embankment. If sufficient protection is not employed against preferential seepage the results will likely be valueless and the expense of the entire installation wasted.

A serious consequence of inadequate installation procedure would be the increased likelihood of hydraulic fracture initiating if the trench were connected to the upstream shell. Therefore designers should never consider

running trenches from the lower core into the upstream shell, and this should not be done in the upper core without considerable justification and consideration of the possible consequences. Considerable attention is required during the design and installation to ensure that the hydraulic properties of the instrument-lead trenches are similar to the surrounding core material.

8.3 Selection of Piezometer Type

Some conclusions are drawn regarding piezometer types used in embankment dams.

Hydraulic 'embankment type' piezometers are excellent and should be used where possible. Their main attraction is simplicity of operation, the facility for de-airing and in-situ testing. If adequate care is taken during installation their performance is completely satisfactory.

Electric piezometers require special attention in partly saturated zones. The choice of a high air entry stone does not remove the possibility that the tip is recording pore air pressure in zones of low stress. Their design precludes the possibility of flushing or in-situ testing. They have been proven susceptible to overvoltage failures from lightning strikes unless very special attention is paid to overvoltage protection.

Pneumatic piezometers generally lack a deairing facility and in-situ tests are normally impossible. Long lead lengths and certain lead types may present problems.

Operator error is not uncommon. Insufficient evidence is available in the literature regarding the long term behaviour and accuracy of these piezometers.

In many instances electric and pneumatic piezometers may be excellent choices but it is the author's opinion that where practical hydraulic 'embankment type' piezometers should be used in partly saturated compacted-fill embankments. Their suitability and long term reliability have been adequately demonstrated in the literature. If a variety of piezometer types are employed then care must be exercised to ensure that different piezometer types are placed within zones of similar potential. In a few locations it is desirable to provide a hydraulic piezometer close to the alternate type, to serve as a calibration check. In this manner an adequate description of the pore pressure distribution may still be possible if a particular piezometer type malfunctions. It must be remembered that once a malfunction occurs it may be impossible to replace that piezometer and it will certainly be very expensive to do so.

8.4 Recommendations for Further Research

Based on the work presented here the following is recommended for further research.

1. The effect of rotation of principal stresses on the pore pressure parameters require further attention.

2. Further investigation is required into the shape of the steady state phreatic surface in a core where the unsaturated or capillary fringe flow is considered. Particularly useful would be investigation of case histories which indicate the phreatic surface with time.
3. In order that transient flow may be successfully analysed it is necessary to provide a more accurate description of the storage coefficient and its sensitivity to parameters such as degree of saturation, compaction water content, porosity, degree of compaction, stress history, and grain size distribution.
4. A particularly important area of research would be an investigation of hydraulic fracture. It may be possible to use induced hydraulic fracture as an indicator of degree of arching in critical zones of the core. This in turn could be related to the likelihood of hydraulic fracture occurring on reservoir filling. Earth pressure cells have not been very successful in embankments to date, but perhaps they could be used in conjunction with hydraulic fracture tests to determine in-situ stress states more accurately.

references

- Barden, L. and Sides, G. R. 1967. The Diffusion of Air Through the Pore Water of Soils. Proc. 3rd Asian Regional Conf. on Soil Mech. and Fdn. Engg. , 1, pp .
- Bishop, A. W., and Henkel, D.J., 1962. The Triaxial Test. Arnold, London.
- Bishop, A. W. 1957. Some Factors Controlling the Pore Pressures set up during the Construction of Earth Dams. Proc. 4th. Int. Conf. Soil Mech. and Fdn. Engg., 2, pp. 294-300.
- Bishop A. W., 1954. The Use of Pore Pressure Coefficients in Practice. Geotechnique, 4, pp. 148-152.
- Bishop, A. W., Kennard, M. F., and Vaughan, P. R. 1964. Developments in the Measurement and Interpretation of Pore Pressure in Earth Dams. Trans. 8th Int. Congr. of Large Dams, 2, Q29-R4, pp. 47-71.
- Blight, G. E. 1970. Construction Pore Pressures in two Sloping-Core Rockfill Dams. Trans. 10th Int. Congr. on Large Dams, Montreal, 1, pp. 269-290.
- Brahma, S. P., and Harr, M. E. 1962. Transient Development of Free Surface in a Homogeneous Earth Dam. Geotechnique, 12, pp. 283-302.
- Broms, B. B. and Casbarian, A. O. 1965. Effects of Rotation of the Principal Stress Axes and of the Intermediate Principal Stress on the Shear Strength. Proc. 6th. Int. Conf. on Soil Mech. and Fdn. Engg., Montreal, 1, pp. 178-183.

- Caseco Consultants Ltd., Mica Project. Reports on Dam Instrumentation 1969-1979. Vancouver, B. C.
- Caseco Consultants Ltd., Mica Project. Dam Instrumentation Construction Notes. 1969-1972. Vancouver, B. C.
- Casagrande, A. 1937. Seepage Through Dams. New England Waterways Assoc., LI, June 1937, pp. 245-336.
- Cedergren, H. R. 1967. Seepage, Drainage and Flow Nets. Wiley. New York.
- Chan, W. K. 1972. The Development and Dissipation of Construction Pore Pressure in the Core of Mica Dam. M. Eng. Report. Dept. of Civil Engineering, University of Alberta, Edmonton, Alberta.
- Chang, C. 1976. Analysis of Consolidation of Earth and Rockfill Dams. Ph.D. Thesis, Dept. of Civil Engineering, University of California, Berkeley, California.
- Charles, J. A. 1977. Discussion on paper by Kulhawy and Gurtowski.(1976). Jnl. of the Geotechnical Div. Proc. A.S.C.E.,103, pp. 663-665.
- Desai, C.S., and Sherman, W.C. 1971. Unconfined Transient Seepage in Sloping Banks. Jnl. Soil Mech. and Fdn. Div., A.S.C.E, 97, Feb. 1971, pp. 357-374.
- Dvinoff, A. H. 1970. Response of the Phreatic Surface in Earthen Dams due to Headwater Fluctuations. Ph.D. Thesis, Purdue University, Lafayette, Indiana. 156 pages.
- Dvinoff, A. H., and Harr, M. E. 1971. Phreatic Surface Location after Drawdown. Jnl. Soil Mech. Fdn. Div. Proc.

- A.S.C.E., 97, pp. 47-58.
- Fredlund, D. G. 1973. Volume Change Behaviour of Unsaturated Soils. PhD. Thesis, Dept. of Civil Engineering, University of Alberta, Edmonton, Alberta.
- Freeze, R. A. 1971. Influence of the Unsaturated Flow Domain on Seepage through Earth Dams. Water Resources Research, 7, pp.929-941.
- Freeze, R. A. and Cherry, J. A. 1979. Groundwater. Prentice Hall.
- Guther, H. 1972a. Axisymmetric and Plane Flow in Porous Media. Users Manual, Soil Mechanics No. 16, Dept. of Civil Engineering, University of Alberta, Edmonton, Alberta.
- Guther, H. 1972b. M.Sc. Thesis, Dept of Civil Engineering, University of Alberta, Edmonton, Alberta.
- Hanna, T.H. 1973. Foundation Instrumentation. Trans. Tech. Publications, pp. 69-122.
- Henkel, D. J. 1960. The Shear Strength of Saturated Remoulded Clays. Research Conf. Shear Strength of Cohesive Soils, A.S.C.E., Boulder, pp. 533-554.
- Hilf, J. W. 1948. Estimating Construction Pore Pressures in Rolled Earth Dams. Proc. 2nd. Int. Conf. Soil. Mech. and Fdn. Engg., 3, pp. 234-240.
- Hosking, A. D., and Hilton J. I. 1963. Instrumentation of Earth Dams on the Snowy Mountains Scheme. Proc. 4th. Australia-New Zeland Conf. on S.M.F.E. pp. 251-262.
- Insley, A. E. and Hillis, S. F. 1965. Triaxial Shear.

- Characteristics of a Compacted Till under Unusually High Confining Pressures. 6th. Int. Conf. on Soil Mech. and Fdn. Engg., 1, Montreal, pp. 244-248.
- Kazda, I. 1979. Numerical Modeling of Seepage in Earth and Rockfill Dams. 3rd. Int. Conf. on Numerical Methods in Geomechanics, Aachen, 2nd.-6th. April 1979, pp. 257-261.
- Kealy, C. D., and Busch, R. A. 1971. Determining Seepage Characteristics of Mill-tailings Dams by the Finite Element Method. U. S. Bureau of Mines. Report of Investigations, No. 7477.
- Kjaernsli, B., and Torblaa, I. 1968. Leakage Through Horizontal Cracks in the Core of Hyttejuvet Dam. Norges Geoteknishe Institut, Nr. 80., Oslo.
- Koppula, S.D. 1970. The Consolidation of Soil in Two Dimensions and with Moving Boundaries. Ph.D. Thesis. Dept. of Civil Engineering, University of Alberta, Edmonton, Alberta.
- Kulhawy, F. H., and Duncan, J. M. 1970. Nonlinear Finite Element Analysis of Stresses and Movements in Oroville Dam. Geotechnical Engineering Report No. TE-70-2, Dept. of Civil Engineering, University of California, Berkeley, California.
- Kulhawy, F. H., and Gurtowski, T.M. 1976. Load Transfer and Hydraulic Fracturing in Zoned Dams. Jnl. of the Geotechnical Engineering Division, A.S.C.E., 102, Sept. 1976, pp.963-974. and Discussions.
- Lambe, T. W., and Whitman, R.V. 1969. Soil Mechanics. Wiley,

New York.

- Lambe, T. W. 1967. Stress Path Method. Jnl. of Soil Mech. and Fdn. Div., A.S.C.E., 93, SM6, pp. 309-331.
- Law, K. T., and Holtz, R. D. 1978. A Note on Skempton's A Parameter with Rotation of Principal Stress. Geotechnique, 28, pp. 57-64.
- Law, T. C. 1975. Deformations of Earth Dams during Construction. Ph.D. Thesis Dept. of Civil Engineering, University of Alberta, Edmonton, Alberta.
- Lee, K. L., Morrison, R. A., and Haley, S. C. 1969. A note on the Pore Pressure Parameter B. Proc. 7th. Int. Conf. Soil Mech. and Fdn. Engg. Mexico City. 1969. pp. 231-239.
- Little, A.L. 1973. Experiences with Instrumentation for Embankment Dam Performance. Field Instrumentation in Geotechnical Engineering, Butterworths.
- Mackellar, D.C.R., Nunn, D. J., and Pells, P.J.N. 1973. Instrumentation of some Embankment Dams in Southern Africa. Field Instrumentation in Geotechnical Engineering. Butterworths.
- Meidal, P., and Webster, J.L. 1973. Mica: One of the World's Largest Structures. Water Power, June, 1973, pp. 201-210; and July, 1973, pp. 245-249.
- Middlebrooks, E. J., Penman, C. D., and Dunn, I. S. 1978. Wastewater Stabilization of Pond Linings. Special Report 78-28, Nov. 1978, U. S. Army Corps. of Engineers, C.R.R.E.L., Hanover, N. H.

- Mitchell, J. K., Hooper, D. R., and Campanella, R. G. 1965. Permeability of Compacted Clay. *Jnl. of Soil Mech. Fdn. Div., A.S.C.E.*, 91, pp. 41-65.
- Mylrea, F.H. 1969. Geology of Mica Damsite, Columbia River, British Columbia. *Proc. of the Geol. Assoc. of Canada*, 20, Feb, 1969.
- Neuman, S. P., and Witherspoon, P. A. 1970. Finite Element Method of Analyzing Steady Seepage with a Free Surface. *Water Resources Research*, 6, pp. 889-897.
- Nobari, E. S., and Duncan, J. M. 1972. Effect of Reservoir Filling on Stresses and Movements in Earth and Rockfill Dams. Geotechnical Engineering Report No. TE-72-1, Dept. of Civil Engineering, University of California, Berkeley, California.
- Nussbaum, H. 1976. Mica Dam Embankment Performance. Unpublished. Caseco Consultants. Vancouver.
- Nussbaum, H., and Stevenson, G. W. 1976. Performance of Mica Dam Embankment. Paper Presented at Joint Meeting of CEA Hydraulic Power Section and CANCELD, 23th-24th. Sept., 1976.
- Nussbaum, H. 1979. Personal Communication.
- Penman, A. D. M. 1975. Earth Pressures Measured with Hydraulic Piezometers. A.S.C.E. Speciality Conference on In-Situ Measurement of Soil Properties, held at N. Carolina State University, at Raleigh, N. C.
- Pinkerton, I., and McDonnell, A. D. 1964. Behaviour of Tooma Dam. *Trans. 8th. Int. Congr. on Large Dams*, 2, pp.

351-376.

- Richards, B. G., and Chan, C. Y. 1969. Prediction of Pore Pressures in Earth Dams. Proc. 7th Int. Conf. on Soil Mech. and Fdn. Engg., 2, Aug. 1969, Mexico, pp. 355-362.
- Rollins, M. B., and Dylla, A. S. 1970. Bentonite Sealing Methods Compared in the field. Jnl. Irrig. and Drainage Division, A.S.C.E., 96, pp.
- Schober, W. 1967. Behaviour of the Gepatsch Rockfill Dam. Trans. 9th Int. Congr. on Large Dams, Istanbul, Q34-R39, pp. 677-699.
- Schober, W. 1970. The Interior Stress Distribution of the Gepatsch Rockfill Dam. Trans. 10th Int. Congr. on Large Dams, Montreal, Q36-R10, 1, pp. 169-187.
- Scott, J. D., and Kilgour, J. 1967. Experience with some Vibrating Wire Instruments. Canadian Geotechnical Journal, 4, pp. 100-123.
- Sherman, W. C., and Clough, G. W. 1968. Embankment Pore Pressures During Construction. Jnl. Soil Mech. and Fdn. Div., A.S.C.E., 94, pp. 527-553.
- Sherard, J. L., Woodward, R. J., Gizienski, S. F., and Clevenger, W. A., 1963. Earth and Earth-Rock Dams. Wiley, New York.
- Sherard, J. L. 1973. Embankment Dam Cracking. Embankment - Dam Engineering Casagrande Volume, R. C. Hirschfield and S. J. Poulos, eds., Wiley-Interscience, New York. pp. 271-353.
- Sides, G. R., and Barden, L. 1967. The Effects of Time on

- the Undrained Pore Pressure in Compacted Clay. Proc. 3rd Asian Regional Conf. on Soil Mech. and Fdn. Engg., 1, pp. 308-311.
- Simmons, J. V. 1974. Three-Dimensional Analysis of Mica Dam. M.Sc. Thesis. Dept. of Civil Engineering, University of Alberta, Edmonton, Alberta.
- Skempton, A.W. 1954. Pore Pressure Coefficients A and B. Geotechnique, 4, pp.143-147.
- Skempton, A.W. 1961. Horizontal Stresses in Overconsolidated London Clay. Proc. 5th Int. Conf. Soil Mech. Fdn. Engg., Paris, 1, pp. 351-357.
- Skempton, N. A. 1975. Mica Dam Embankment Stress Analysis. Jnl. of the Geotech. Div., A.S.C.E., 101, pp. 229-242.
- Speedie, M. G. 1963. Discussion on paper by Hosking and Hilton. Proc. of 4th Australian-New Zealand Conf. on S.M.F.E. 1963. p. 331.
- Stevenson, D. 1978. Drawdown in Embankments. Geotechnique, 28, pp.273-280.
- Taylor, R. L., and Brown, C. B. 1967. Darcy Flow Solutions with Free Surface. Jnl. Hydraulics Division, A.S.C.E., 93, pp. 25-33.
- United States Bureau of Reclamation. 1963. Earth Manual. U.S. Govt. Printing Office, Washington D. C. Appendix Des. E-27,E-28, pp. 650-699.
- Vaughan, P. R. 1965. Field Measurements in Earth Dams. Ph.D. Thesis, University of London, 1.
- Vaughan, P. R. 1973. The Measurement of Pore Pressures with

Piezometers. Field Instruments in Geotechnical Engineering, Butterworths.

Vaughan, P. R. 1969. A Note on Sealing Piezometers in Boreholes. Geotechnique, 19, pp. 405-413.

Webster, J. L. 1970. Mica Dam Designed with Special Attention to Control of Cracking. Trans. 10th Int. Congr. on Large Dams, Montreal, Q36-R30, 1, pp. 487-510.

Webster, J. L., and Lowe, W. I. 1971. Instrumentation for Earth and Rockfill Dams. Proc. Int. Conf. on Pumped Storage Development, American Water resources Assoc., pp. 238-247.

Wei, C. Y., and Shieh, W. Y. J. 1979. Transient Seepage Analysis of Guri Dam. Jnl. of the Technical Councils, A.S.C.E., 105, pp. 135-147.

Zienkiewicz, O. C. 1971. The Finite Element Method in Engineering Science, McGraw Hill, London.